Characterising the urinary acylcarnitine and amino acid profiles of patients with HIV/TB co-infection, using LC-MS metabolomics

C Pretorius

orcid.org 0000-0001-8021-6992

Dissertation accepted in partial fulfilment of the requirements for the degree *Master of Science in Biochemistry* at the North-West University

Supervisor: Dr L Luies

Graduation May 2024

ACKNOWLEDGEMENTS

The following individuals and institutions are acknowledged herein for their contributions to the fulfilment of this dissertation.

- The South African Tuberculosis Vaccine Initiative and the Desmond Tutu HIV Centre, located at the University of Cape Town (South Africa), for providing the urine samples used in this study.
- The North-West University for the postgraduate bursary that financed my M.Sc. degree.
- Dr Laneke Luies, my supervisor, for your effort put into this project, guidance, and aid in the writing of this dissertation. Your attention to detail has been invaluable in this regard. I appreciated your go-getter attitude and fighting spirit. Without it, I would still be waiting for my isotopes to arrive.
- My family, for your patience and all the sacrifices you made for my studies. Thank you for all the warm welcomes and the special treatment I received at home.
- Cara Olivier, for being a good colleague and even better friend, thank you for all the lunch breaks and your company in the office.
- The M.Sc. “study” group. For all the good times we had together and for taking my mind off work every now and then.
- Everyone who helped me with the LC-MS, thank you for all your patience. Arno Smith, for showing me the ropes on the instrument. Ms Carien van der Berg, for your crucial guidance and knowledge with the method validation. Mr Peet Jansen van Rensburg, for your relentless efforts to fix the LC-MS whenever it was misbehaving. Tarien Jacobs, for your general advice and assistance with the quantification software. Prof Zander Lindeque, for advice, not only with the LC-MS, but also with the statistics of this study. The BOSS lab, for letting me use their instrumentation. The Mitochondrial Research Lab, for providing me with the reference standards I used for the LC-MS.
- The Centre for Human Metabolomics, for the urine amino acid analysis.
- My God, for all the opportunities, guidance and strength given for this project.

SUMMARY

This study comprises a comprehensive investigation of the urinary acylcarnitine and amino acid profiles in patients with HIV, TB, and HIV/TB co-infection using LC-MS metabolomics. It addresses a critical gap in current research by exploring the metabolic interplay in HIV/TB co-infection, a domain less extensively studied compared to the individual effects of HIV and *Mtb* infection. Recognising the potential of metabolomics in enhancing our understanding of HIV/TB co-infection and its immunological impact on host metabolism, this research aimed to characterise the urinary metabolome of individuals afflicted by these conditions. Such insights are pivotal for developing novel treatments and diagnostic strategies to effectively manage the HIV/TB syndemic.

In this pursuit, urine samples from 9 HIV/TB co-infected, 7 HIV-only, and 41 TB-only patients, along with 32 healthy controls, were analysed. The analysis employed three targeted HPLC-MS/MS methods, allowing for the distinct assessment of urinary amino acids using the ChromSystems MassChrom® Amino Acid Analysis kit, as well as acylcarnitines and the tryptophan derivative 5-hydroxyindoleacetic acid (5-HIAA) through newly established and validated methods. The validation of these methods encompassed a thorough evaluation of selectivity, linearity, precision, and accuracy, ensuring the reliability of the findings.

The results revealed significant alterations in the amino acid metabolome across all infected cohorts. Notably, there was a marked decrease in tryptophan and glycine levels, coupled with increased saccharopine and hydroxykynurenine levels. Enhanced lysine degradation via the saccharopine pathway was evident in HIV/TB co-infected and TB-only patients, as indicated by a significantly increased saccharopine/lysine ratio. While amino acid levels predominantly decreased in the HIV-only patients, an increase was observed in those with TB-only compared to healthy controls. The co-infected cohort did not exhibit a clear trend, suggesting a complex interplay of metabolic processes in the co-infection state. Although changes in acylcarnitines and 5-HIAA were not statistically significant, there were indications of generally elevated medium-chain acylcarnitines in the TB-only and HIV/TB co-infected cohorts. These findings point towards an altered net protein turnover, inflammation, lipid and amino acid catabolism, and potentially diabetic-like hyperglycaemia in the HIV/TB co-infected state, predominantly driven by *Mtb* infection. Furthermore, this study lays the groundwork for future research aiming to identify robust disease markers, as it suggests that the effects of HIV and *Mtb* infection on the amino acid metabolome are attenuated in the co-infected state. Overall, this study not only contributes to a deeper understanding of the metabolic complexities associated with HIV, TB, and their co-infection but also opens new avenues for targeted therapeutic interventions in managing these challenging infectious diseases.

Keywords: HIV/TB co-infection; targeted; LC-MS; acylcarnitines; amino acids; 5-hydroxyindoleacetic acid

TABLE OF CONTENTS

LIST OF FIGURES

Chapter 2:

Chapter 3:

Chapter 4:

LIST OF TABLES

Chapter 1:

Chapter 2:

Chapter 3:

Chapter 4:

Appendix A:

Appendix B:

LIST OF ABBREVIATIONS

Abbreviation	Meaning	Abbreviation	Meaning
5-HIAA	5-Hydroxyindoleacetic acid	GI	Gastrointestinal
5-HIAA_IS	5-Hydroxyindole-3-acetic acid-^{13}C3	H_2O	Water
AIDS	Acquired immunodeficiency syndrome	HCl	Hydrochloric acid
ACN	Acetonitrile	HIV	Human immunodeficiency virus
ART	Antiretroviral therapy	HPLC-MS/MS	High-performance liquid chromatography-tandem mass spectrometry
ATP	Adenosine triphosphate	IDO1	Indolamine 2,3-dioxygenase 1
ANOVA	Analysis of variance	IL	Interleukin
BCAA	Branched chain amino acids	IRIS	Immune reconstitution inflammatory syndrome
BCG	Bacillus Calmette-Guérin	LC-MS	Liquid chromatography-mass spectrometry
C2	Acetyl-L-carnitine	LTBI	Latent tuberculosis infection
C3	Propionyl-L-carnitine	MDR-TB	Multi-drug resistant TB
C4	Butyryl-L-carnitine	MRM	Multiple reaction monitoring mode
C5	Isovaleryl-L-carnitine	MS/MS	Tandem mass spectrometer
C6	Hexanoyl-L-carnitine	*Mtb*	*Mycobacterium tuberculosis*
C8	Octanoyl-L-carnitine	*m/z*	Mass-to-charge ratio
C10	Decanoyl-L-carnitine	NAD(P)	Nicotinamide adenine dinucleotide (phosphate)
C12	Dodecanoyl-L-carnitine	NMR	Nuclear magnetic resonance spectroscopy
CCR5	C-C chemokine receptor 5	NWU	North-West University
CD4+	Cluster of differentiation 4 positive	RD1	Region of difference 1
CDP	Cytidine diphosphate	RNA	Ribonucleic acid
COVID-19	Coronavirus disease of 2019	RSD	Residual standard deviation
CNS	Central nervous system	SATVI	South African Tuberculosis Vaccination Initiative
CV	Coefficient of variation	SNAE	Serious non-AIDS events
dMRM	Dynamic multiple reaction monitoring	TB	Tuberculosis
DTSV	Desmond Tutu HIV Centre	TCA	Tricarboxylic acid
DNA	Deoxyribonucleic acid	TNF	Tumour necrosis factor
FDR	False discovery rate	UCT	University of Cape Town
GC-MS	Gas chromatography-mass spectrometry	USA	United States of America
GI	Gastrointestinal	WHO	World Health Organization

CHAPTER 1: PREFACE

1.1. Problem statement

Until the coronavirus disease of 2019 (COVID-19) pandemic, tuberculosis (TB) was the leading cause of death from a single infectious agent (Zimmer *et al.*, 2022). Human immunodeficiency virus (HIV) infection, with no known cure, actively compromises the host's immune system (Boasso *et al.*, 2009; Sankaranantham, 2019). The interaction between TB and HIV is notably bidirectional and synergistic. HIV patients are about 20 times more susceptible to *Mycobacterium tuberculosis* (*Mtb*) infection, while TB accelerates HIV infection by upregulating the host's immune response, including T cell activation and increased expression of receptors for HIV replication (Saharia & Koup, 2013). This interplay exacerbates the deterioration of immune functions, leading to profound metabolic consequences. The metabolic impacts, however, are poorly understood. Metabolomics offers a promising avenue to explore these unknowns. While separate metabolomics studies on HIV and TB exist [reviewed by Liebenberg *et al.* (2021)], the metabolic profile of HIV/TB co-infected remains underexplored. Previous studies have identified a myriad of amino acids and acylcarnitines that undergo significant alterations in both HIV-only and TB-only infected states, rendering them appealing candidates for a targeted metabolic investigation of the co-infected state. Additionally, this study includes 5-hydroxyindoleacetic acid (5-HIAA) due to its potential significance in neurotransmitter metabolism, which may be perturbed in the co-infected state. A detailed metabolic characterisation, focusing on urinary acylcarnitine and amino acid profiles, could enhance our understanding of the co-infected state and inform future studies aimed at improving treatment, diagnosis, and monitoring of HIV/TB co-infected individuals.

1.2. Aim

The aim of this study is to characterise the urinary acylcarnitine and amino acid (including the tryptophan derivative 5-HIAA) profiles of patients with HIV/TB co-infection using targeted liquid chromatography-mass spectrometry (LC-MS) metabolomics.

1.3. Objectives

To achieve the aforementioned aim, the study sets forth the following objectives:

1. To setup and perform a partial validation of two LC-MS/MS methods for the quantification of urinary acylcarnitines and 5-HIAA.

2. To analyse the urinary (a) acylcarnitines and (b) amino acids (with an additional focus on the tryptophan derivative 5-HIAA) of all collected samples (n=114) and appropriate quality controls (QCs) using LC-MS/MS.

3. Undertake data processing, clean-up, and statistical analyses to identify significant metabolite markers.

4. Interpret the data in light of existing literature to determine the overall impact of HIV/TB co-infection on profiles a–c by comparing treatment naïve HIV/TB co-infected (n=9), HIV-positive (n=7) and TB-positive (n=41) groups to healthy controls (n=32).

1.4. Structure of dissertation

This dissertation adheres to the guidelines of the North-West University (NWU), Potchefstroom Campus, South Africa, for completion of the degree Master of Science (Biochemistry). It is structures as follows:

Chapter 1 introduces the study, covering the problem statement, aim, objectives, and structure of this dissertation.

Chapter 2 provides a literature review on the basic pathophysiology of HIV infection, TB, HIV/TB co-infection, and the known metabolomic consequences.

Chapter 3* details the study design, encompassing sample collection and storage, analytical methods standardisation, validation, application, and data processing and statistical analysis.

Chapter 4* presents method validation results, patient urine sample analyses, and characterises the amino acid, 5HIAA and acylcarnitine metabolome in HIV, TB, and HIV/TB co-infection.

Chapter 5 gives the conclusion, addressing the study's aim and objectives, and offers recommendations for future metabolomic studies.

All references utilised are listed following Chapter 5.

Supplementary information is provided in Appendices A and B.

**Chapters 3 and 4 are in drafting process for journal submission.*

1.5. Author contributions

The contributions of the main author of this dissertation (Mr Charles Pretorius), co-authors, and co-workers to this dissertation and related research outputs are outlined in Table 1.1. The following statement from the main author and supervisor confirms their roles and grants permission for the use of the study's data and conclusions in this dissertation: "I declare that my role in this study, as indicated in Table 1.1, accurately reflects my actual contributions, and I consent to the publication of this work as part of the M.Sc. dissertation of Mr Charles Pretorius.

Dr Laneke Luies
(supervisor)

Mr Charles Pretorius
(M.Sc. candidate)

Table 1.1: Researchers involved in this study.

Co-author	Collaborator	Contribution
Mr Charles Pretorius (B.Sc. Hons. Biochemistry)		Conceptualised, planned, executed experiments (including the setup and partial validation of the acylcarnitine and 5-HIAA methods as well as the application of these methods on patient urine samples), analysed data, and wrote the dissertation and all associated documents and publications, together with the supervisor
Dr Laneke Luies (Ph.D. Biochemistry)		Supervisor: Conceptualised and co-ordinated all aspects of the study, including study design, planning, execution, writing of the dissertation and all associated documents
	The South African Tuberculosis Vaccine Initiative and the Desmond Tutu HIV Centre at the Institute of Infectious Disease and Molecular Medicine, University of Cape Town, Cape Town, South Africa	Collected and provided all urine samples and associated clinical information
	Centre for Human Metabolomics	Conducted the urine amino acid analysis of this study

CHAPTER 2: LITERATURE OVERVIEW

2.1. A basic understanding of HIV/AIDS

The HIV/acquired immune deficiency syndrome (AIDS) epidemic remains a global burden despite recent advances in prevention and treatment strategies. In 2022, an estimated 39 million people were living with HIV, contributing to about 630 000 deaths according to the most recent Joint United Nations Programme on HIV/AIDS statistics (UNAIDS, 2023). Historically, it is believed that HIV crossed species from non-human primates to humans during the 20th century. The virus gained global recognition in the early 1980s following reports of a group of young, previously healthy homosexual men (ages 29–33 years) presenting with symptoms of severe immune deficiency (Gottlieb *et al.*, 1981). Subsequent studies in the following years successfully isolated and identified HIV, firmly establishing it as the causative agent of AIDS (Barré-Sinoussi *et al.*, 1983; Gallo *et al.*, 1984; Levy *et al.*, 1984).

HIV is either classified as type 1 (HIV-1) or type 2 (HIV-2), which is speculated to have evolved from non-human primate immunodeficiency viruses from Central African chimpanzees (Gao *et al.*, 1999), and the West African sooty mangabeys, respectively (Hirsch *et al.*, 1989). There are various similarities between HIV-1 and HIV-2, which include their modes of transmission, intracellular mechanisms of replication, and both cause the host to have increased susceptibility to a similar variety of opportunistic infections. HIV-1, however, differs clinically from HIV-2 in that a more rapid immunological deterioration occurs in patients infected with HIV-1, and geographically in that HIV-1 infection has spread globally. On the other hand, HIV-2 infection mostly occurs in West African regions and European countries with socioeconomic links to these regions Therefore, all references in this dissertation to HIV implies HIV-1 due to its more severe pathological effect on the host and its far greater geographical spread (Nyamweya *et al.*, 2013).

HIV is a retrovirus which is distinguished from other viruses by the presence of ribonucleic acid (RNA) genome and reverse transcriptase enzymes in the subgroup known as lentiviruses, owing to its ability to infect non-dividing cells effectively, such as tissue macrophages (Chiu *et al.*, 1985; Liu & Berkhout, 2014). HIV transmission can occur when biofluids such as semen, blood, breast milk, or vaginal fluids infected with HIV enter another person's body. Subsequently, the virus can spread through target cells as a free viral particle or in a cell-associated form (Hübner *et al.*, 2009; Sourisseau *et al.*, 2007). Although HIV can infect macrophages as previously mentioned, its primary target is the cluster of differentiation 4 positive (CD4+) helper T lymphocytes (Klatzmann *et al.*, 1984). HIV fuses with CD4+ cells through binding with the viral spike protein complex (gp160), consisting of gp120 and gp41 proteins, followed by the association of the gp120 protein with the host cell chemokine receptors [C-C chemokine receptor 5 (CCR5) or C-X-C chemokine receptor 4] (Guilhaudis *et al.*, 2002). After fusion, single-strand RNA is reverse transcribed by a reverse transcriptase enzyme to synthesise HIV deoxyribonucleic acid (DNA), which is integrated into the host cell DNA by DNA integrase. The host cells' enzymes are then

utilised to transcribe integrated HIV DNA, and to synthesise and cleave viral proteins used to form mature virions. The mature virions are then released from the host cell and infect more cells (Craigie, 2012; Deeks *et al.*, 2015; Gilboa *et al.*, 1979).

HIV infection is well known to be associated with a progressive loss in CD4+ cells (Jaffar *et al.*, 1997). However, there remains uncertainty on the exact mechanism(s) by which CD4+ cell depletion occurs during HIV infection and several hypotheses have been formed to explain this occurrence, as reviewed by Le Hingrat *et al.* (2021). The previously explained fusion and replication of HIV can lead to the direct loss of the infected CD4+ cells via several mechanisms. This includes cytolysis induced by viral budding and/or syncytium formation, HIV-specific cytotoxic T lymphocyte-mediated death, and activation of caspase-3 and/or Bax in cells undergoing productive infection leading to apoptosis (Borrow *et al.*, 1994; Gandhi *et al.*, 1998; Laforge *et al.*, 2007; Leonard *et al.*, 1988; Petit *et al.*, 2002). The CD4+ cell loss, however, has been shown to significantly exceed the amount of infected CD4+ cells (Li *et al.*, 2005; Mattapallil *et al.*, 2005), which is most likely linked to: (i) bystander apoptosis initiated by viral proteins, such as gp120 inducing apoptosis in cells nearby after interacting with CD4 and chemokine receptors (Boirivant *et al.*, 1998; Estaquier *et al.*, 1994); (ii) immune activation leading to the synthesis of tumour necrosis factor (TNF)-receptors (FasL and Fas) by infected peripheral blood mononuclear cells (such as CD4+ cells) causing nearby uninfected CD4+ T cells to have increased susceptibility to activation-induced cell death (Estaquier *et al.*, 1995; Sloand *et al.*, 1997); (iii) abortive HIV infection leading to inflammasome-dependent caspase-1 activity resulting in an inflammatory form of cell death (pyroptosis) of CD4+ cells (Doitsh *et al.*, 2010); and (iv) capturing of CD4+ cells by neutrophil extracellular traps which are formed during HIV infection due to neutrophils becoming overwhelmed from the phagocytosis of translocated microbes (Sivanandham *et al.*, 2018).

CD4+ cells orchestrate a myriad of immune responses, mainly through the production and secretion of cytokines such as interleukin (IL)-10, IL-4, and IL-6 mediating the activity of immune cells, B-lymphocytes, and cytotoxic T (CD8+) cells (Estaquier *et al.*, 1995; Sofi *et al.*, 2009; Yang *et al.*, 2016; Yang *et al.*, 2017). It is therefore unsurprising that a progressive loss of CD4+ cells eventually lead to the immunological deterioration of HIV-infected patients. HIV infection can be classified into three stages, acute infection (2–4 weeks after infection the patient may experience flu-like symptoms and will have a severely high viral load), chronic infection (characterised by clinical latency where replication persists at a lower rate and most patients are asymptomatic), and AIDS (characterised by certain opportunistic infections and a CD4+ cell count <200 cells/mm^3 blood) (Hernandez-Vargas & Middleton, 2013). The gut-associated lymphoid tissue of the gastrointestinal (GI) tract is a vastly affected site during HIV infection due to a higher percentage of its CD4+ cells having increased expression of the CCR5 co-receptor (Anton *et al.*, 2000; Poles *et al.*, 2001). HIV can directly disrupt the mucosal epithelial barrier, leading to the translocation of bacteria and viruses. Mucosal epithelial cells of the GI tract respond to the translocated HIV envelope glycoproteins by upregulating inflammatory cytokines while microbial products from the GI tract can cause systemic immune activation (Brenchley

et al., 2006; Caradonna *et al.*, 2000; Nazli *et al.*, 2010). Therefore, the GI tract is a site that can significantly contribute to inflammation and systemic immune activation in HIV-infected patients.

The fourth-generation serum test, currently the gold standard for HIV diagnosis, represents a significant advancement in early detection. It can identify the HIV p24 antigen and antibodies against the virus, enabling detection approximately 14 days post-exposure — much sooner than antibody-only tests (Alexander, 2016). Early detection is crucial, as HIV viral replication and transmissibility are markedly increased during the early infection stage (Selik & Linley, 2018). In addition, this test distinguishes between HIV-1 and HIV-2, exhibiting high sensitivity and specificity, making it a pivotal tool in managing the HIV/AIDS pandemic (Alexander, 2016). For instance, Bio-rads' fourth-generation test, approved by the Food and Drug Administration in 2011, showed a 100% specificity and 99.9 to 100% sensitivity in a study involving 9150 patients (Bentsen *et al.*, 2011).

The clinical presentation of AIDS varies based on the types of opportunistic infections to which patients are exposed (Piot & Colebunders, 1987). Common presentations of AIDS include pneumocystis carinii pneumonia, toxoplasmosis, oesophageal candidiasis, and TB, contributing to HIV-associated morbidity and mortality (Jankowska *et al.*, 2001). Significant advances have, however, been made in the management of these opportunistic infections with anti-retroviral treatment (ART) resulting in an enhanced life expectancy of HIV patients (Johnson *et al.*, 2013; Zolopa *et al.*, 2009). There are currently six classes of ART, categorised based on their molecular mechanisms and resistance profiles. These classes include nucleoside-analogue reverse transcriptase inhibitors, non-nucleoside reverse transcriptase inhibitors, protease inhibitors, co-receptor (CCR5) antagonists, fusion inhibitors, and integrase strand transfer inhibitors (Arts & Hazuda, 2012).

There is currently no vaccine against HIV, as the development of a vaccine has been hampered by the virus' ability to effectively evade antibody neutralisation due to the conformational flexibility and metastability of the HIV envelope glycoproteins (gp120 and gp41), combined with its dynamic glycosylation states and genetic diversity (Gaschen *et al.*, 2002; Lopez Angel & Tomaras, 2020). As for a cure, the eradication of HIV in patients has proven to be near impossible, with the possible exceptions of two patients who have received bone allogeneic stem cell transplants of cells that do not express the CCR5 co-receptor, thereby preventing HIV cell infection and replication (Allers *et al.*, 2011; Gupta *et al.*, 2020). Unfortunately, multiple attempts using similar procedures were unsuccessful in curing HIV infection and the feasibility of this approach is limited due to the inadequate availability of CD4+ cells not expressing the CCR5 co-receptors with the requirement for human leukocyte antigen matching to assure that the stem cells are suitable for transplant (Kuritzkes, 2016; Zou *et al.*, 2013). The main barrier in the eradication of HIV, however, lies in the ability of the virus to latently infect resting CD4+ cells and macrophages. These cells carry an integrated copy of the HIV genome and are used as stable reservoirs (Chun *et al.*, 1995; Chun *et al.*, 1997; Embretson *et al.*, 1993). This is problematic as latently infected cells can persist even when viral replication is inhibited through ART (Finzi *et al.*, 1997).

Continued ART is essential in the management of HIV since, even after prolonged use of ART drugs, which can decrease the HIV viral load to undetectable levels, discontinued use of ART can result in the re-emergence of HIV (Chun *et al.*, 2010; Hermankova *et al.*, 2001). This, in turn, can lead to an increased risk of opportunistic infections, poor clinical outcomes, and death (Makunde *et al.*, 2012; Rachlis *et al.*, 2015). Drawbacks of continuous ART using drugs such as abacavir, may lead to cardiovascular diseases (Lang *et al.*, 2010), whereas tenofovir disoproxil fumarate can cause both renal dysfunction (Brennan *et al.*, 2011) and bone mineral density loss (Bedimo *et al.*, 2012). This contributes to serious non-AIDS events (SNAE) which are defined as clinical events excluded from the criterium of AIDS-defining events, such as psychiatric impairment, malignancies, cardiac events, hepatic and renal diseases, and bone disorders (Centers for Disease Control and Prevention, 1992). In contrast to the decreasing AIDS-related deaths, the occurrence of SNAE-related mortality and morbidity has increased in the ART era. However, this cannot only be attributed to ART toxicities as previously mentioned but is also related to HIV directly causing organ dysfunction, underlying co-infections and co-morbidities, coagulopathy, and inflammation relating to immune activation. A detailed discussion concerning SNAE and their aetiology is beyond the scope of this dissertation, however, several reviews discussing this topic have been published (Deeks *et al.*, 2013; Hsu & Sereti, 2016; Lang *et al.*, 2010; Masiá *et al.*, 2013).

2.2. A basic understanding of *Mtb*/TB

TB is an infectious disease caused by the bacillus *Mtb*. This bacterium can infect a myriad of organ systems, including the GI system, central nervous system (CNS), musculoskeletal system, reproductive system, and most frequently, the respiratory system (Mathiasen *et al.*, 2020; Mbuh *et al.*, 2019; Terracciano *et al.*, 2020). *Mtb* transmission occurs via inhalation of infectious aerosol particles released from close contacts, potentially leading to latent tuberculosis infection (LTBI). Patients with LTBI are asymptomatic and cannot transmit the disease. If the infection progresses, however, active TB can develop, and symptoms will show (Luies & Du Preez, 2020). The maintenance of LTBI, as well as the aetiology and mechanism of disease progression from LTBI to active TB, is not yet fully understood. Immune suppression, a major risk factor for active TB, can occur due to various reasons. These include people taking immunosuppressants for autoimmune diseases or organ transplants (Keane & Bresnihan, 2008; Sidhu *et al.*, 2014), having diabetes mellitus (Jeon & Murray, 2008), and most notably, HIV infection (Selwyn *et al.*, 1989).

During initial infection, the host's innate immune system elicits a response that results in the phagocytosis of *Mtb* by phagocytes such as dendritic cells, neutrophils, and macrophages (De Martino *et al.*, 2019; Weiss & Schaible, 2015). Generally, this phagocytosis leads to the fusion of the phagosomes of the phagocytes with their lysosomes, forming what is known as phagolysosomes. This process (phagosome maturation) is inhibited by *Mtb*, as it modifies the phagosomal environment to support bacterial survival inside macrophages. This inhibition of phagosome maturation is achieved by the reduction of phagosome-lysosome fusion (Armstrong & Hart, 1971), phagosomal acidification (Barker

et al., 1997), and the acquisition of lysosomal markers and characteristics by the phagosome (Clemens & Horwitz, 1995; Xu *et al.*, 1994). Following the interaction of *Mtb* with macrophages and dendritic cells, inflammation is initiated by the release of pro-inflammatory cytokines such as IL-12 and TNF-α (Kassa *et al.*, 2016). If the macrophage fails to eliminate the *Mtb*, the bacteria will continue to multiply within the macrophage (Cambier *et al.*, 2014). This results in the recruitment of monocytes to the site of infection to contain the bacteria (Muller & Randolph, 1999) and eventually leads to granuloma formation in the lungs (De Martino *et al.*, 2019). Granulomas are organised, compact immunological structures constituting macrophages, multinucleated giant cells, and epithelioid immune cells. These immune cells are each surrounded by a layer of T lymphocytes, forming part of the initial response to *Mtb*. As such, granulomas are described as a pathological hallmark of TB (Ndlovu & Marakalala, 2016; Silva Miranda *et al.*, 2012). The role of these tuberculous granulomas in the host-pathogen relationship remains controversial. Granulomas were initially presumed to primarily function as a host-protective structure. For example, an early study using mouse models showed that the containment of *Mtb* in the pulmonary granuloma correlated with increased life span, delayed disease progression and a capacity to sustain much higher bacterial loads as it prevented necrotising interstitial pneumonitis from occurring (Davis & Ramakrishnan, 2009; Pagán & Ramakrishnan, 2015). More recently, however, the view of the granuloma as a host-protective structure has shifted to a host- and pathogen-protective structure. Davis and Ramakrishnan (2009) showed that mycobacteria can enhance the recruitment of new macrophages to nascent granulomas wherein their motility is increased. This, in turn, enhances the phagocytosis of infected apoptotic macrophages leading to increased infected macrophages. After departing from the granuloma, macrophages facilitate haematogenous dissemination, which allows the bacteria to infect other sites and subsequently leads to the formation of secondary granulomas. Mycobacteria have also been shown to enhance granuloma formation through the secretion of region of difference 1 (RD1) products in a study using a zebrafish model wherein granuloma formation failed to occur after infection with RD1-deficient mycobacteria (Volkman *et al.*, 2004). These are merely a few examples of the growing body of evidence supporting the view that the granuloma also serves as a pathogen-protective structure, which could play a pivotal role in the maintenance of LTBI by improving the survival of both the host and pathogen.

If the *Mtb* infection progresses and the host develops active pulmonary TB, the clinical manifestations commonly include chronic cough, coughing up blood (haemoptysis), fever, loss of appetite, weight loss (cachexia) and night sweats (Loddenkemper *et al.*, 2016). Death usually occurs due to septic shock, TB-related cachexia, respiratory failure, and haemoptysis if the host fails to recover from the infection and disease progression is severe enough (Fløe *et al.*, 2018; Lin *et al.*, 2014; Seyed Mohammad & Nejad, 2008). Cachexia is defined as a complex metabolic syndrome characterised by muscle atrophy with or without loss of fat tissue associated with an underlying illness (Evans *et al.*, 2008). This is considered a clinical hallmark of pulmonary TB (Luies & Du Preez, 2020). It is estimated that 1.4 million HIV-negative people and an additional 187 000 HIV-positive people died as a result of TB globally in 2021 (Falzon *et al.*, 2023). TB is, however, a curable disease through treatment regimens generally consisting

of a combination of antibiotics such as isoniazid, rifampin, ethambutol, and pyrazinamide. Notwithstanding these treatment regimens, TB remains a global health problem, especially in developing countries such as India, Indonesia and South Africa, which the World Health Organization (WHO) has classified as high TB burden countries (World Health Organization, 2021). This can be attributed to multiple barriers hampering the successful treatment of TB in these countries. These include a lack of knowledge and the perception of TB health care and treatment; logistical complications such as long distances to health care and/or lack of transport; household income loss; stigmatisation from the general community, family, and health care operatives; and unfavourable drug reactions (Pradipta *et al.*, 2021). The resulting treatment failure serves as a high-risk factor for multi-drug resistant TB (MDR-TB) (Mulu *et al.*, 2015), which is defined as *Mtb* resistant to isoniazid and rifampin. MDR-TB is one of the main reasons TB has such a high mortality rate (Seung *et al.*, 2015). Unfortunately, even after successful treatment, TB-related morbidity does not necessarily end, as treated patients can be left with significant long-term health issues such as chronic obstructive airway disease, fibrosis and bronchiectasis (Meghji *et al.*, 2016; Willcox & Ferguson, 1989).

Regarding the prevention of TB, the Bacillus Calmette-Guérin (BCG) vaccine is currently the sole TB vaccine in general use. Although this vaccine has a high efficacy against TB in infants, its efficacy against pulmonary TB in adults remains inconsistent (Abubakar *et al.*, 2013). This inconsistency may be linked to variability in the BCG strain used for vaccination and exposure to mycobacteria that are not *Mtb*, leading to either masking or blocking. This is supported by a study using a mouse model which suggested that there are differences in the immunogenicity of different BCG strains and that these differences could cause variable efficacy in the BCG vaccine. The possible masking effect of the BCG vaccine is supported by studies performed in London and Malawi where the subjects from London showed a stronger immunological response to the BCG vaccine compared to the subjects from Malawi, which may be related to the Malawi subjects being more desensitised to the vaccine from exposure to environmental mycobacteria (Black *et al.*, 2002). The blocking effect hypothesis is supported by a study using a mouse model which suggests that immunity required from certain environmental mycobacterium inhibits the multiplication of the BCG vaccine required for vaccine efficacy (Brandt *et al.*, 2002).

Another important contributor to the persistence and resurgence of the TB pandemic is the HIV/AIDS pandemic, which has not only led to an increase in disease progression, susceptibility, and severity of the TB disease in HIV-infected patients, but also to complications in the management of the TB pandemic by affecting the treatment, prevention, and diagnosis of TB.

2.3. The HIV/TB syndemic

The resurgence of TB in the United States of America (USA) from the mid-1980s, after a period of decline from the 1950s to the early 1980s, was primarily attributed to the emergence of HIV (Gottlieb *et al.*, 1981). Other contributing factors to this resurgence included the rise of MDR-TB, migration from Asia to the USA, reduced resources for TB prevention and eradication efforts, and non-adherence to

prescribed drug regimens by patients (Hellman & Gram, 1993). A meta-analysis conducted by Sultana *et al.* (2021) that included a total of 54 studies observed an increased risk of MDR-TB within HIV-infected individuals. The duration of MDR-TB treatment regimens is around three-fold higher than that of TB due to their weak sterilizing activity, with MDR-TB treatment regimens lasting 18–24 months (Seung *et al.*, 2015) compared to the six-month duration of non-multidrug resistant TB treatment regimens (World Health Organization, 2021). This increased risk of MDR-TB in HIV-infected people and the subsequently increased duration of treatment needed to eradicate the mycobacterium demonstrates how HIV contributes to the perseverance of TB.

HIV-infected people are estimated to be 20 times more likely than HIV-seronegative people to develop active TB in high-burden settings (World Health Organization, 2013). This increased susceptibility HIV-infected people have to TB can be attributed to the loss of Th1-polarised CD4+ cells. This is largely due to these cells being a primary source of interferon-gamma (IFN-λ), an activator of macrophages capable of overcoming the ability of *Mtb* to inhibit phagolysosome formation (possibly through stimulation of the autophagic pathway) and kill it via nitric oxide-induced apoptosis (Herbst *et al.*, 2011; Kumar, 2017). CD4+ cells also assist in controlling *Mtb* infection by hampering CD8+ cell exhaustion and enhancing these cells' effector functions (Lu *et al.*, 2021). It is therefore unsurprising that lower CD4+ counts, which occur in HIV-infected people, are linked to more severe clinical presentations such as fever and weight loss (Schutz *et al.*, 2010).

The synergistic relationship between HIV and TB can be described as bidirectional, meaning that TB also contributes to the pathogenesis of AIDS in HIV-infected people as these patients have been reported to progress to AIDS faster than those without co-infections (Ganji *et al.*, 2016). This synergistic effect of TB on HIV infection can be attributed to several molecular mechanisms resulting in the enhanced replication and growth of HIV in *Mtb*-infected hosts. This includes the upregulation of the host's immune response through T cell activation, linked to the increased expression of the CCR5 co-receptors on *Mtb*-specific CD4+ cells, resulting in enhanced entry of HIV into these CD4+ cells (Geldmacher *et al.*, 2010). Furthermore, in *Mtb*-infected cells, increased expression of transcription factors (such as the nuclear factor of activated T cells 5 and nuclear factor-κB) occurs, which promotes transcription of HIV through binding with the HIV-1 long terminal repeat, serving as a promotor region for the transcription of the HIV genome (Falvo *et al.*, 2011; Ranjbar *et al.*, 2012).

The HIV pandemic complicates TB prevention through the BCG vaccine. Gasper *et al.* (2017) found that administering BCG to infants increases their susceptibility duration to HIV infection, as evidenced by a rise in activated CD4+ cells targeted by HIV. While BCG, derived from *Mycobacterium bovis*, is generally harmless, it can cause disseminated BCG infection, potentially affecting bones, lymph nodes, liver, joints, and spleen. This condition is primarily fatal and occurs mainly in immunocompromised infants, such as those with HIV, who have received the BCG vaccine (Han *et al.*, 2000; Ong *et al.*, 2020). Therefore, the WHO advises against administering the BCG to vaccine to children with

symptomatic HIV infection (World Health Organization, 2007). Furthermore, HIV infection has been shown to reduce the BCG vaccine's efficacy against extrapulmonary TB (Arbeláez *et al.*, 2000).

Mtb infection is mostly detected by examining sputum for acid-fast bacilli through microbiological culture-based methods. The sensitivity of smear microscopy has been shown to be decreased in patients co-infected with HIV due to decreased density of *Mtb* present within their sputum (Mugusi *et al.*, 2006). This decreased sensitivity has not only been observed in co-infected patients with low CD4+ cell counts but also in patients with CD4+ cell counts greater than 500, which highlights the detrimental effect HIV-seroconversion has on the immune response against *Mtb* (Gupta *et al.*, 2013; Ngabonziza *et al.*, 2016). TB diagnosis is further complicated in co-infected patients due to these patients often being unable to provide a sufficient amount of sputum for *Mtb* detection, especially in those with severe immune destruction (World Health Organization, 2015). Inaccurate diagnosis of LTBI is also common in HIV-infected individuals. LTBI is diagnosed by either the tuberculin skin test or an IFN- λ release assay (Carranza *et al.*, 2020). Limitations to these diagnostic methods include the increased false-negative or indeterminate results obtained in patients with a low CD4+ cell count, as is commonly the case with HIV-infected patients (Oliveira *et al.*, 2017; Sawhney & Sharma, 2006). This is problematic since TB disease prevention by LTBI screening and treatment, along with antiretroviral therapy (ART) initiation, are key components in the management of HIV-infected patients (Bares & Swindells, 2020).

Although ART initiation has proven to decrease TB incidence at a population and individual level, the incident rates of TB in HIV-infected individuals and the risk of TB-related mortality remain elevated in these individuals (Lawn *et al.*, 2006). In addition, drug-to-drug interactions, increased TB-immune reconstitution inflammatory syndrome (IRIS) occurrence, and drug toxicity present complications in terms of TB treatment in HIV patients (Shankar *et al.*, 2014). These can result in high discontinuation of treatment rates for either TB or HIV, consequently having to re-introduce drugs through a difficult and prolonged process which could increase mortality and morbidity due to the delay in treatment (Schutz *et al.*, 2010).

In addition, a novel complication to this syndemic has emerged. Years of progress in the provision of essential TB and HIV services and the attenuation of the burden of these diseases have been undone by the COVID-19 pandemic. Most notably, there has been a colossal global reduction in the number of patients newly diagnosed and reported with TB. Furthermore, the COVID-19 pandemic has hampered HIV treatment and research while less access to diagnosis and treatment facilities for TB has led to an increase in the number of TB-related deaths (Chenneville *et al.*, 2020; World Health Organization, 2021). In 2020, a multiple model projection based on the setting of the COVID-19 pandemic predicted HIV- and TB-related deaths to increase in high-burden settings such as South Africa by an estimated 10% and 20%, respectively, by the year 2025 (McQuaid *et al.*, 2020). This predicted rise is supposedly due in part to the diminished diagnostic and treatment capacities during the pandemic.

2.4. Metabolomics as a prospect for investigating the HIV/TB syndemic

Metabolomics, the study of metabolite composition of cells, tissues, or biofluids, presents an appealing approach for enhancing our understanding and characterisation of the intricate metabolic alterations induced by HIV/TB co-infection. Metabolomics methodologies are typically described as either untargeted or targeted. Untargeted metabolomic analysis provides a comprehensive overview of all the measurable small molecular compounds, known and unknown, in a sample, while targeted metabolomics focuses on specific, chemically characterised and annotated metabolites (Roberts *et al.*, 2012). Metabolites can be recognised as immediate disease markers in some instances, such as for the diagnosis of inborn metabolic disorders, making metabolomics a powerful tool (Gowda *et al.*, 2008). Metabolite abundances in biological specimens often directly correlates with pathogenic mechanisms, reflecting an organism's phenotype over time, serving as downstream indicators of proteomic, transcriptomic, and genomic expressions (Alonso *et al.*, 2015; Gerszten & Wang, 2008). Analysing differences in metabolic pathways can reveal underlying disease mechanisms. If potential specific disease-related metabolic markers are identified (typically in an untargeted manner), the design of specific assays becomes straightforward (in a targeted approach). These targeted assays are cost-effective, simple, and offer high specificity and sensitivity (Yoshida *et al.*, 2012). Molecular disease markers can eventually serve as efficacy markers during drug development, treatment monitoring, and disease progression assessment (Clish, 2015). While current clinical application of metabolomics in infectious disease diagnosis is limited, primarily to inborn metabolic disorders, its potential in guiding the adaptation of existing methods or leading to the development of new diagnostic techniques is significant. Metabolomics holds the potential to assist in the development of improved diagnostic techniques and treatment strategies for TB (Luies *et al.*, 2017) and associated adverse effects, and enable early interventions, ultimately reducing mortality and morbidity in co-infected patients (De Villiers & Loots, 2013).

While multiple studies have investigated the metabolic profiles of individuals with HIV (Peltenburg *et al.*, 2018; Williams *et al.*, 2012) or TB (Luies & Loots, 2016; Zhou *et al.*, 2013), proving metabolomics as a useful tool in understanding these diseases, research on the co-infected state remains limited. Silva *et al.* (2019) analysed HIV/TB and HIV/TB-IRIS cohorts to identify distinguishing metabolites, aiding in TB-IRIS diagnosis. Additionally, two studies investigated indolamine 2,3-dioxygenase 1 (IDO1) activity by measuring plasma tryptophan and kynurenine levels. Both studies observed decreased tryptophan levels and increased kynurenine levels in HIV/TB co-infection compared to TB infection alone, strongly suggesting increased IDO1 activity in the co-infected state (Adu-Gyamfi *et al.*, 2017; Collins *et al.*, 2020). IDO1 catalyses tryptophan in the first and rate-limiting step of kynurenine formation, influencing the immune response through multiple mechanisms (Zhai *et al.*, 2019), including tryptophan depletion, modulation of CD4+ T cell responses, induction of immune tolerance, and inflammation control (Johnson *et al.*, 2013; Silva *et al.*, 2002; Zhang *et al.*, 2013). Increased IDO1 activity has proven ineffective against HIV and *Mtb* infection. This may be due to mycobacteria's ability

to synthesise tryptophan *de novo*, making them less affected by tryptophan depletion resulting from increased IDO1 activity. Furthermore, it could lead to increased host tolerance to *Mtb* through enhanced tryptophan catabolism (Gautam *et al.*, 2018; Zhang & Rubin, 2013) and contribute to disease severity in HIV patients due to its immunosuppressive effects, essentially caused by the inactivation of CD8+ cells targeting HIV-infected cells (Frumento *et al.*, 2002; Kandanearatchi & Brew, 2012; Mbongue *et al.*, 2015; Terness *et al.*, 2002; Wang *et al.*, 2019).

Silva *et al.* (2019) demonstrated that metabolomics can effectively distinguish HIV/TB co-infection from related disease states, such as HIV/TB-IRIS. Furthermore, Adu-Gyamfi *et al.* (2019) and Collins *et al.* (2020) found differences in the metabolomic profiles of individuals with HIV, TB, and the co-infected state. These comparisons were, however, limited to tryptophan and kynurenine levels in all three disease states. The first comprehensive metabolic characterisation of the HIV/TB co-infected state has only recently been published (Herbert *et al.*, 2023). In this untargeted study, the serum metabolic profiles were measured for healthy controls, untreated TB-positive, as well as treated and untreated HIV/TB co-infected patients. The study specifically compared the co-infected group to healthy controls, co-infected patients to TB-only cases, and treated co-infected patients to untreated co-infected individuals. It was observed that co-infection with HIV and *Mtb* primarily affected the amino acid and lipid metabolism. The key metabolic alterations, such as the elevated α-ketobutyric acid, proline, glycerol, and depleted hydroxyproline levels, were noted specifically when comparing the HIV/TB co-infected group to healthy controls were mainly attributed to a state of depleted energy levels and inflammation. Given the numerous barriers in eradicating HIV and TB, the impact of disease synergy on co-infected patients' clinical presentation, and the challenges in disease management, including diagnosis, treatment, and vaccination highlighted in this dissertation, it is imperative to enhance our approach to managing the HIV/TB syndemic. Metabolomics presents an attractive tool for disease characterisation, offering insights into the pathophysiology of the co-infected state that could significantly improve syndemic management and, ultimately, contribute to eradication.

2.5. A Further look into tryptophan metabolism during HIV/TB co-infection

Tryptophan serves as a precursor for kynurenine and is also the exclusive precursor in the synthesis of serotonin through the serotonin pathway. In this pathway, tryptophan initially undergoes conversion to L-5-hydroxytryptophan, catalysed by tryptophan hydroxylase 1 or 2, which is subsequently transformed into serotonin by L-amino acid decarboxylase (Roth *et al.*, 2021). The liver plays a significant role in removing serotonin from the plasma, where it undergoes conversion into 5-hydroxyindole acetaldehyde and subsequently into 5-HIAA through the actions of monoamine oxidase and aldehyde dehydrogenase, respectively (Figure 2.1). This resulting 5-HIAA is excreted in urine and serves as the primary urinary metabolite for serotonin. As such, in clinical chemistry, urinary 5-HIAA levels are routinely measured for the diagnosis and monitoring of carcinoid tumours, which secrete an excess of serotonin (Clark *et al.*, 2017; Kema *et al.*, 2000). In humans, approximately 90% of serotonin is synthesised in the

enterochromaffin cells of the GI tract, while an estimated 10% originates from serotonergic neurons within the CNS (Roth *et al.*, 2021). Beyond its role as a neurotransmitter in the CNS, serotonin also functions as a blood factor and neurohormone that regulates the function of various peripheral organs and systems (De Deurwaerdère & Di Giovanni, 2020).

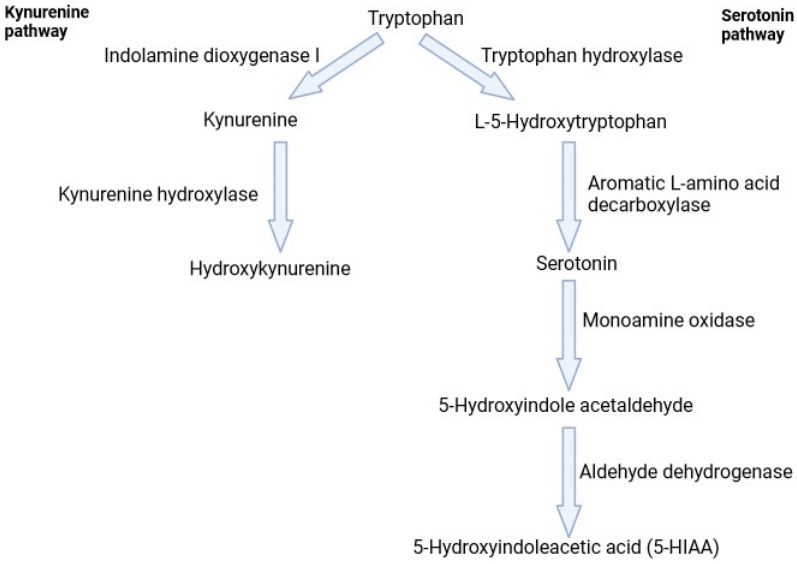

Figure 2.1: Tryptophan metabolism in HIV/TB co-infection. *This figure provides a simplified illustration of tryptophan metabolism, highlighting two key pathways: the synthesis of kynurenine and its derivative, 3-hydroxykynurenine, via the kynurenine pathway, and the formation of serotonin and its primary marker in urine, 5-hydroxyindoleacetic acid, via the serotonin pathway. This underscores the dual role of tryptophan as a precursor in both pathways and demonstrates the metabolic processes leading to the production of these significant metabolites. The diagram also emphasizes the clinical relevance of 5-hydroxyindoleacetic acid as a diagnostic marker in urine. Created by Biorender.com and adapted from Höglund et al. (2019).*

In contrast to the well-studied kynurenine pathway, the serotonin pathway has received less attention in individuals infected with HIV and *Mtb*. Brain serotonin pathway activity is well known to decrease with low tryptophan intake or availability (Van Donkelaar *et al.*, 2011). Similarly, this activity has been shown to decrease on a systemic level as indicated by reduction of blood and urine 5-HIAA levels in patients with diarrhoea and healthy subjects after acute tryptophan depletion (Chojnacki *et al.*, 2022; Honig *et al.*, 2004). A study conducted on the striatum (a brain structure) of pigtailed macaques infected with simian immunodeficiency virus (like HIV) revealed a significant loss of serotonin during acute and chronic infection, along with enhanced kynurenine activity. Even after treatment with ART, these altered metabolite concentrations did not fully return to their nominal values (Drewes *et al.*, 2015). Targeted studies have also indicated that serotonin levels are significantly reduced in the plasma of untreated HIV-infected patients (Peltenburg *et al.*, 2018), and in the serum of patients with active TB (Cho *et al.*, 2020). Additionally, Collins *et al.* (2020) reported a significant increase in plasma 5-HIAA concentrations in TB patients after treatment, although 5-HIAA levels in untreated patients with active TB did not significantly differ from the control group. These studies collectively suggest that serotonin synthesis can be disrupted, potentially due to tryptophan depletion resulting from enhanced kynurenine

pathway activation. Furthermore, it has already been demonstrated that kynurenine pathway activity is increased to a greater extent in the context of HIV/TB co-infection compared to HIV and *Mtb* infection alone (Adu-Gyamfi *et al.*, 2019; Collins *et al.*, 2020). However, it remains unclear whether this phenomenon leads to further decreases in serotonin levels in individuals with HIV/TB co-infection.

2.6. Amino acids during pathogenic infections

Amino acids are the fundamental building blocks of proteins. Of the numerous amino acids found in the human body, approximately 20 are traditionally classified as either "essential" or "non-essential". Essential amino acids are less efficiently synthesised from metabolic intermediates, making them vital for dietary intake (Hou & Wu, 2018; Hou *et al.*, 2015). Amino acids are pivotal in the context of infectious diseases due to their various immunological functions. These include activating immune cells such as T lymphocytes, B lymphocytes, macrophages, and natural killer cells, regulating cellular redox state, gene expression and lymphocyte proliferation, synthesising cytotoxic substances and antibodies, and modulating inflammatory responses (Grohmann & Bronte, 2010; Tomé, 2021). Furthermore, amino acid metabolism directly combats viral and bacterial infections. For example, phenylalanine catabolism by the interleukin 4-inducible 1 enzyme generates phenylpyruvate and peroxide, which has antimicrobial effects. When amino acid levels are low, it triggers the activation of general control nonderepressible 2 kinase, an enzyme known to inhibit the replication of RNA viruses such as the dengue virus and HIV (Afroz *et al.*, 2020; Del Pino *et al.*, 2012).

Apart from their roles as protein building blocks and immune system regulators, amino acids regulate various other functions in the human body, as reviewed by (Wu, 2013) and (Wu, 2010). Notably, in the context of pathogenic infections, amino acids play a crucial role in nutrient and energy metabolism. This is because the immune response demands increased energy while infections can lead to reduced nutrient intake related to a loss of appetite (Exton, 1997; Rao *et al.*, 2017; Yang *et al.*, 2021). As a result, amino acids like glutamine and alanine can serve as alternative sources for the tricarboxylic acid (TCA) cycle or gluconeogenesis, ultimately contributing to energy production in immune cells (Newsholme & Newsholme, 1989; Newsholme *et al.*, 2003; Wu *et al.*, 1991). The significance of amino acids lies in their ability to provide insights into the pathophysiological state of individuals with infections. This is due to their pivotal role in regulating the host's immune system and their connection to altered energy and nutrient balances resulting from infection, which can affect systemic amino acid levels.

2.6.1. Amino acid metabolism within HIV-infected and TB patients

Numerous studies have examined the systemic metabolic profiles of individuals with HIV-only and *Mtb*-only infections, with a focus on serum (Sitole *et al.*, 2019; Weiner *et al.*, 2012; Zhou *et al.*, 2013), plasma (Ding *et al.*, 2020; Li *et al.*, 2018; Peltenburg *et al.*, 2018), and to a lesser extent, urine (Luies & Loots, 2016; Munshi *et al.*, 2013). These investigations have revealed various perturbations in amino acid metabolism, as summarised in Tables 2.1, 2.2 and 2.3. These investigations, represented in

Tables 2.1, 2.2 and 2.3, are examples of studies that have identified significant alterations in amino acids at the systemic level. For this, online resources such as ScienceDirect and PubMed were used to search for articles including key words like amino acids, TB, and HIV. Inclusion criteria included studies published after 2010 which compared TB-only or HIV-only with healthy controls. These metabolic disruptions are primarily attributed to the host's immune response to infection and the body's efforts to sustain energy metabolism during illness. Cachexia, a persistent feature of HIV, TB, and co-infection (Chang *et al.*, 2013; Siddiqui *et al.*, 2009; Siddiqui *et al.*, 2022), is characterised by altered metabolism due to infection and malnutrition (see Section 2.2) (Ding *et al.*, 2020; Gelato *et al.*, 2007; MacAllan *et al.*, 1998; Sashindran & Thakur, 2020). However, the underlying causes of cachexia in HIV and TB patients may vary, with HIV-associated cachexia more linked to GI malabsorption, potentially stemming from the depletion of CD4+ cells in the GI tract (see Section 2.1) (Brenchley & Douek, 2008; Clay & Crutchley, 2014; Paton *et al.*, 1999). On the other hand, TB related cachexia seems to stem from the acute inflammatory response from the infection with *Mtb* (Luies & Du Preez, 2020; Schwenk & Macallan, 2000; Wanke, 2004).

Table 2.1: Perturbed systemic amino acid levels in untreated HIV-infected individuals compared to healthy controls.

Compound	Directionality*	Analytical platform utilised#	Matrices and references
Alanine	↓ ↓	LC-MS NMR	Plasma (Peltenburg *et al.*, 2018) Urine (Munshi *et al.*, 2013)
Glutamate/glutamic acid	↑ ↑ ↑	NMR and GC-MS NMR MS/MS	Serum (Sitole *et al.*, 2019) Urine (Munshi *et al.*, 2013) Plasma (Scarpelini *et al.*, 2016)
Tryptophan	↓ ↓ ↓	GC-MS LC-MS/GC-MS LC-MS	Serum (Sitole *et al.*, 2019) Plasma (Li *et al.*, 2018) Plasma (Peltenburg *et al.*, 2018)
Phenylalanine	↑	NMR and GC-MS	Serum (Sitole *et al.*, 2019)
Methionine	↓	LC-MS	Plasma (Peltenburg *et al.*, 2018)
Tyrosine	↓ ↓	LC-MS GC-MS	Plasma (Peltenburg *et al.*, 2018) Serum (Sitole *et al.*, 2019)
Histidine	↓	LC-MS/GC-MS	Plasma (Li *et al.*, 2018)
Asparagine	↓	LC-MS	Plasma (Peltenburg *et al.*, 2018)
Aspartate/aspartic acid	↑ ↑	GC-MS MS/MS	Serum (Sitole *et al.*, 2019) Plasma (Scarpelini *et al.*, 2016)
Lysine	↓	NMR	Plasma (Munshi *et al.*, 2013)

**Directionality indicates the untreated HIV-infected individuals compared to the healthy controls.*

#For studies where the specific analytical platform was not explicitly mentioned, a "/" is used to indicate that either LC-MS or GC-MS could have been utilised.

Abbreviations: GC-MS: gas chromatography-mass spectrometry; LC-MS: Liquid chromatography-mass spectrometry; MS/MS: tandem mass spectrometry; NMR: nuclear magnetic resonance.

Table 2.2: Perturbed systemic amino acid levels in treated HIV patients compared to healthy controls.

Compound	Directionality*	Analytical platform utilised#	Matrices and references
Alanine	↓ ↓	LC-MS NMR	Plasma (Peltenburg *et al.*, 2018) Urine (Munshi *et al.*, 2013)
Glutamate/Glutamic acid	↑ ↑ ↑	NMR and GC-MS MS/MS NMR	Serum (Sitole *et al.*, 2019) Plasma (Scarpelini *et al.*, 2016) Urine (Munshi *et al.*, 2013)
Tryptophan	↓ ↓	GC-MS LC-MS/GC-MS	Serum (Sitole *et al.*, 2019) Plasma (Li *et al.*, 2018)
Phenylalanine	↑	NMR and GC-MS	Serum (Sitole *et al.*, 2019)
Methionine	↓	LC-MS	Plasma (Peltenburg *et al.*, 2018)
Tyrosine	↑	GC-MS	Plasma (Sitole *et al.*, 2019)
Aspartic acid	↑ ↑	GC-MS MS/MS	Serum (Sitole *et al.*, 2019) Plasma (Scarpelini et al., 2016)
Lysine	↓	NMR	Plasma (Munshi *et al.*, 2013)

**Directionality indicates the HIV-infected individuals compared to the healthy controls.*

#For studies where the specific analytical platform was not explicitly mentioned, a "/" is used to indicate that either LC-MS or GC-MS could have been utilised.

Abbreviations: GC-MS: gas chromatography-mass spectrometry; LC-MS: Liquid chromatography-mass spectrometry; MS/MS: tandem mass spectrometry; NMR: nuclear magnetic resonance.

As previously mentioned, alanine and glutamine play essential roles in gluconeogenesis. Consequently, alanine levels have consistently been found to be significantly decreased in both *Mtb* (Weiner *et al.*, 2018; Zhou *et al.*, 2013) and HIV-infected (Munshi *et al.*, 2013; Peltenburg *et al.*, 2018) patients. On the other hand, glutamine tends to decrease mainly in TB patients (Cho *et al.*, 2020; Ding *et al.*, 2020; Vrieling *et al.*, 2018; Weiner *et al.*, 2012). However, Zhou *et al.* (2013) observed increased glutamine levels in TB patients, attributing this to increased proteolysis aimed at supplying the amino acids required for gluconeogenesis. Glutamine levels in HIV patients, in contrast, have shown less consistency, possibly due to variations in CD4+ cell counts (McKnight *et al.*, 2014). Inactive CD4+ cells may contribute to increased glutamine levels in TB patients, as observed by Zhou *et al.* (2013). The interplay between HIV infection, TB, and metabolic changes underscores the need to include HIV/TB co-infected individuals with known CD4+ cell counts in metabolic studies focused on TB alone, as it can ease the interpretation of results (Table 2.3).

Table 2.3: Perturbed systemic amino acid levels in Mtb-infected patients compared to healthy controls.

Compound	Directionality*	Analytical platform utilised#	Matrices and references	HIV participants excluded**
Alanine	↓	NMR	Serum (Zhou *et al.*, 2013)	No
	↓	NMR	Plasma (Vrieling *et al.*, 2018)	Yes
Glutamate/glutamic acid	↑	NMR	Serum (Zhou *et al.*, 2013)	Yes
	↑	LC-MS	Serum (Cho *et al.*, 2020)	Yes
	↑	LC-MS	Plasma (Ding *et al.*, 2020)	No
Glutamine	↑	NMR	Serum (Zhou *et al.*, 2013)	No
	↓	LC-MS/GC-MS	Serum (Weiner *et al.*, 2012)	Yes
	↓	LC-MS	Serum (Cho *et al.*, 2020)	Yes
	↓	NMR	Plasma (Vrieling *et al.*, 2018)	Yes
	↓	LC-MS	Plasma (Ding *et al.*, 2020)	No
Tryptophan	↓	LC-MS/GC-MS	Serum (Weiner *et al.*, 2012)	Yes
	↓	NMR	Plasma (Vrieling *et al.*, 2018)	Yes
	↓	LC-MS	Plasma (Collins *et al.*, 2020)	Yes
	↓	LC-MS	Plasma (Ding *et al.*, 2020)	No
Phenylalanine	↑	NMR	Serum (Zhou *et al.*, 2013)	No
	↑	NMR	Plasma (Vrieling *et al.*, 2018)	Yes
	↓	GC-MS	Serum (Che *et al.*, 2013)	Yes
	↓	LC-MS	Plasma (Ding *et al.*, 2020)	No
Tyrosine	↑	NMR	Serum (Zhou *et al.*, 2013)	No
Histidine	↓	LC-MS/GC-MS	Serum (Weiner *et al.*, 2012)	Yes
	↓	NMR	Plasma (Vrieling *et al.*, 2018)	Yes
	↓	LC-MS	Plasma (Vrieling *et al.*, 2019)	Yes
	↓	LC-MS	Plasma (Ding *et al.*, 2020)	No
Arginine	↑	LC-MS	Plasma (Vrieling *et al.*, 2019)	Yes
Cysteine	↓	LC-MS/GC-MS	Serum (Weiner *et al.*, 2012)	Yes
	↓	LC-MS	Plasma (Ding *et al.*, 2020)	No
Methionine	↓	LC-MS	Serum (Cho *et al.*, 2020)	Yes
	↓	LC-MS	Plasma (Ding *et al.*, 2020)	No
Asparagine	↓	LC-MS	Serum (Cho *et al.*, 2020)	Yes
	↓	LC-MS	Plasma (Ding *et al.*, 2020)	No
Aspartate/Aspartic acid	↓	LC-MS	Plasma (Vrieling *et al.*, 2019)	Yes
	↑	LC-MS	Serum (Cho *et al.*, 2020)	Yes
	↑	LC-MS	Plasma (Ding *et al.*, 2020)	No
Lysine	↑	NMR	Serum (Zhou *et al.*, 2013)	No
	↓	LC-MS	Plasma (Ding *et al.*, 2020)	No
Glycine	↓	NMR	Serum (Zhou *et al.*, 2013)	No
Leucine	↓	LC-MS	Plasma (Ding *et al.*, 2020)	No
Isoleucine	↑	NMR	Serum (Zhou *et al.*, 2013)	No
Threonine	↓	LC-MS	Plasma (Ding *et al.*, 2020)	No

**Directionality indicates the Mtb-infected individuals compared to the healthy controls.*

***Studies where the TB-positive groups were tested for HIV for exclusion are indicated as "Yes".*

Abbreviations: GC-MS: gas chromatography mass-spectrometry; LC-MS: Liquid chromatography-mass spectrometry; MS/MS: tandem mass spectrometry; NMR: nuclear magnetic resonance.

The literature consistently reports elevated glutamate in both HIV-infected and TB patients, often accompanied by a decreased glutamine/glutamate ratio in TB patients (Cho *et al.*, 2020; Ding *et al.*, 2020; Scarpelini *et al.*, 2016; Sitole *et al.*, 2019; Zhou *et al.*, 2013). *Mtb* is suggested to convert glutamine to glutamate to maintain cellular pH and for redox balance, potentially explaining increased glutamate levels in TB patients (Cho *et al.*, 2020). In HIV-infected patients, increased glutamate levels, along with elevated cysteine concentrations, may be linked to oxidative stress and/or the onset of HIV-related neurological conditions (Sitole *et al.*, 2019). Moreover, both HIV-infected and TB patients consistently exhibit decreased levels of amino acids involved in pro- and anti-inflammatory responses, specifically tryptophan and histidine, due to chronic inflammation characteristic of these infections (Li *et al.*, 2018; Sitole *et al.*, 2019; Weiner *et al.*, 2018). Tryptophan degradation by the kynurenine pathway suppresses hyperinflammation by reducing the formation of highly inflammatory Th17 cells (Favre *et al.*, 2010). Histidine serves as a precursor for histamine which contributes to pro- and anti-inflammatory reactions by interacting with histamine receptors, influencing the synthesis and secretion of inflammatory mediators and cytokines (Branco *et al.*, 2018; Huang *et al.*, 2018).

Methionine has been observed to be decreased in both HIV (Munshi *et al.*, 2013; Peltenburg *et al.*, 2018), and *Mtb*-infected patients (Cho *et al.*, 2020; Ding *et al.*, 2020). In TB patients, this decline may be linked to increased glutathione synthesis, as the glutathione substrate, cysteine, derived from methionine, has also been found to be lower in individuals with active TB (Ding *et al.*, 2020; Weiner *et al.*, 2012). This could be due to the glutathione recycling, supported by decreased 5-oxyproline in active TB patients, an important component in the gamma-glutamyl cycle related to glutathione recycling (Che *et al.*, 2018). Glutathione, a vital antioxidant, is synthesised throughout the body and present in most cells (Kerksick & Willoughby, 2005). The disrupted glutathione recycling may indicate decreased antioxidant capacity in individuals with active TB (Liebenberg *et al.*, 2021). Altered amino acid metabolism in HIV-infected individuals may also affect lipid metabolism, as studies have demonstrated negative correlations between plasma lysine and total L-carnitine with viral loads in HIV-infected patients (Butorov, 2017).

2.7. Acylcarnitine perturbations during HIV and *Mtb* infection

Acylcarnitines are acyl-CoA molecules, essentially activated fatty acids, conjugated with L-carnitine to facilitate their transport into the mitochondrial matrix. This process is part of the carnitine shuttle (Figure 2.2), which plays a pivotal role in cellular fatty acid catabolism through β-oxidation. The carnitine shuttle is a complex, multi-step process that starts with carnitine palmitoyltransferase I, which couples long-chain fatty acid-CoAs with L-carnitine, leading to the formation of acylcarnitine derivatives. These acylcarnitines are then transported from the cytosol to the intermembrane space of the mitochondrion. Carnitine-acylcarnitine translocase facilitates their transport through the inner mitochondrial membrane and into the matrix, in exchange for L-carnitine being transported out of the matrix. Finally, within the mitochondrial matrix, acylcarnitines are converted back into their acyl-CoA

counterparts by carnitine palmitoyltransferase II, ultimately undergoing β-oxidation to generate short-chain acetyl-CoAs (Melone *et al.*, 2018; Qu *et al.*, 2016; Schooneman *et al.*, 2013).

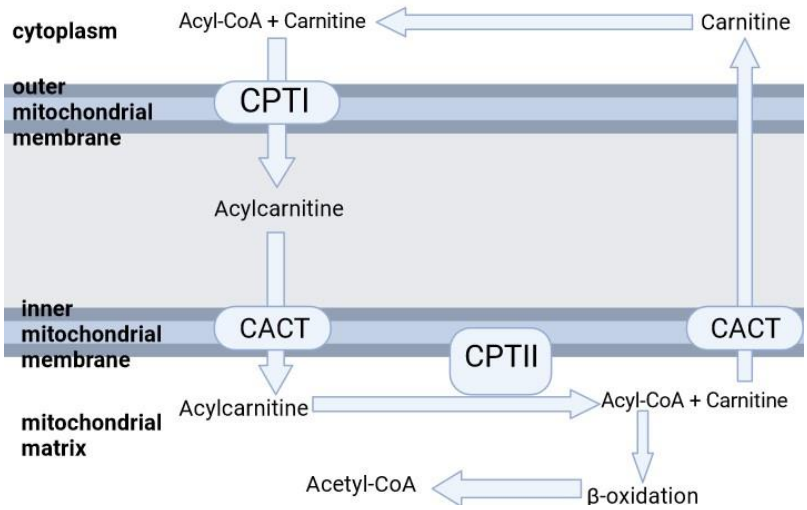

Figure 2.2: The carnitine shuttle in cellular fatty acid metabolism. *The diagram illustrates the steps involved in transporting activated fatty acids (acyl-CoA molecules) into the mitochondrial matrix for β-oxidation. Key enzymes and components are depicted, including carnitine palmitoyltransferase I and II, which catalyse the conjugation and reconversion of acyl-CoAs with L-carnitine. The shuttle's role in generating acetyl-CoAs, crucial for energy production in cells, is also highlighted.Created by Biorender.com and adapted from (Qu et al., 2016). Abbreviations: CPTI: carnitine palmitoyltransferase I; CACT: carnitine acylcarnitine transferase; CPTII: carnitine palmitoyltransferase II.*

Acylcarnitine analysis is a valuable tool for screening fatty acid oxidation disorders, including conditions like medium-chain L-3-ketoacyl-CoA dehydrogenase deficiency, carnitine palmitoyl-transferase I deficiency, and carnitine uptake defects. It provides insights into an individual's fatty acid β-oxidation status and can also indicate certain organic acid metabolism disorders (Rinaldo *et al.*, 2008). Interestingly, the carnitine shuttle is thought to be one of the most significantly altered metabolic pathways in TB patients, as revealed by an untargeted LC-MS study conducted on plasma (Phuoc Long *et al.*, 2022). Notably, L-carnitine deficiency has been shown to be prevalent in TB patients, with nearly half of the study population in Iran with TB presenting with such a deficiency (Hatamkhani *et al.*, 2013). Additionally, Che *et al.* (2018) found increased levels of long-, medium-, and short-chain acylcarnitines, coupled with decreased levels of long-chain free fatty acids in tuberculous pleural effusions when compared to malignant pleural effusions. This suggests that fatty acids are transported more rapidly for β-oxidation as their carnitine derivatives, resulting in lowered free fatty acid levels and increased acylcarnitine levels. This phenomenon could be attributed to increased fatty acid β-oxidation in TB patients, related to increased energy expenditure (Che *et al.*, 2018).

A similar trend emerges in HIV-infected individuals concerning their acylcarnitine profiles. Plasma samples from HIV immunological nonresponsive patients, who exhibit poor immunological recovery after ART initiation, showed increased levels of long- and medium-chain acylcarnitines (Qian *et al.*,

2021). Interestingly, these elevated acylcarnitines exhibited an inverse correlation with CD4+ cell count and could potentially serve as markers for evaluating and predicting CD4+ cell levels during long-term ART. This underscores how a metabolomics-based approach focusing on acylcarnitine analysis may enable disease progression monitoring and prediction in HIV-infected patients. Furthermore, increased levels of acylcarnitines and fatty acids in HIV-infected individuals, along with evidence of decreased lipid oxidation due to mitochondrial dysfunction, have been reported in other studies (Li *et al.*, 2018; Luies *et al.*, 2017; Scarpelini *et al.*, 2016).

Of significant note is that while both *Mtb*- and HIV-infected individuals exhibited increased levels of acylcarnitines in these studies, the underlying causes of this elevation appear to differ. TB patients displayed increased lipid oxidation, whereas HIV-infected individuals showed signs of decreased lipid oxidation. This difference was evident in the levels of fatty acids, where TB patients had reduced levels (precursors for lipid oxidation), and HIV-infected individuals had increased fatty acid levels (Che *et al.*, 2018; Li *et al.*, 2018). It remains unexplored whether disrupted lipid oxidation, as seen with HIV infection, combined with increased fatty acid transport as acylcarnitine derivatives, observed in *Mtb*-infected patients, would lead to even higher acylcarnitine levels in HIV/TB co-infected patients. Furthermore, the ability of *Mtb* to utilise fatty acids as an alternative carbon source, as highlighted in recent metabolomics research (Beukes *et al.*, 2023), suggests a potential mechanism by which *Mtb* infection could influence systemic metabolic profiles in TB patients. This aspect offers an intriguing area for further investigation, particularly in the context of HIV/TB co-infection.

2.8. Exploring the role of amino acid and acylcarnitine metabolism in the metabolic characterisation of HIV/TB co-infection

Amino acids play a fundamental role in regulating the host's immune system, while acylcarnitines support energy homeostasis during infection. Consequently, it is unsurprising that several altered amino acids and acylcarnitines have been identified in the context of HIV-only and *Mtb*-only, as discussed above. Amino acids, along with their metabolic derivatives like serotonin and 5-HIAA, as well as acylcarnitines, offer valuable insights into unique metabolic perturbations induced by the synergistic effect of these two infections in co-infected individuals. Targeted metabolomics, a previously successful approach for accurately identifying and quantitatively measuring systemic levels of amino acids, amino acid derivatives, and acylcarnitine levels in humans, emerges as an attractive method for addressing these uncertainties related to the metabolic profile of HIV/TB co-infection (Giesbertz *et al.*, 2015; Phipps *et al.*, 2020).

CHAPTER 3: METHODOLOGY

3.1. Introduction

As discussed in Section 2.6.1, urine has previously been employed to investigate the metabolome of individuals with HIV and *Mtb* infection, although not as extensively as serum and plasma. The advantages of using urine instead of serum or plasma include non-invasive collection, improved subject compliance without the need for preparation, reduced interferences from lipids and proteins, simple sample preparation, and its complex chemical matrix containing various hydrophilic compounds such as amino acids and carbohydrates (Bouatra *et al.*, 2013; Khamis *et al.*, 2017). Although urine is traditionally considered sterile (Bouatra *et al.*, 2013), subsequent studies have refuted this claim, demonstrating the presence of bacteria in healthy adult males and females (Kogan *et al.*, 2015; Wolfe & Brubaker, 2015). To address variation in sample volume, urine production, and dilution effects, creatinine normalisation is necessary for spot urine collection (Heymsfield *et al.*, 1983). This is achieved by dividing the concentration of the analytes of interest by the urinary creatinine concentration, as creatinine excretion is considered relatively stable under normal circumstances. However, the primary limitation of this method is that creatinine excretion rates may vary due to intra- and inter-individual differences. Timed urine collection methods, such as 24-hour urine collection, are alternatives but pose challenges in proper complete collection (Alessio *et al.*, 1985; Wagner *et al.*, 2010). Furthermore, urinary metabolite concentrations are more sensitive to changes due to acute dietary intake compared to other biofluids like plasma or saliva (Walsh *et al.*, 2006).

LC-MS is a powerful analytical technique that separates compounds in a column based on their interactions with the mobile and stationary phases. This separation depends on various chemical properties, like charge, polarity, and size, determined by the type of stationary phase used (Rusli *et al.*, 2022). After separation, compounds of interest are ionised, and their ions and/or fragment ions are analysed based on their respective mass-to-charge ratios (Pitt, 2009). LC-MS offers several advantages over the other analytical platforms such as gas chromatography-mass spectrometry (GC-MS) and nuclear magnetic resonance spectroscopy (NMR). It enables the analysis of a broader range of compounds, including non-volatile and thermically unstable compounds, simplifying sample preparation compared to GC-MS, which requires extra derivatisation steps (Perez *et al.*, 2016; Xiao *et al.*, 2012). LC-MS also offers higher sensitivity compared to NMR (Emwas, 2015), and has a high specificity and coverage depth with relatively low reagent costs. Despite its advantages, LC-MS has some disadvantages, including ion suppression, high running costs, low chromatographic resolution, and high signal-to-noise ratio (De Villiers & Loots, 2013).

In targeted metabolomic studies, LC-MS employs a tandem mass spectrometer (MS/MS) as the mass analyser, often using multiple reaction monitoring (MRM) mode. Such an LC-MS platform is referred to as high-performance liquid chromatography-tandem mass spectrometry (HPLC-MS/MS). In

HPLC-MS/MS set in MRM mode, after the separation of an analyte, the eluting analyte is first selected by the mass-to-charge ratio (*m/z*) of its ionised form, known as the precursor ion, using the first mass spectrometer. The precursor ion is then further fragmented to form specific product ions selected by the second mass spectrometer, which is used to identify and quantify the analyte of interest after detection (Pitt, 2009). The specificity and coverage depth of HPLC-MS/MS, along with the separation achieved by the liquid chromatography system, allow the instrument to identify compounds with a level one confidence, the highest level of confidence according to the Metabolomics Standards Initiative (Malinowska & Viant, 2019).

3.2. Experimental design

The broad outline of the experimental design is indicated in Figure 3.1 As part of a larger study (ethics no. NWU-00355-20-A1), urine samples (n=114) were collected by the South African Tuberculosis Vaccine Initiative (SATVI) and Desmond Tutu HIV Centre (DTHC) at the University of Cape Town (UCT). These samples were categorised into six subgroups based on the patients' HIV, TB, and treatment status.

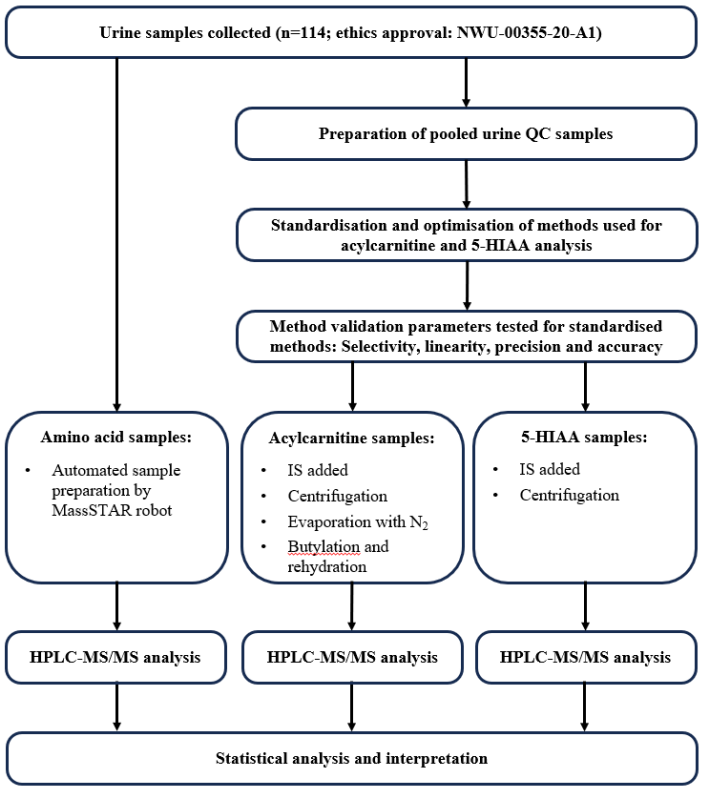

Figure 3.1: Outline of the experimental design. *This study can be divided into amino acid, acylcarnitine, and 5-hydroxyindoleacetic acid (5-HIAA) analyses. The process began with urine sample collection and categorisation, followed by specific metabolite analyses using validated techniques. The design incorporates a specialised kit for amino acids and two HPLC-MS/MS methods that were set up and partially validated for acylcarnitines and 5-HIAA, aiming to address the study's objectives in understanding HIV/TB co-infection. Abbreviations: QC: quality control; IS: internal standard; HPLC-MS/MS: High performance liquid chromatography-tandem mass spectrometry.*

The urine samples were aliquoted for amino acid, acylcarnitine and 5-HIAA analysis. For acylcarnitine and 5-HIAA analysis, a pooled urine QC sample was prepared using small aliquots (50 µL) from each individual sample. Urinary amino acid sample preparation and analysis was performed using the ChromSystems MassChrom® Amino Acid Analysis kit (supplied by Separations, Johannesburg, South Africa) along with the kit's own included QC samples (*MassCheck*® controls, order no. 0474, 0475, 0476) according to the manufacturer's instructions. This kit, however, only analyses the kynurenine pathway of tryptophan as it quantifies urinary tryptophan, kynurenine and hydroxykynurenine.

To provide a more comprehensive understanding of tryptophan metabolism in HIV/TB co-infected patients, urinary 5-HIAA was quantified by setting up and validating an HPLC-MS/MS method adapted from Clark *et al.* (2017). For urine acylcarnitine analysis, an additional HPLC-MS/MS method was established and validated. This step was necessary due to several instrumental and methodological considerations. The pre-existing HPLC-MS/MS methods either employed different liquid chromatography systems and columns that were no longer accessible or utilised direct injection protocols which were deemed unsuitable for this specific study. These limitations, particularly the potential for interferences in acylcarnitine detection with direct injection methods, prompted the development of a new chromatographic approach. Furthermore, the unavailability of publications using the same instrumentation necessitated this development and validation of a new method on the recently acquired 6470 QQQ instrument, known for its high sensitivity. Thus, the analysis of amino acids, acylcarnitines and 5-HIAA required three separate HPLC-MS/MS methods, the latter two needing setup and validation. Validation parameters for both 5-HIAA and acylcarnitine methods included selectivity, linearity, accuracy, and precision. These validated methods were applied to all urine samples for acylcarnitine and 5-HIAA analyses after sample preparation, fulfilling the first objective. In both the acylcarnitine and 5-HIAA analyses, all prepared samples were divided and analysed separately in six batches, with a QC sample injected at the beginning, middle and end of each batch analysis to assess repeatability. Finally, the acquired data from 32 controls, 41 patients with untreated TB, 7 patients with untreated HIV and 9 patients with untreated HIV/TB co-infection, was subjected to statistical analyses and interpreted to gain further insights into the biological status of the HIV, TB, and the HIV/TB co-infected state, addressing the second and third objectives, respectively.

3.3. Ethical approval

This investigation was conducted in compliance with the Declaration of Helsinki and International Conference on Harmonisation Guidelines. Ethical approval for the larger study was granted by the Research Ethics Committees of North-West University (NWU; reference no. NWU-00355-20-A1) and the University of Cape Town (reference no 680/2013). Additionally, this sub-study received ethical approval (reference no. NWU-00355-20-A1-02). Each participant provided written informed consent to participate in the study.

3.4. Cohort demographics

As previously outlined in Section 3.2, urine samples (n=114) for this study were collected as part of a larger project by SATVI and DTHC at UCT (ethics no. NWU-00355-20-A1) between March 2015 and August 2018. Participants, aged 18 to 69 years, were residents of the Masiphumelele and Ocean View Townships and surrounding areas in Cape Town, Western Cape Province. Participants were categorized into subgroups based on their HIV, TB, and treatment status. HIV status confirmation was conducted through standard serum testing (Fearon, 2005), while active pulmonary TB diagnosis was made using GeneXpert. In addition to these diagnostic details, supplementary information about the population includes CD4+ counts, lifestyle habits (e.g., smoking status), viral load (for HIV-positive individuals), chest X-ray results, current TB-related symptoms, age, sex, height, and weight was obtained (see Table 3.1. To ensure robustness of the results, lifestyle confounders were not considered for exclusion. Rigorous inclusion criteria were applied: individuals with concurrent diseases (including hypertension, cancer, liver disease, kidney disease and non-TB lung disease), those on over-the-counter or chronic medication, or who were pregnant, or lactating were excluded to minimize confounding factors. This selective process was crucial for maintaining the study's integrity and ensuring reliable results. Due to the WHO's "test and treat" policy, samples from untreated HIV and HIV/TB co-infected patients are difficult to obtain, explaining the relatively small sample cohorts (World Health Organization, 2021). All samples were managed according to UCT's standard operating procedures and stored in bio-freezers at NWU, with restricted access to authorized personnel only, ensuring sample integrity.

Table 3.1: Cohort demographics and clinical information.

	HIV-/TB-	**HIV+/TB-**	**HIV-/TB+**	**HIV+/TB+**
No. of patients (%)	32	7	41	9
Age (years), mean ± (range)	34 ± 3.3	37 ± 5.3	33 ± 3.6	34 ± 3.3
Gender, male:female ratio	3:8	5:4	3:1	3:1
Smokers in the group, no. of patients	12	3	25	3
CD4+ cell count (cells/mm^3 blood), mean ± SD	N/A	259.9 ± 264.2	N/A	26.9 ± 20.4
Viral load (copies/mL), range	N/A	unavailable	N/A	<20 – 22

Abbreviations: SD: Standard deviation; HIV-/TB-: healthy controls; HIV+/TB-: HIV-positive individuals only; HIV-/TB+: TB-positive individuals; HIV+/TB+: HIV/TB co-infected.

3.5. Samples collection, storage, and transport

Spot urine samples were collected using standard urine-collection-vials. Within a two-hour window following collection, the samples were promptly transported to UCT and frozen at -80°C. Anonymised samples were carefully placed on dry ice and transported to the NWU, Focus Area of Human Metabolomics: Laboratory of Infectious and Acquired Diseases (HM-SOP-ADM03-ver 001: "Procedure for the import and export of biological samples"). Here, samples were stored in a -80°C

freezer until the commencement of the metabolomics analysis. The freezer housing the urine samples was equipped with an alarm that would send notifications in the event of temperature fluctuations.

3.6. Reagents and chemicals

Isotopically labelled internal standards for the acylcarnitine method were purchased from LGC Standards included deuterium-labelled L-carnitine-d3 hydrochloric acid (HCL) (C0_ISCas: 350818-62-1), acetyl-L-carnitine-d3 HCl (Cas: 1334532-17-0), propionyl-L-carnitine-d3 HCl (Cas: 1334532-19-2), butyryl-L-carnitine-d3 HCl (Cas: 1334532-21-6), isovaleryl-L-carnitine-d9 HCl (Cas: 1334532-23-8), hexanoyl-L-carnitine-d3 HCl (Cas: 2483831-95-2), octanoyl-L-carnitine-d3 HCl (Cas: 1334532-24-9), decanoyl-L-carnitine-d3 HCl (Cas: 2483831-87-2), dodecanoyl-L-carnitine-d3 HCl (Cas: 2687960-76-3), myristoyl-L-carnitine-d9 HCl (Cas: 1334532-25-0), palmitoyl-L-carnitine-d3 HCl (Cas: 1334532-26-1) and octadecanoyl-L-carnitine-d3 HCl (Cas: 2245711-27-5). ^{13}C-labelled 5-hydroxyindole-3-acetic acid-^{13}C3 (5-HIAA_IS; Cas: 51-16-0) was purchased from Toronto Research Chemicals and used as internal standard for the 5-HIAA method. Unlabelled standards used during method validation were purchased from Merck, and, for the acylcarnitine method, included acetyl-L-carnitine (C2; Cas: 3040-38-8), propionyl-L-carnitine (C3; Cas: 20064-19-1), butyryl-L-carnitine (C4; Cas: 25576-40-3), isovaleryl-L-carnitine (C5; Cas: 31023-24-2), hexanoyl-L-carnitine (C6; Cas: 22671-29-0), octanoyl-L-carnitine (C8; Cas: 25243-95-2), decanoyl-L-carnitine (C10; Cas: 1492-27-9), dodecanoyl-L-carnitine (C12; Cas: 2466-77-5) and 5-HIAA (Cas: 54-16-0) for the 5-HIAA method. Synthetic urine from Industrial Analytical (Pty) Ltd was used during the validation of the acylcarnitine method. LC-MS grade solvents, namely acetonitrile (ACN; Cas: 75-05-8), methanol (MeOH; Cas: 67-56-1) and water (H_20; Cas: 7732-18-5), were from Honeywell, Burdick & Jackson, supplied by Anatech, South Africa. Formic acid (Cas: 64-18-6) from Merck KGaA, Darmstadt, Germany, was used as the mobile phase modifier while acetyl-chloride (Cas: 75-36-5) and 1-butanol (Cas: 71-36-3), also from Merck, were used for the butylation of acylcarnitines. All reagents used for the amino acid analysis, including the mobile phases, internal standards, calibrators, and QCs were included in the ChromSystems MassChrom® Amino Acid Analysis kit (supplied by Separations, Johannesburg, South Africa).

3.7. Preparation of isotope working solutions

Two separate isotope working solutions were meticulously prepared for urine acylcarnitine and 5-HIAA analyses:

1. An acylcarnitine isotope stock solution, containing all acylcarnitine isotopes listed in Section 3.6, was prepared to a final concentration of 3 µmol/L in H_2O. From this stock solution, a 3 mL aliquot was taken and further diluted with H_2O by a factor of ten to obtain an acylcarnitine isotope working solution with a final concentration of 0.3 µmol/L.

2. The 5-HIAA_IS isotope was sonicated in 1 mL of ACN:H_2O (50:50) for 4 minutes at 40°C to facilitate the dissolution of the compound. This solution was then further diluted in a volumetric flask with the same solvent to make 50 mL of a 51.1 µmol/L (10 ppm) 5-HIAA_IS working solution.

Both isotope working solutions were stored at 4°C for the duration of the validation and patient urine analysis (to prevent multiple freeze thaw cycles potentially causing degradation of the isotopes) and were stored at -20ºC otherwise. All isotopically labelled standards used in this study were designed to possess a mass that exceeded that of their unlabelled counterparts by at least 3 Da. This precaution was taken to prevent possible signal interference between the two species within the MS/MS system. For the analysis of 5-HIAA, a ^{13}C-labelled internal standard isotope was selected over a deuterium labelled isotope. This choice was based on experiments conducted by Clark *et al.* (2017), which revealed that the deuterium-labelled isotope did not co-elute effectively with 5-HIAA, adversely impacting 5-HIAA quantification. Co-elution of an isotopically labelled internal standard with the analyte of interest is important for quantification as it allows the internal standard to minimise potential matrix effects (Hewavitharana *et al.*, 2018). In contrast, the ^{13}C-labelled isotope did not have this drawback. Moreover, compared to deuterium-labelled isotopes, ^{13}C-labelled isotopes are favoured for their enhanced stability, particularly considering the potential for deuterium exchange when deuterium-labelled isotopes are dissolved in protic solutions (such as H_2O, methanol, 1-butanol, etc.) (Triebl & Wenk, 2018).

3.8. Setup of acylcarnitine and 5-HIAA methods

As stated in Section 3.2, this study employed three HPLC-MS/MS-based methods to analyse urinary amino acids, acylcarnitines, and 5-HIAA. The amino acid analysis utilised a ChromSystems MassChrom® kit, which had previously been validated by the Centre of Human Metabolomics (CHM) for diagnostic purposes. Notably, CHM's protocol includes automated sample preparation using the Hamilton Microlab Star liquid handler, deviating from the manual preparation indicated by the kit. For the acylcarnitine and 5-HIAA analyses, modified versions of pre-existing validated methods were employed. The acylcarnitine analysis method originally developed the Biotransformation and Oxidative Stress Status laboratory, NWU, and the 5-HIAA method from Clark *et al.* (2017) were adapted to suit different HPLC-MS/MS instrumentation and reverse-phase columns. These adaptations, detailed in Section 3.9, required standardisation to assess sensitivity and selectivity, involving optimisation of multiple reaction monitoring (MRM) transitions and mobile phase gradients for chromatographic resolution.

3.8.1. Instrumentation and software used for the acylcarnitine and 5-HIAA methods

The HPLC-MS/MS system used for both the acylcarnitine and 5-HIAA analyses consisted of an Agilent 1260 Infinity II autosampler, an Agilent 1290 Infinity binary pump, and an Agilent 6470 MS/MS with positive electrospray ionisation. For data acquisition, Agilent MassHunter Data Acquisition software

was used, while Agilent MassHunter QQQ Quantitative software was used for the quantification of analytes of interest.

3.8.2. Preparation of standard working solutions for method standardisation

For method standardisation, stock solutions with known concentrations of unlabelled acylcarnitine standards dissolved in H_2O and a working solution of 5-HIAA (52.3 µmol/L [10 ppm]) dissolved in ACN:H_2O (50:50) were used. Detailed information about these stock solutions and all other acylcarnitine working solutions prepared and used in this study can be found in APPENDIX A (Table A1). An acylcarnitine method standardisation working solution was created by combining a 100 µL aliquot of each acylcarnitine stock solution, which was then used for optimising MRM transitions and chromatographic separation.

3.8.3. Preparation and butylation of acylcarnitine tuning mix for standardisation

To prepare the acylcarnitine tuning mixes used for standardisation, 100 µL aliquots of the acylcarnitine method standardisation working solution and 100 µL aliquots of the acylcarnitine isotope working solution were each combined in three vials. The resulting solutions were dried under a stream of nitrogen and subjected to butylation as follows: A fresh 3 N butanolic HCl solution was prepared by slowly adding acetyl chloride to 1-butanol on ice until a 1:4 ratio of acetyl chloride to 1-butanol was achieved.

The dried tuning mixes were then incubated in 200 µL of 3 N butanolic HCl for 30 minutes and dried again using nitrogen streaming. The dried butylated acylcarnitine tuning mixes were subsequently reconstituted in 100 µL of ACN:H_2O (50:50) and incubated at room temperature for 30 minutes whereafter they were vortexed and aspirated into a vial containing a pulled insert for analysis by HPLC-MS/MS. The injection volume was kept at 1 µmol/L for all further acylcarnitine analysis.

3.8.4. Sample preparation for urinary 5-HIAA method standardisation

For standardisation of the 5-HIAA and 5-HIAA_IS methods, samples were prepared by simply combining 50 µL of the 5-HIAA_IS isotope working solution to 50 µL of the 5-HIAA standard working solution in a pulled insert vial for analysis. For all further 5-HIAA analysis, the injection volume was kept at 1 µmol/L.

3.8.5. Optimisation of MRM transitions for analytes

The MRM transitions for 5-HIAA, butylated acylcarnitines, and their labelled isotopes were optimised using MassHunter Optimizer software. This involved directly injecting the urinary acylcarnitine and 5-HIAA tuning mixes into the MS/MS system. For each analyte, the software selected the most abundant product ion formed from the respective precursor ion, along with the optimal transition conditions for quantification. For 5-HIAA and its isotopically labelled standard, the second most abundant product ion was also selected as a qualifier ion. The ratio of the response between the qualifier and quantifier ions

was used to confirm the identity of 5-HIAA and its labelled counterpart during analysis, ensuring specificity and sensitivity (Angeles & Aga, 2018).

3.8.6. Chromatographic separation

3.8.6.1. Chromatographic separation for acylcarnitine analysis

To achieve separation of acylcarnitines, a reverse phase chromatography technique with gradient elution was applied, focusing on separating isobaric acylcarnitines, such as C5 and valeryl-L-carnitine, which have similar MRM transitions according to the Human Metabolome Database. This was essential to avoid inaccuracies due to compounds like C4 and isobutyryl-L-carnitine, known for sharing transitions, as highlighted in research by (Mels *et al.*, 2011). The aqueous phase consisted of H_2O with 0.1% formic acid, while the organic phase was composed of ACN with 0.1% formic acid. To determine the most suitable column for the analyses, two columns were evaluated: the Agilent Zorbax SB-Aq C18 column (150 × 2.1 mm, 3.5 µm) and the Phenomenex Luna C8 column (150 × 2 mm, 5 µm). An acylcarnitine tuning sample was first injected into the HPLC-MS/MS system using each column. The gradient was initially set from 5% to 95% ACN over 17 minutes to determine the retention time of each butylated acylcarnitine and isotope on both columns, with the MS/MS set on MRM mode. After establishing the retention times of the butylated acylcarnitines and isotopes, both columns were used to analyse a 10 µL aliquot of the pooled urinary QC sample. The rationale behind using pooled urine QC samples, as opposed to blank urine, stemmed from their complexity and variability, which mirrors that of normal urine, containing a multitude of potential interfering analytes. During the validation phase, these pooled QCs were spiked with standards to assess selectivity (Section 3.9.4). Furthermore, for precision and accuracy tests, spiked blank urine samples were utilised, providing a comprehensive evaluation of matrix effects and analytical interferences (Section 3.9.3.). The pooled urine QC sample was first prepared for HPLC-MS/MS analysis in a microcentrifuge tube by adding 100 µL of acylcarnitine isotope working solution and 30 µL of ACN. Subsequently, the sample was centrifuged for 10 minutes at 12 000 g and 4°C. After centrifugation, the remaining supernatant was transferred to a vial and butylated as described in Section 3.8.3. The pooled urine QC was analysed to detect any possible interference from analytes present in urine that could co-elute with the analytes of interest.

During the use of both columns, co-elution of butylated C4 and C5 initially occurred with unknown analytes (Figure 3.2 A and B). Although co-elution of C4 was not initially clear, it was indicated by the fact that the peak that was supposedly C4 had a slightly shorter retention time to its deuterated analogue internal standard. This is unusual as deuterated analogues generally are slightly more hydrophilic and therefore have slightly shorter retention times compared to their non-deuterated counterparts in reverse phase LC (Achouba *et al.*, 2023). With a similar gradient, the Phenomenex Luna C8 column demonstrated superior separation of C5 and was therefore used for all further acylcarnitines analyses. To achieve sufficient separation of C5 with the Phenomenex Luna C8 column, the gradient was decreased, and multiple isocratic elution steps were inserted. This elongated the run time from

17 minutes to 32 minutes per sample analysed. This confirmed that there was a co-eluting compound interfering with the detection of C4 and although the separation of C4 improved with the extended run time, it still could not be fully separated from this unknown analyte. Therefore, C4 was excluded from all subsequent analysis. A visual comparison illustrating the separation of C4 and C5 with the Phenomenex Luna C8 column in the short and long run time is provided in Figure 3.2 B and C, respectively. This further highlighted the need for chromatographic separation for acylcarnitine analysis.

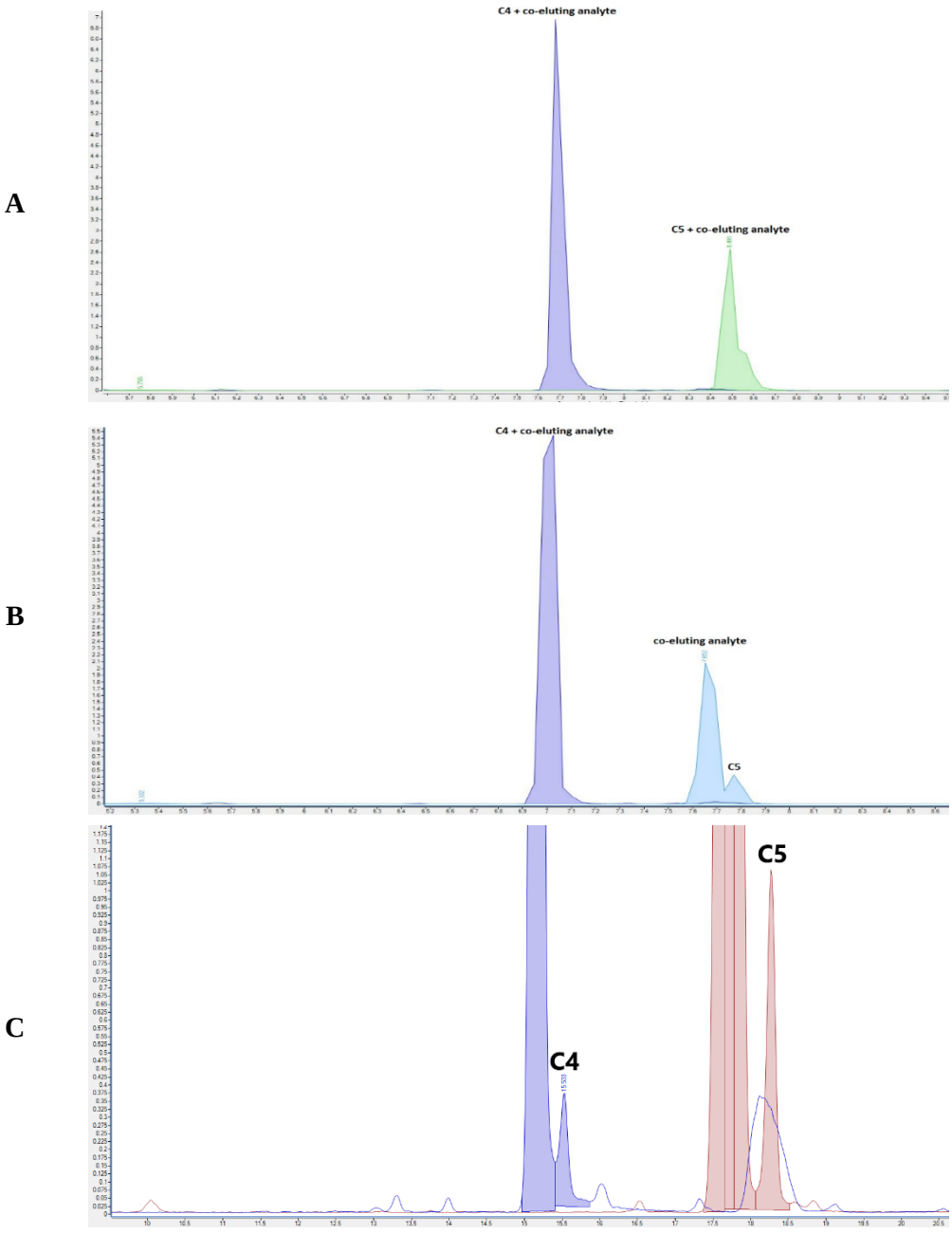

Figure 3.2: Chromatographic separation of acylcarnitines. *The chromatograms demonstrate the butylated C4 and C5 alongside unknown co-eluting analytes. It compares the initial separation with the (A) Agilent Zorbax SB-Aq C18 column and the (B) Phenomenex Luna C8 column, showing (C) improved separation with the Luna C8 column after optimising the mobile phase gradient and adding isocratic steps.Abbreviations: C4: butylated butyryl-L-carnitine; C5: butylated isovaleryl-L-carnitine.*

To re-equilibrate the column after each sample analysis, a post-run time of three minutes was set with the mobile phase composition set to 5% organic phase solution. The Phenomenex Luna C8 column not only provided superior chromatographic separation but also enhanced the method's overall robustness. Its large particle size (5 μm) ensured consistently low backpressures, well below the HPLC-MS/MS system's maximum pressure limit (600 bar).

3.8.6.2. Chromatographic separation for 5-HIAA analysis

To achieve separation for 5-HIAA and 5-HIAA_IS, reverse-phase chromatography was employed using the Phenomenex Luna C8 column. The aqueous and organic mobile phase solvents used were H_2O and methanol with 0.05% formic acid, respectively.

The 5-HIAA and 5-HIAA_IS standardisation working solution was initially injected into the HPLC-MS/MS system. An initial gradient was set, ranging from 5% to 95% methanol over 14 minutes, to determine the retention times of the compounds of interest. Hereafter, a pooled urine QC sample was prepared by centrifugation of 50 μL of the urine QC mixed with 50 μL of the 5-HIAA_IS working solution at 12 000 g for 10 minutes in a microcentrifuge tube. The supernatant was transferred to a pulled insert in a vial for analysis. The urine QC was analysed using this gradient to detect possible interference from co-eluting compounds. The column effectively separated 5-HIAA and 5-HIAA_IS from any analytes in the pooled QC urine sample that had similar MRM transitions.

To decrease the run time required per sample, the initial organic phase composition was adjusted to 15% methanol, which was then increased to 100% after 11 minutes, where it was kept for 2 minutes to ensure the removal of very non-polar compounds, if present, by the end of each sample run. This reduced the overall run time from 14 to 13 minutes. A post-run time of 4 minutes was set at a mobile phase composition of 15% organic phase after each sample run. For reference, the gradient elution conditions used in the acylcarnitine and 5-HIAA analysis methods are summarised in Table 3.2 below.

Table 3.2: Gradient elution conditions for acylcarnitine and 5-HIAA analysis.

Acylcarnitine analysis			**5-HIAA analysis**		
Time (min)	**ACN (%)**	**FR (mL/min)**	**Time (min)**	**Methanol (%)**	**FR (mL/min)**
0	5	0.3	**0**	15	0.3
15	25	0.3	**6**	33	0.3
17	25	0.3	**11**	100	0.3
18	30	0.3	**13**	100	0.3
19	30	0.3			
28.5	64.3	0.3			
31	100	0.5			
32	100	0.5			

Abbreviations: 5-HIAA: 5-hydroxyindoleacetic acid; min: minutes; ACN: acetonitrile; FR: flow rate.

3.8.7. Specifications of the MS/MS used for urinary acylcarnitine and 5-HIAA analysis

To enhance the resolution of the acylcarnitines analysed, the MS/MS was set to dynamic MRM (dMRM) mode instead of MRM. This mode allows the MS/MS to only monitor the analyte of interest in the timeframe of the sample run when the analyte of interest is expected to elute from the liquid chromatography system. As a result, the MRM transition cycle times are reduced, giving the MS/MS system more time to analyse the eluting analytes of interest. This improved the overall peak shapes for the monitored acylcarnitines and subsequently the accuracy and precision of the analysis (Stone *et al.*, 2009).

For the dMRM mode used during acylcarnitine analysis, retention times of each analyte of interest obtained from previous MRM analysis with the acylcarnitine standards alone were selected with a delta analysis time of 2 minutes. The source parameters and optimised MRM/dMRM transitions used in both methods are summarised below in Table 3.3 and Table 3.4, respectively.

Table 3.3: Source parameters for acylcarnitine and 5-HIAA analyses.

Method	Acylcarnitine analysis	5-HIAA analysis
Gas temperature (˚C)	280	150
Gas flow (L/minute)	9	8
Nebulizer (psi)	45	20
Sheath gas temperature (˚C)	400	300
Sheath gas flow (L/minute)	12	12
Capillary voltage (V)	4500	3000
Nozzle voltage (V)	500	0

Table 3.4: MRM transitions for acylcarnitines and 5-HIAA analysis.

Analyte	Precursor ion (m/z)	Product ion (m/z)	Fragmentor voltage (V)	Collision energy (V)
C2	260.2	85.1	159	32
C2 IS	263.2	85.1	101	24
C3	274.2	85.1	111	24
C3 IS	277.2	85.1	107	26
C5	302.2	85.1	102	26
C5 IS	311.1	85.1	122	26
C6	316.2	85.1	121	24
C6 IS	319.3	85.1	117	30
C8	344.2	85.1	129	28
C8 IS	347.3	85.1	107	30
C10	372.3	85.1	144	32

C10 IS	375.3	85.1	117	30
C12	400.3	85.1	159	32
C12 IS	403.3	85.1	107	30
5-HIAA	192.1	146	80	16
5-HIAA (qualifier)	192.1	118.1	80	34
5-HIAA IS	195.17	148	80	18
5-HIAA IS (qualifier)	195.17	120.1	80	34

Abbreviations: IS: internal standard; C2: acetyl-L- carnitine; C3: propionyl-L-carnitine; C5: isovaleryl-L-carnitine; C6: hexanoyl-L-carnitine; C8: octanoyl-L-carnitine; C10: decanoyl-L-carnitine; C12: dodecanoyl-L-carnitine; 5-HIAA: 5-hydroxyindoleacetic acid.

3.9. Validation of standardised acylcarnitine and 5-HIAA methods

Method validation is a crucial process aimed at ensuring the accuracy, precision, and consistency of test data generated in a laboratory, ultimately confirming the suitability of an analytical method for its intended purpose (Das, 2011; González *et al.*, 2014). Three main types of validation are recognised: full validation, partial validation, and cross-validation. A full validation becomes necessary when a new method is introduced or when a new compound is incorporated into and existing method. It entails a comprehensive assessment of various essential validation parameters, such as selectivity, linearity, accuracy, precision, sensitivity, matrix effects, stability, and reproducibility. When minor adjustments are made to an established method, such as changes in sample preparation or transition between laboratories, a partial validation may be conducted. This type of validation often focuses on within-run accuracy and precision, providing a near full validation. In the context of research, a cross-validation is essential when comparing two different analytical techniques within the same study. To achieve cross-validation, the same QC sample is analysed using both techniques, with the results ideally exhibiting a discrepancy of no more than 15% (González *et al.*, 2014).

For this investigation, two distinct methods using the same HPLC-MS/MS instrument were established. One method was for acylcarnitine analysis, while the other was for urinary 5-HIAA analysis. It is important to clarify that although validated methods exist for analysing urinary acylcarnitines and 5-HIAA, these were developed on different HPLC-MS/MS systems. In our study, given the unique setup of our instrumentation, which involved a different MS/MS and LC system potentially affecting sensitivity and selectivity, a partial validation of both methods was deemed appropriate. Similar method validation parameters were applied to both methods to effectively assess the capabilities and limitations of our specific HPLC-MS/MS instrument.

3.9.1. Linearity and calibration curves

Linearity characterises the relationship between the analyte's response and its actual concentration, ensuring accurate quantification within the calibration curve's concentration range (Moosavi &

Ghassabian, 2018). The calibration curve should cover the anticipated concentration range of the analyte in the samples to be analysed, with a minimum of six data points (González *et al.*, 2014). A literature review was conducted to determine the typical concentrations of acylcarnitines and 5-HIAA in urine (Bouatra *et al.*, 2013). Additionally, a previous study at the NWU, Focus Area Human Metabolomics: Laboratory of Infectious and Acquired Diseases examined urinary acylcarnitine levels in patients with pulmonary TB and healthy controls, revealing relatively low values, especially for medium-chain acylcarnitines (C6, C8, C10, and C12). The study underscored the need for method validation to ensure sufficient sensitivity. For 5-HIAA, literature suggested moderate quantities in urine with little variance (Bouatra *et al.*, 2013; Clark *et al.*, 2017). Ten calibration points were selected for each analyte to accommodate potential non-linear regions at the extremes. Any data points displaying non-linearity were excluded to ensure the calibration curve accurately reflected a linear relationship between the analyte response and concentration. Thus, the calibration curves for each analyte comprised seven to ten data points, providing a reliable basis for quantification.

Three calibration working solutions were prepared for acylcarnitines, with concentrations diluted to 24 µmol/L (C2), 8 µmol/L (C3 and C5), and 0.16 µmol/L (medium-chain acylcarnitines: C6, C8, C10, and C12). Calibration samples were created by adding the required amounts from each working solution to the same vial, followed by drying and butylation (see Section 3.8.3). All acylcarnitine calibration samples were analysed within a single batch.

For 5-HIAA, calibrators were prepared by adding the necessary amount of the 5-HIAA standard working solution to a vial, diluted with ACN:H_2O (50:50), and 50 µL of the 5-HIAA_IS working solution. Due to the 5-HIAA standard working solution's concentration limitation (52.3 µmol/L [10 ppm]), the 5-HIAA working solution was dried and resuspended in 50 µL of ACN:H_2O (50:50) and 5-HIAA_IS working solution for calibrators of 50, 75, and 100 µmol/L.

Finally, a 100 µL aliquot of each acylcarnitine and 5-HIAA calibration solution was transferred to a vial containing a pulled insert and analysed by their standardised HPLC-MS/MS method. Additional information on calibrators is available in APPENDIX A (Table A2).

3.9.2. Limit of detection and lower limit of quantification

The limit of detection (LOD) is generally defined as the smallest concentration of an analyte that can be distinguished from background noise by a particular method, although it may not necessarily be quantifiable. On the other hand, the lower limit of quantification (LLOQ) is the minimum concentration of an analyte that can be quantified with acceptable accuracy and precision by a method (Armbruster & Pry, 2008). Common methods for determining the LOD and LLOQ include calculation from the signal-to noise-ratio, calculation using the standard deviation of blank samples, and linear regression (Shrivastava & Gupta, 2011).

For this investigation, a linear regression approach was used to estimate the LOD and LLOQ of each analyte. This approach assumes a linear correlation between the analyte response obtained from the instrument used and its concentration. Linear regression was deemed applicable for this study, as the linear regions for all analytes were defined, as described in Section 3.9.1. Equations 3.1 and 3.2 were used to estimate the LOD and LLOQ, respectively, from the calibration curve of each analyte. The standard deviation (σ) of the y-residuals and the y-intercept of each calibration curve were divided by the slope of the curve (S), then multiplied by three or ten to obtain the estimated LOD and LLOQ, respectively. The upper limit of quantification (ULOQ) for each analyte was set at the highest concentration within the linear region of its calibration curve.

$$LOD = 3 \times \frac{\sigma}{S} \tag{3.1}$$

$$LLOQ = 10 \times \frac{\sigma}{S} \tag{3.2}$$

3.9.3. Precision and accuracy

Precision refers to the closeness between homogenous samples analysed in replicate and is typically measured as the residual standard deviation (RSD) or the coefficient of variation (CV), expressed as a percentage of the replicates analysed (Kumar *et al.*, 2012). Precision demonstrates whether a method can reproducibly quantify an analyte of interest. On the other hand, accuracy is defined as the closeness of agreement between the measured concentration of an analyte and its true concentration.

For this investigation, the intra-batch and inter-batch precision and accuracy were evaluated for both the urinary acylcarnitine and 5-HIAA methods. Intra-batch assays measure within-run precision and accuracy, while inter-batch assays evaluate between-run accuracy and precision over a certain time period (González *et al.*, 2014). QC samples covering the entire calibration range and consisting of concentrations at least three times the LLOQ, close to the middle of the range, and near the ULOQ were used for precision and accuracy tests. Additionally, the intra-batch and inter-batch precision and accuracy of the analytes of interest at their LLOQ were determined by a fourth QC sample (González *et al.*, 2014). The QC samples used during the validation of the acylcarnitine method are denoted as follows: acylcarnitine low quality control (ACLQC), medium quality control (ACMQC), high quality control (ACHQC), and the acylcarnitine lower limit of quantification (ACLLOQ). QC samples used during the validation of the urine 5-HIAA method are referred to as the 5-HIAA low quality control (5HLQC), medium quality control (5HMQC), high quality control (5HHQC), and 5-HIAA lower limit of quantification quality control (5HLLOQ). RSD (or CV) values obtained for an analyte measured by an analytical method should ideally not exceed 15% for low QC, medium QC, and high QC samples, or 20% for LLOQ samples when determining the intra-batch and/or inter-batch precision. For the determination of intra-batch and inter-batch accuracy, the measured concentration of an analyte should not differ with more than 15% from the actual concentration of the low QC, medium QC, and high QC

samples, while a deviation of less than 20% is acceptable for the LLOQ samples (González *et al.*, 2014; Whitmire *et al.*, 2011).

In separate conical tubes, three working solutions were prepared for the ACLQC, ACMQC, and ACHQC samples, consisting of C2, the other short-chain acylcarnitines, and the medium-chain acylcarnitine standards. These solutions were individually prepared in H_2O at twice the concentration of their selected high QC value. Additionally, two additional working solutions were prepared for the ACLLOQ acylcarnitine samples, containing acylcarnitines (C2 and C3) and acylcarnitines (C5, C6, C8, C10 and C12) at twice the concentration of their LLOQ [see APPENDIX A (Table A1)]. The necessary amount of the appropriate working solution for the ACLQC, ACMQC, ACHQC, and ACLLOQ samples was then added to a vial. Subsequently, 10 µL of synthetic urine and 100 µL of the acylcarnitine isotope working solution were introduced. These samples were subjected to drying with a stream of nitrogen and butylation (see Section 3.8.3), for subsequent analysis.

For the preparation of the 5HLLOQ and 5HLQC samples, 50 µL of the 5-HIAA standard working solution, diluted to the required concentration, and 50 µL 5-HIAA_IS working solution were added to a vial. The concentrations of 5HMQC and 5HHQC exceeded that of the available working solution. Therefore, after combining the required volumes of 5-HIAA working solution and 50 µL of the 5-HIAA_IS solution, these samples were dried with nitrogen, and subsequently resuspended in 100 µL ACN:H_2O (50:50) for 30 minutes. Hereafter, the resulting solutions were transferred with the 5HLLOQ and 5HLQC samples to a vial containing a pulled insert before analysis could commence.

To assess the precision and accuracy of both the urinary acylcarnitine and 5-HIAA methods, triplicates of their respective low QC, medium QC, high QC and LLOQ validation samples were prepared and analysed separately daily for five consecutive days (hence 15 observations in total for each QC sample). Refer to APPENDIX A (Table A3) for additional information regarding these QC samples. Equations 3.3 and 3.4 were utilised to determine the precision (RSD, %) and accuracy (%). The calibration curves obtained in Section 3.9.1, along with the appropriate internal standard and analyte response were employed to quantify all analytes of interest, as shown by Equation 3.5.

$$Precision\ (RSD, \%) = \frac{standard\ deviation}{mean} \times 100 \tag{3.3}$$

$$Accuracy\ (\%) = \frac{mean\ concentration\ measured}{true\ concentration} \times 100 \tag{3.4}$$

$$Concentration = \left(\frac{analyte\ response}{internal\ standard\ response} - yintersept\right) \times \begin{bmatrix} internal \\ standard \end{bmatrix} \div \begin{matrix} calibration \\ curve\ slope \end{matrix} \tag{3.5}$$

3.9.4. Selectivity

In analytical chemistry, selectivity generally refers to the method's ability to distinguish the compound of interest from other analytes within the matrix that may co-elute or interfere with its detection (Reilly *et al.*, 2020).

To assess the selectivity of the urinary acylcarnitine method, 10 µL from the pooled urine QC sample was spiked with acylcarnitines at the concentration of the ACLQC samples, using the same acylcarnitine standard working solutions prepared for the precision and accuracy tests. To the spiked sample, along with 10 µL of a non-spiked pooled QC urine sample, 100 µL of the acylcarnitine isotope working solution and 30 µL of ACN was added. After centrifugation at 12 000 g for 10 minutes at 4ºC, the QCs were dried using nitrogen and butylated for HPLC-MS/MS analysis, following the procedure described in Section 3.8.3. Hereafter, the spiked and non-spiked QC samples were analysed together.

Similarly, the selectivity of the urinary 5-HIAA method was evaluated by analysing a spiked pooled QC urine sample alongside a non-spiked QC urine sample. To prepare the 5-HIAA spiked QC sample, 50 µL of the 5-HIAA_IS working solution and a 25 µL aliquot of a 5-HIAA standard solution at the same concentration as the 5HLQC were added to 25 µL of the pooled QC. For the non-spiked QC sample, 50 µL of the pooled QC and 50 µL 5-HIAA_IS working solution were combined in a microcentrifuge tube. Following centrifugation at 12 000 g for 10 minutes at 4°C, the resulting supernatant was transferred to pulled insert vial for analysis.

3.10. Urine sample preparation and HPLC-MS/MS analysis

3.10.1. Sample preparation for acylcarnitine analysis

Pooled QC and patient samples were prepared by adding 100 µL of the acylcarnitine isotope working solution and 30 µL of ACN to 10 µL of each urine sample in a microcentrifuge tube. Following centrifugation at 12 000 g for 10 minutes at 4°C, the samples were transferred to a vial, dried using nitrogen, and butylated for HPLC-MS/MS analysis (see Section 3.8.3).

3.10.2. Sample preparation for 5-HIAA analysis

Pooled QC and patient samples were prepared using a "dilute and shoot" method described by Clark *et al.* (2017). The 5-HIAA_IS working solution (50 µL) was added to 50 µL of urine in a microcentrifuge tube and centrifuged at 12 000 g for 10 minutes at 4°C. The resulting supernatant was transferred to a pulled insert in a vial and was ready for analysis.

3.10.3. HPLC-MS/MS analysis of urine acylcarnitines and 5-HIAA

All urine samples (n=114) and six pooled QC aliquots prepared were randomised and divided into six batches, separately prepared, and analysed using both the validated urine acylcarnitine and 5-HIAA

sample processing and HPLC-MS/MS methods. Before each batch analysis, the instrument was equilibrated by injecting a blank sample containing H_2O. This blank sample was reinjected and analysed midway through and after each batch to assess potential carry-over effects during analysis. Throughout each batch, a QC urine sample was analysed at the beginning, middle, and end to gauge the between-batch reproducibility, measured as the RSD (%) for each analyte of interest of the urine QC samples. Quantification of the response of the analytes of interest, along with their corresponding internal standards and calibration curves, was conducted using Excel. Additionally, a principal component analysis (PCA) scores plot created by MetaboAnalyst (version 5.0) was employed to visually inspect the clustering of urine QC samples in comparison to patient urine samples, specifically for the acylcarnitine analysis (see Section 4.3.). The urine analysis for acylcarnitine and 5-HIAA spanned a duration of six and three days, respectively.

3.10.4. Amino acid analysis

Amino acid analysis via HPLC-MS/MS was performed using the ChromSystems MassChrom® Amino Acid Analysis kit, following the manufacturer's instructions. This comprehensive kit facilitates the quantification of 52 amino acids and creatinine in a urine sample. The preparation of the patient urine and QC samples provided with the kit (*MassCheck*® controls, order no. 0474, 0475, 0476) were automated using the MassSTAR robot. The liquid handler added 50 µL of the Internal Standard Mix (order no. 75246) and 600 µL of the Dilution Buffer (order no. 75205) to 20 µL of urine/QC sample in a 96-well plate. After centrifugation at 2000 g for 5 minutes, 200 µL of the resulting supernatant was transferred to a Collection Plate (order no. 75058), sealed with a heat seal. The extract was then analysed via HPLC-MS/MS using settings provided with the kit. The run time per urine sample was 19.1 minutes. All urine samples were analysed within three separate batches in a randomised order. QC samples from the kit were analysed in triplicate: at the beginning, middle, and end of each batch. The precision was assessed using RSD (%) values of QC samples. The kit includes its own analytical column (order no. 75100), which was utilised for analysis. The HPLC-MS/MS system employed was an Agilent Infinity 1290 binary pump with a 6470 MS/MS. Positive electrospray ionisation was utilised, with the MS/MS mode set to MRM mode. Agilent MassHunter Data Acquisition software and MassHunter QQQ Quantitative software were used for data acquisition and quantification, respectively.

3.11. Data processing

After quantification of all metabolites of interest in the patient urine samples with their respective methods, concentrations of metabolites below their calculated LOD were replaced with a zero value. Hereafter, creatinine normalisation was performed by dividing the concentration of all metabolites by the creatinine concentration determined with the ChromSystems MassChrom® Amino Acid Analysis kit (Section 3.10.4). All urine concentrations used during statistical analysis were expressed as µmol/L per mmol/L creatinine.

3.12. Statistical analysis

Statistical analyses were conducted on the HPLC-MS/MS results from urine samples of untreated individuals infected with either HIV-only, TB-only, and those with untreated HIV/TB co-infection, in addition to the healthy control group. MetaboAnalyst (version 5.0) was used for the statistical evaluation of the amino acid and acylcarnitine results. For the amino acid and acylcarnitine datasets, all zero values were replaced by one-fifth of the lowest recorded value for each respective feature, followed by log-transformation and auto-scaling. PCA was used to visually assess separation between the amino acid and acylcarnitine profiles. For identifying potentially significantly alterations in these datasets, one-way analysis of variance (ANOVA) was performed on both datasets, with Fisher's least significant difference used for post-hoc analysis. A threshold of 0.05 was set for both the maximum false discovery rate (FDR) and p-value in these analyses, applying the criteria to control for false positives and to determine statistical significance, respectively.

The 5-HIAA data analysis was simpler; the zero values were replaced by one-fifth of the lowest 5-HIAA concentration, but no transformation or scaling was necessary. Instead, three separate two-tailed T-tests, conducted in Excel, compared the 5-HIAA levels of the healthy controls with those of the three untreated infected cohorts. A p-value smaller than 0.05 indicated significant alterations.

CHAPTER 4: RESULTS AND DISCUSSION

4.1. Method validation results for acylcarnitine and 5-HIAA analysis methods

4.1.1. Linearity

Linearity for each analyte was assessed by plotting the response of the analyte divided by its respective internal standard against the expected concentration of the analyte standard divided by the internal standard concentration. The linear concentration ranges comprised 7–10 data points, and the coefficient of determination (R^2) for all calibration curves ranged from 0.9986 to 0.9999, indicating a strong linear relationship between the response and concentration (Schober *et al.*, 2018). The concentration range, linear range, and R^2 values for each compound are summarised in Table 4.1. The calibration curves for all acylcarnitines and 5-HIAA are provided in APPENDIX B (Table B1), with the calibration curve of C6 shown in Figure 4.1 as an example.

Table 4.1: Calibration curve parameters for acylcarnitines and 5-HIAA.

	C2	C3	C5	C6	C8	C10	C12	5-HIAA
Range analysed (µmol/L)	0.05–12	0.005–4	0.005–4	0.0002–0.08	0.0002–0.08	0.0002–0.08	0.0002–0.08	0.1–100
Linear range (µmol/L)	0.1–12	0.005–1.5	0.005–0.75	0.0002–0.08	0.0002–0.08	0.0002–0.08	0.0024–0.08	0.5–100
R^2	0.9999	0.9988	0.9999	0.9999	0.9998	0.9986	0.9988	0.9997

Abbreviations: C2: acetyl-L-carnitine; C3: propionyl-L-carnitine; C5: isovaleryl-L-carnitine; C6: hexanoyl-L-carnitine; C8: octanoyl-L-carnitine; C10: decanoyl-L-carnitine; C12: dodecanoyl-L-carnitine; 5-HIAA: 5-hydroxyindoleacetic acid.

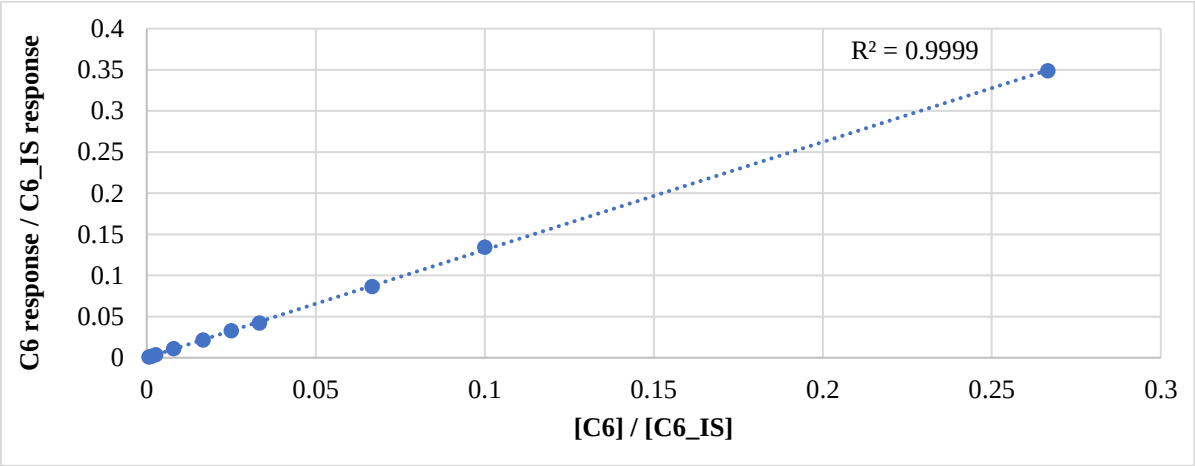

Figure 4.1: Calibration curve for hexanoyl-L-carnitine. *This calibration curve was constructed using ten concentration levels and demonstrates the linearity of the response of C6 in relation to its concentration, an essential aspect of method validation. The linear relationship is underscored by a high coefficient of determination (R^2). Abbreviations: C6: hexanoyl-L-carnitine; C6_IS: hexanoyl-L-carnitine internal standard.*

4.1.2. LOD and LLOQ of acylcarnitines and 5-HIAA

The LLOQ and LOD values for both the acylcarnitine and 5-HIAA analysis methods were consistent with the linear ranges of their respective calibration curves. The estimated LLOQ and LOD concentrations for acylcarnitines, particularly for the medium-chain acylcarnitines, were notably low. These values, in conjunction with the ULOQ values, are presented in Table 4.2.

Table 4.2: Estimated LOD, LLOQ and ULOQ concentrations for acylcarnitines and 5-HIAA.

	C2	C3	C5	C6	C8	C10	C12	5-HIAA
LOD (µmol/L)	0.096	0.048	0.004	0.0008	0.0009	0.0026	0.0033	1.7
LLOQ (µmol/L)	0.32	0.16	0.013	0.0026	0.003	0.0086	0.011	5.68
ULOQ (µmol/L)	12	1.5	0.75	0.08	0.08	0.08	0.08	100

Abbreviations: LOD: Limit of detection; LLOQ: Lower limit of quantification; ULOQ: Upper limit of quantification; C2: acetyl-L-carnitine; C3: propionyl-L-carnitine; C5: isovaleryl-L-carnitine; C6: hexanoyl-L-carnitine; C8: octanoyl-L-carnitine; C10: decanoyl-L-carnitine; C12: dodecanoyl-L-carnitine; 5-HIAA: 5-hydroxyindoleacetic acid.

These low LLOQ values underscore the sensitivity of the methods, especially in detecting medium-chain acylcarnitines. The ULOQ values establish the upper limit for quantification, ensuring the methods cover a wide dynamic range. The precision and accuracy of these values were thoroughly validated during experiments, affirming the reliability and robustness of the acylcarnitine and 5-HIAA analysis methods.

4.1.3. Precision and accuracy

For the acylcarnitine analysis method, most acylcarnitines demonstrated sufficient precision. Intra-batch precision exhibited RSD values below 20% for the ACLLOQ samples and below 15% for the QC samples at low (ACLQC), medium (ACMQC), and high (ACHQC) concentrations. Inter-batch precision was generally acceptable, except for C12 at the ACMQC. Notably, C12's inter-batch accuracy exceeded a 15% deviation of its actual concentration at ACLQC. Additionally, the measured intra-batch and inter-batch concentrations of C12 and C10 at the ACLLOQ exceeded the 20% deviation threshold.

The 5-HIAA analysis method demonstrated excellent precision and accuracy. The low (5HLQC), medium (5HMQC), and high (5HHQC) samples had RSD values below 3%, with accuracy values deviating less than 3% from their actual concentrations in both intra-batch and inter-batch assays. The highest RSD was noted in the inter-batch analysis of the LLOQ (5HLLOQ) samples at 7.08%, with the most deviation from their actual concentration by 6.48%.

A summary of all intra-batch and inter-batch precision and accuracy results for both the acylcarnitine and 5-HIAA analysis methods are presented in Table 4.3. The results generally fall within acceptable

ranges, indicating the reliability and robustness of both methods. Specific deviations highlight areas for potential improvement or closer monitoring in future analyses.

Table 4.3: Precision and accuracy results for the acylcarnitine and 5-HIAA analysis methods.

Compound	Intra-batch precision and accuracy							
	Low QC		Medium QC		High QC		LLOQ	
	RSD (%)	Accuracy (%)	RSD (%)	Accuracy (%)	RSD (%)	Accuracy (%)	RSD (%)	Accuracy (%)
C2	1.67	102.45	0.77	105.13	1.32	103.41	0.11	99.77
C3	1.56	103.13	1.47	99.58	0.21	101.23	1.78	101.28
C5	0.77	105.64	0.98	103.74	0.23	106.05	0.78	98.07
C6	1.58	107.05	0.70	107.20	1.12	108.96	0.97	97.61
C8	2.03	105.53	0.77	105.66	0.34	108.10	2.42	92.41
C10	3.02	109.02	2.20	108.79	0.03	113.00	5.24	120.99
C12	3.92	96,26	3.11	88.78	0.45	88.35	2.99	162.68
5-HIAA	2.61	97.13	1.50	99.42	1.42	98.97	1.71	100.16
Compound	**Inter-batch precision and accuracy**							
	Low QC		**Medium QC**		**High QC**		**LLOQ**	
	RSD (%)	**Accuracy (%)**	**RSD (%)**	**Accuracy (%)**	**RSD (%)**	**Accuracy (%)**	**RSD (%)**	**Accuracy (%)**
C2	2.36	101.32	1.75	104.23	0.99	103.11	1.26	99.27
C3	3.97	102.37	1.27	100.68	0.56	101.36	0.17	103.07
C5	1.77	102.85	1.48	102.48	1.35	103.66	1.80	96.00
C6	1.50	105.77	1.35	106.78	1.14	107.19	3.44	93.27
C8	1.89	106.55	2.36	107.68	0.72	108.49	3.98	88.65
C10	3.26	108.92	4.16	111.50	1.52	111.16	3.82	124.97
C12	8.20	94.32	19.00	94.67	8.32	79.73	7.88	177.00
5-HIAA	1.39	98.36	1.03	99.58	0.88	99.56	7.08	106.48

Abbreviations: QC: quality control; LLOQ: lower limit of quantification; RSD: residual standard deviation; C2: acetyl-L-carnitine; C3: propionyl-L-carnitine; C5: isovaleryl-L-carnitine; C6: hexanoyl-L-carnitine; C8: octanoyl-L-carnitine; C10: decanoyl-L-carnitine; C12: dodecanoyl-L-carnitine; 5-HIAA: 5-hydroxyindoleacetic acid.

4.1.4. Selectivity

Selectivity is crucial for ensuring accurate detection of target analytes within complex matrices. In the acylcarnitine analysis, the examination of pooled QC urine samples, both non-spiked and spiked with acylcarnitines, revealed no interference, confirming the method's reliability. Figure 4.2 illustrates the chromatograms with distinct peaks for (A) short-chain acylcarnitines and (B) medium-chain acylcarnitines in both the pooled QC urine and spiked pooled QC urine samples.

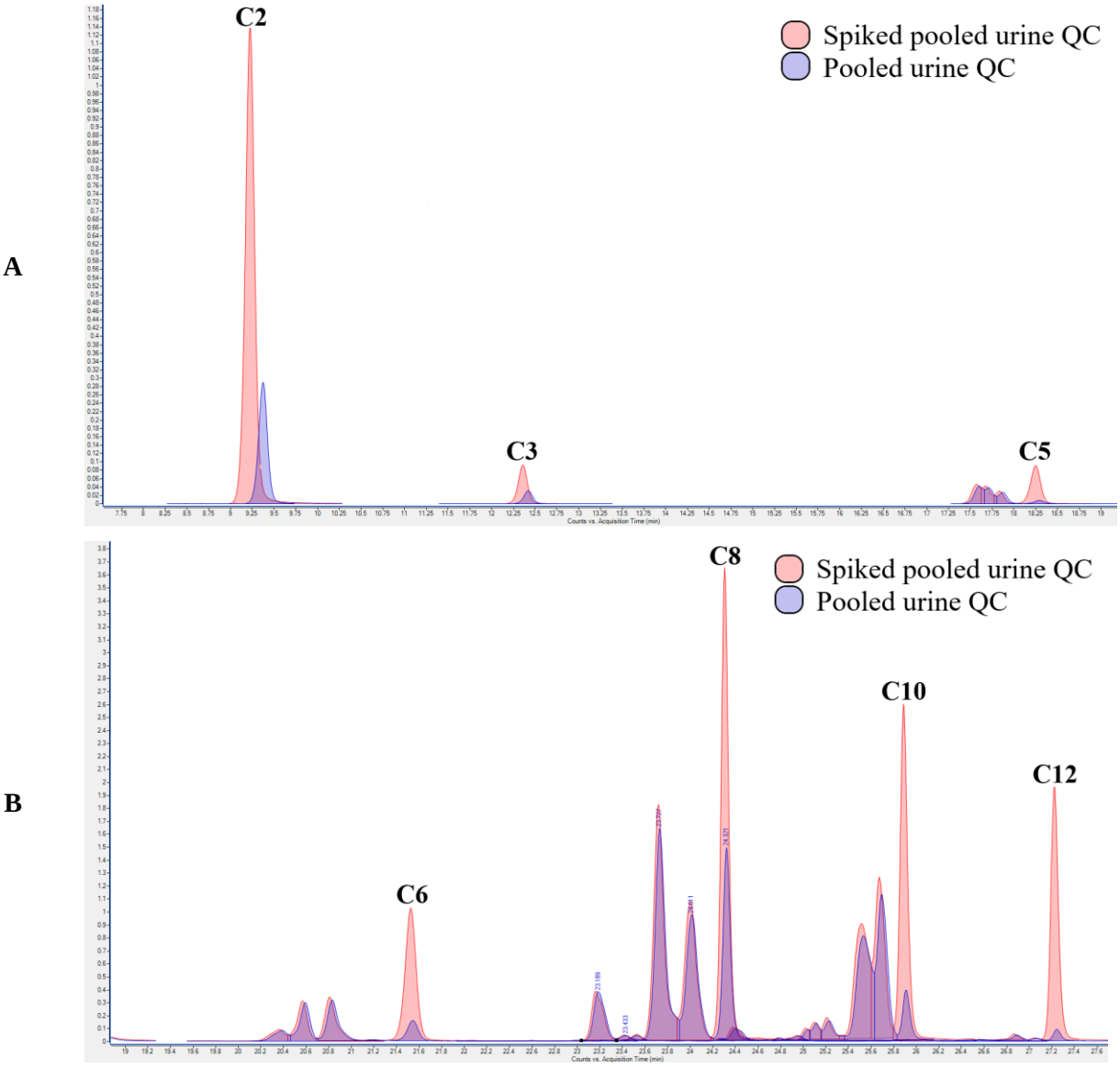

Figure 4.2: Acylcarnitine selectivity in chromatographic analysis. *The overlaid chromatograms of pooled QC urine and spiked QC urine samples analysed for acylcarnitine content demonstrate the method's selectivity and ability to differentiate and quantify (A) short-chain and (B) medium-chain acylcarnitines.Abbreviations: QC: quality control; C2: acetyl-L-carnitine; C3: propionyl-L-carnitine; C5: isovaleryl-L-carnitine; C6: hexanoyl-L-carnitine; C8: octanoyl-L-carnitine; C10: decanoyl-L-carnitine; C12: dodecanoyl-L-carnitine.*

Similarly, for the 5-HIAA analysis, chromatograms of non-spiked and 5-HIAA spiked pooled QC urine samples indicated no interference and confirmed the identity of 5-HIAA in the pooled QC urine sample, as shown in Figure 4.3.

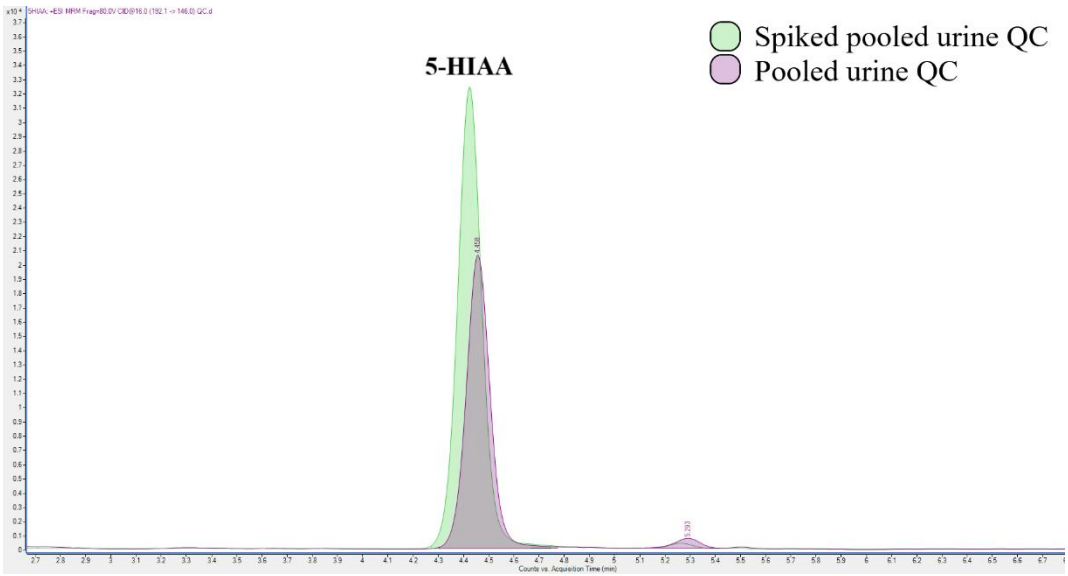

Figure 4.3: 5-Hydroxyindoleacetic acid (5-HIAA) selectivity in chromatographic analysis. *Overlaid chromatograms of non-spiked and spiked pooled urine QC samples analysed for 5-HIAA. The absence of interference in the detection confirms the method's selectivity in accurately identifying 5-HIAA.*

The absence of interference in both methods underscores their high selectivity, which is vital to prevent false positives or misinterpretation in metabolite identification and quantification. Employing spiked samples not only confirms the absence of interference but also validates the identity of the analysed compounds, enhancing the overall robustness of the analytical approach.

4.1.5. Validation outcomes for acylcarnitine and 5-HIAA: Sensitivity and precision challenges

The acylcarnitine analysis method's overall validation results appear promising, demonstrating high sensitivity. This is evident from the calibration curves' linear regions, which adequately cover the expected acylcarnitine concentration ranges in urine, and the relatively low estimated LOD and LLOQ values derived from these curves. While precision and accuracy measurements were generally sufficient, there were notable exceptions. These include the accuracy of C10 at LLOQ levels, the inter-batch precision of C12 in ACMQC samples, and the accuracy of C12 in both ACLLOQ and ACLQC samples. Regarding the accuracy issues with C12, it is unlikely that this is related to its solubility in water (urine), as C12 remains soluble despite being more hydrophobic than shorter chain acylcarnitines. Additionally, solubility does not typically affect the detection of a compound by MS. These findings suggest an inverse correlation between the molecular weight of medium-chain acylcarnitines and the method's sensitivity, as shown by increasing estimated LOD and LLOQ values relative to the molecular weight of the medium-chain acylcarnitines tested. This inverse correlation might be linked to variations in ionisation efficiency or product ion formation due to the size of the medium-chain acylcarnitines, potentially impacting the detection of product ions (Li *et al.*, 2021). The method also demonstrated high selectivity, with no interferences observed in both spiked and non-spiked urine QC samples.

The 5-HIAA method exhibited satisfactory linearity and low estimated LOD and LLOQ values, covering the expected 5-HIAA concentration range in urine. Both the precision and accuracy of this method, combined with its selectivity, underscore its repeatability and suitability for accurately and selectively quantifying 5-HIAA in urine, making it a viable method for this investigation. Furthermore, the simplicity and speed of the sample preparation process minimise the potential for analytical errors, thereby enhancing the method's repeatability.

4.2. Evaluating the cohort demographics of this study

The demographics of the four cohorts (see Section 3.4), including age, male/female ratio, and the number of smokers, showed no significant differences. However, the sample sizes were relatively small, especially of the HIV-only (n=7) and HIV/TB co-infected (n=9) cohorts. This limitation was due to the WHO's "test and treat" policy, which made obtaining untreated HIV and TB samples challenging (World Health Organization, 2021). Thus, this study is exploratory in nature and aims to guide future research in identifying biomarkers for HIV/TB co-infection rather than discovering them directly.

4.3. Data quality of the patient urine samples

The quality of patient sample data was assessed using pooled QC urine samples analysed before and during sample analysis, alongside the validation parameters for acylcarnitine and 5-HIAA analysis. QC samples were analysed concurrently to prevent significant errors from instrumentation and/or the analyst. Both acylcarnitine and 5-HIAA analyses showed no trends indicating analyte variation related to run-order, suggesting an absence of within-batch drift. The RSD (%) values for between-batch QC samples remained below the 15% cutoff recommended by the Food and Drug Administration for targeted analysis, indicating minimal batch effects (Food and Drug Administration, 2018). Figure 4.4 further illustrates this with a PCA scores plot showing the clustering of acylcarnitine QC samples (Godzien *et al.*, 2015). Despite sufficient selectivity and linearity in the acylcarnitine method, some intra- and inter-batch precision and accuracy results for C10 and C12 did not meet regulatory guidelines. Nevertheless, during patient sample analysis, concentrations of C10 and C12 were quantified, as they exceeded detection limits in over 50% of the samples and their RSD values were below 15%. This aligns with several published LC-MS-based targeted metabolomic studies that do not specify the use of validated methods with calibrators (Collins *et al.*, 2020; Ding *et al.*, 2020; Peltenburg *et al.*, 2018). The concentrations of other acylcarnitines and 5-HIAA were also predominantly above their detection and quantification limits. Out of 50 amino acids analysed, 37 that were above the detection limit in over 50% of the samples were included in the statistical analysis. Since a diagnostic kit was used for the amino acid analysis, some amino acids are only present with certain diseases. Therefore, it was expected that a certain portion of the amino acids analysed would be below the detection limit. The concentrations of other acylcarnitines and 5-HIAA were also predominantly above their detection and quantification limits. Regarding the amino acid analysis, 37 out of 50 analysed were detected in over 50% of the samples and thus included in the statistical analysis. The absence of certain amino acids (n=13) could

be attributed to their specific presence in certain disease states, as the diagnostic kit used is tailed for inborn errors of metabolism. Acylcarnitine and 5-HIAA creatinine-corrected concentrations and their reference ranges are available in APPENDIX B (Table B2). Most urine acylcarnitine concentrations were below reference ranges, potentially due to dietary factors affecting L-carnitine intake (Kulczyński *et al.*, 2019). The 5-HIAA concentrations were within the reference range in almost patient urine samples.

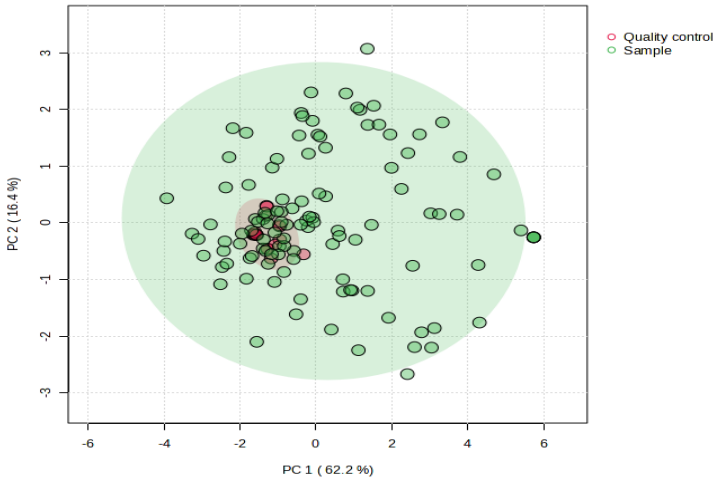

Figure 4.4: Principal component analysis (PCA) scores plot for acylcarnitine analysis. *The plot compares the quality control (QC) samples (in red) with patient urine samples (in green), demonstrating data consistency and absence of significant batch effects.*

4.4. Overview of amino acid and acylcarnitine metabolomes of cohorts

The PCA scores plots for amino acid and acylcarnitine analysis, excluding QC samples, showed no distinct separation between the healthy control group and other experimental groups, as depicted in Figure 4.5. The intra-group variations for amino acids and acylcarnitines across all cohorts were relatively similar. This observation suggests that, multivariately, amino acid and acylcarnitine urine metabolomes do not significantly differ among the cohorts, regardless of HIV, TB, or HIV/TB co-infection status.

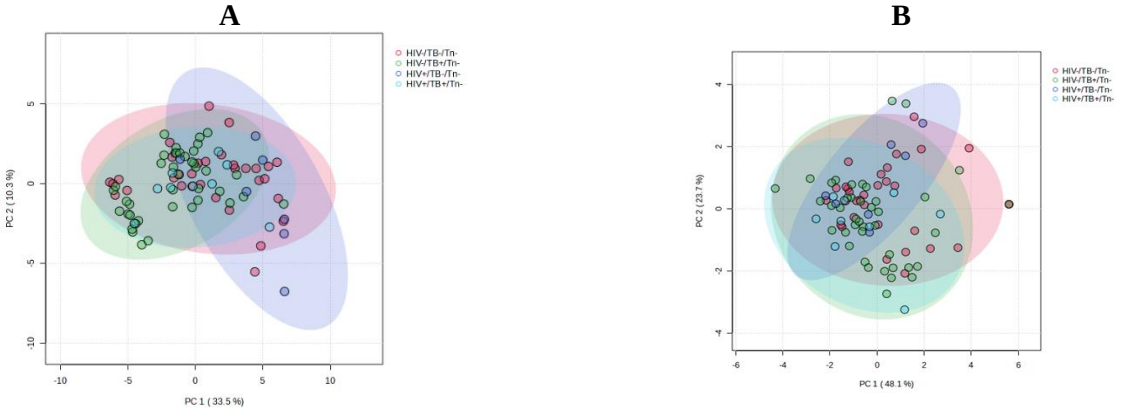

Figure 4.5: PCA scores plots for amino acid and acylcarnitine analysis. *PCA scores plots compare the healthy control group (HIV-/TB-/Tn-) with experimental groups based on (A) amino acid analysis and (B) acylcarnitine analysis, showing no significant separation, indicating similar metabolomic profiles across cohorts.*

4.5. HPLC-MS/MS urine analysis results

4.5.1. Amino acids

For the statistical analysis of amino acid data, the ratios of kynurenine/tryptophan, glutamine/glutamic acid, saccharopine/lysine, and phenylalanine/tyrosine were included as data points. Generally, amino acid levels were decreased in the HIV-only infected group and increased in the TB-only group compared to the healthy control group, as indicated in Table 4.4, which summarises all analysed amino acids and ratios. ANOVA identified 16 individual amino acids and the kynurenine/tryptophan, saccharopine/lysine, and glutamine/glutamic acid ratios as significantly altered between the healthy control and experimental groups (p-value < 0.05) (Table 4.5). Figure 4.6 presents a Venn diagram showing the number of amino acids uniquely altered by the HIV, TB, and HIV/TB co-infected states, and those altered by more than one disease state. In the HIV-only infected group, argininosuccinic acid, phosphoethanolamine, ethanolamine, glutamine, and the glutamine/glutamic acid ratio were significantly decreased. The TB-only cohort showed the most significant disruption in amino acid metabolism, with increases in the kynurenine/tryptophan ratio, kynurenine, leucine, arginine, carnosine, and asparagine, along with a decrease in 3-methylhistidine. No unique alterations were observed in the HIV/TB co-infected group. Both the HIV and TB cohorts showed marked changes in isoleucine and α-aminoadipic acid levels. In the HIV/TB co-infected and HIV groups, and tryptophan levels were decreased, while increases in the saccharopine/lysine ratio, hydroxykynurenine, saccharopine and a decrease in glycine were noted in the HIV/TB co-infected and TB groups. Table 4.5 summarises the significantly altered amino acids and amino acid ratios (n=19), with their statistical analysis results. Notably, only 16 out of the 37 amino acids detected, and three of the ratios, were significantly altered.

Table 4.4: Log-transformed mean abundances of amino acids and ratios included in the statistical analysis.

Compound	**Mean log-transformed concentration (standard deviation)**			
	HIV-/TB-	**HIV+/TB-**	**HIV-/TB+**	**HIV+/TB+**
Amino acids				
1-Methylhistidine	0.333 (0.748)	0.220 (1.151) ↓	-0.291 (1.024) ↓	-0.029 (1.079) ↓
3-Methylhistidine	0.305 (0.933)	0.652 (0.628) ↓	-0.372 (0.942) ↓	0.102 (1.016) ↓
α-Aminoadipic acid	-0.153 (1.059)	-1.109 (0.943) ↓	0.346 (0.735) ↑	-0.171 (1.015) ↓
α-Aminobutyric acid	-0.041 (1.028)	-0.957 (0.904) ↓	0.217 (0.863) ↑	-0.099 (1.024) ↓
β-Alanine	-0.083 (1.028)	-0.582 (0.801) ↓	0.149 (0.948) ↑	0.071 (1.018) ↑
β-Aminoisobutyric acid	-0.109 (1.048)	-0.943 (0.704) ↓	0.185 (0.880) ↑	0.276 (0.998) ↑
Alanine	-0.171 (1.234)	0.225 (1.340) ↑	0.122 (0.748) ↑	-0.121 (0.254) ↑
Anserine	0.038 (1.034)	-0.294 (0.868) ↓	0.004 (0.976) ↓	0.077 (0.987) ↑
Asparagine	-0.209 (1.148)	-0.791 (1.358) ↓	0.338 (0.640) ↑	-0.181 (0.775) ↑
Arginine	-0.316 (1.113)	-0.831 (1.147) ↓	0.314 (0.769) ↑	0.337 (0.446) ↑

Argininosuccinic acid	-0.139 (1.075)	-0.976 (0.573) ↓	0.293 (0.875) ↓	-0.080 (0.849) ↓
Carnosine	-0.132 (1.104)	-0.839 (0.754) ↓	0.358 (0.765) ↑	-0.506 (0.940) ↓
Cystathionine	-0.130 (1.024)	-0.774 (0.724) ↓	0.290 (0.914) ↑	-0.258 (0.929) ↓
Cystine	0.089 (0.865)	-0.837 (1.300) ↓	0.123 (0.815) ↑	-0.224 (1.446) ↓
Ethanolamine	0.159 (0.582)	-1.043 (1.888) ↓	0.134 (0.559) ↓	-0.365 (1.797) ↓
Glutamic acid	0.012 (1.026)	-1.113 (1.081) ↓	0.073 (0.900) ↑	0.490 (0.453) ↑
Glutamine	-0.060 (1.055)	-0.802 (0.969) ↓	0.202 (0.880) ↑	-0.082 (0.924) ↓
Glycine	0.498 (0.857)	0.558 (0.578) ↑	-0.297 (0.901) ↓	-0.851 (0.980) ↓
Histidine	0.291 (1.082)	0.144 (1.114) ↓	-0.174 (0.727) ↓	-0.354 (1.291) ↓
Homocitrulline	0.048 (1.065)	-0.721 (0.605) ↓	0.072 (0.945) ↑	0.062 (0.974) ↑
Hydroxykynurenine	-0.523 (0.857)	-1.014 (0) ↓	0.497 (0.824) ↑	0.385 (1.016) ↑
Hydroxylysine	-0.093 (1.013)	-0.087 (1.318) ↑	0.106 (0.939) ↑	-0.086 (0.816) ↑
Isoleucine	-0.322 (1.053)	-1.272 (0.725) ↓	0.444 (0.673) ↑	0.111 (0.909) ↑
Kynurenine	-0.508 (0.983)	-1.033 (0.529) ↓	0.562 (0.652) ↑	0.051 (0.997) ↑
Leucine	-0.305 (1.112)	-0.923 (1.136) ↓	0.315 (0.699) ↑	0.368 (0.756) ↑
Lysine	0.009 (1.021)	-0.506 (1.459) ↓	0.116 (0.803) ↑	-0.166 (1.091) ↓
Ornithine	-0.234 (1.012)	-0.662 (0.904) ↓	0.275 (0.926) ↑	0.094 (0.837) ↑
Phenylalanine	0.023 (0.907)	-0.500 (1.694) ↓	0.002 (0.889) ↓	0.300 (0.858) ↑
Phosphoethanolamine	-0.085 (1.078)	-1.014 (0.677) ↓	0.333 (0.785) ↑	-0.426 (0.985) ↓
Pyroglutamic acid	-0.225 (1.071)	-0.142 (0.239) ↑	0.144 (1.075) ↑	0.256 (0.191) ↑
Saccharopine	-0.355 (0.976)	-1.092 (0) ↓	0.368 (0.878) ↑	0.435 (0.834) ↑
Serine	0.201 (0.924)	0.689 (0.280) ↑	-0.285 (1.049) ↓	0.050 (0.883) ↓
Taurine	-0.045 (0.988)	-0.100 (1.290) ↓	-0.006 (1.016) ↑	0.266 (0.473) ↑
Threonine	0.063 (1.208)	-0.481 (1.430) ↓	0.092 (0.544) ↑	-0.268 (1.159) ↓
Tryptophan	0.103 (0.941)	-1.090 (1.577) ↓	0.245 (0.646) ↑	-0.638 (1.070) ↓
Tyrosine	0.198 (0.951)	-0.519 (1.678) ↓	-0.087 (0.929) ↓	0.084 (0.382) ↓
Valine	-0.003 (1.078)	-0.725 (1.087) ↓	0.094 (0.909) ↑	0.146 (0.702) ↑
Amino acid ratios				
Glutamine/Glutamic acid	-0.101 (1.01)	-1.054 (0.651) ↑	0.198 (0.913) ↑	0.276 (0.931) ↑
Kynurenine/Tryptophan	-0.510 (0.878)	-1.167 (0) ↓	0.597 (0.730) ↑	0.003 (1.002) ↑
Phenylalanine/Tyrosine	-0.058 (1.008)	-0.587 (1.610) ↓	0.045 (0.864) ↑	0.457 (0.497) ↑
Saccharopine/Lysine	-0.518 (0.743)	-0.952 (0) ↓	0.466 (0.919) ↑	0.456 (1.055) ↑

**The log-transformed data more accurately reflects the data used to identify the ANOVA markers. This approach has been used successfully in other studies (Herbert et al., 2023).*

Blue and ↓: Decreased compared to healthy control group; Red and ↑: Increased compared to healthy control group.

Abbreviations: HIV-/TB-: healthy controls; HIV+/TB-: HIV-only; HIV-/TB+: TB-only; HIV+/TB+: HIV/TB co-infected.

Table 4.5: Statistical analysis results of significantly altered amino acids, arranged according to p-values.

Amino acid/ratio	Means HC HIV TB HIV/TB	P-value	FDR	Post-hoc (Fisher's LSD)
Kynurenine/Tryptophan		< 0.0001	< 0.0001	TB
Kynurenine	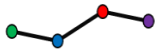	< 0.0001	< 0.0001	TB
Hydroxykynurenine	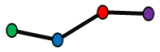	< 0.0001	< 0.0001	TB; HIV/TB
Saccharopine/Lysine	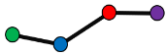	< 0.0001	< 0.0001	TB; HIV/TB
Isoleucine	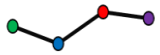	< 0.0001	<0.0001	TB; HIV
Glycine		< 0.0001	0.0004	TB; HIV/TB
Saccharopine	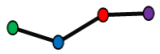	< 0.0001	0.0005	TB; HIV/TB
Tryptophan	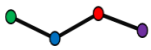	0.0013	0.0072	HIV; HIV/TB
α-Aminoadipic acid	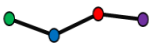	0.0015	0.0073	TB; HIV
Leucine		0.0018	0.0077	TB
Phosphoethanolamine	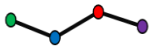	0.0024	0.0096	HIV
Arginine		0.0032	0.0109	TB
Carnosine		0.0033	0.0109	TB
3-Methylhistidine	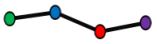	0.0067	0.02	TB
Glutamic acid	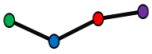	0.0094	0.0262	HIV
Argininosuccinic acid		0.0103	0.0268	HIV
Asparagine	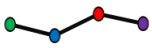	0.0110	0.0269	TB
Glutamine/Glutamic acid	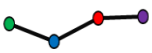	0.0131	0.029	HIV
Ethanolamine	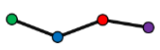	0.0133	0.029	HIV

Abbreviations: HC: healthy controls; HIV: HIV-positive; TB: TB-positive; HIV/TB: HIV/TB co-infected; FDR: false discovery rate; Fisher's LSD: Fisher's least significant difference.

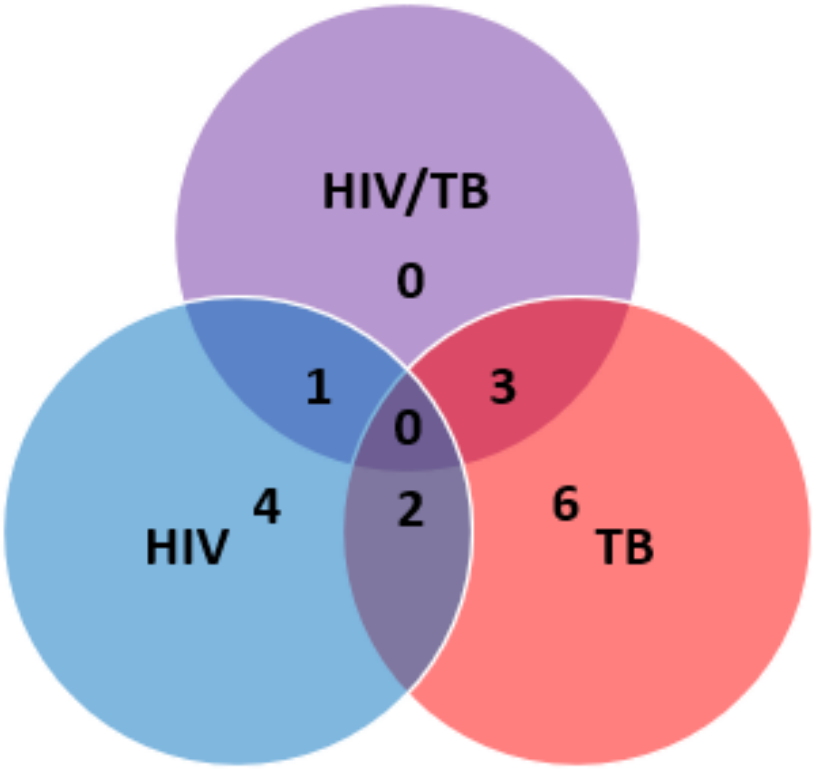

Figure 4.6: Venn diagram of altered amino acids across cohorts. *This Venn diagram illustrates the unique and shared statistically significant amino acids (either increased or decreased) in HIV, TB, and HIV/TB co-infected cohorts, highlighting the distinct metabolic impacts of these disease states. Abbreviations: infected with human immunodeficiency virus only; TB: having tuberculosis; HIV/TB: co-infected.*

4.5.2. Acylcarnitines

While the ANOVA did not find any acylcarnitines significantly altered by HIV, TB, or HIV/TB co-infection, there is a noticeable trend of increased medium-chain acylcarnitines levels in the TB and HIV/TB co-infected groups. Mean concentrations for all medium-chain acylcarnitines (C6, C8, C10 and C12) in these cohorts were higher than in the uninfected control group, with the co-infection group consistently higher compared to the TB-only group. Additionally, short-chain acylcarnitines were observed to be higher in the HIV-only group compared to controls. The ANOVA p-values for medium-chain acylcarnitines were notably lower compared to the short-chain acylcarnitines (see Table 4.6), especially for C6 ($p<0.05$), but their FDR values exceeded the acceptable threshold of 0.05. This possibly due to the small sample sizes of some groups and the close distribution of acylcarnitine levels between cohorts (Pawitan et al, 2015).

Table 4.6: Mean log-transformed acylcarnitine concentrations and statistical analysis.

Acylcarnitine	Means HC HIV TB HIV/TB	P-value	FDR
C2		0.9698	0.9698
C3		0.3493	0.4890
C5		0.4594	0.5359
C6		0.0310	0.1391
C8		0.0696	0.1391
C10		0.0795	0.1391
C12		0.0652	0.1391

Abbreviations: FDR: false discovery rate; Fishers' LSD: Fisher's least significant difference; C2: acetyl-L-carnitine; C3: propionyl-L-carnitine; C5: isovaleryl-L-carnitine; C6: hexanoyl-L-carnitine; C8: octanoyl-L-carnitine; C10: decanoyl-L-carnitine; C12: dodecanoyl-L-carnitine.

4.5.3. Urine 5-HIAA

The statistical analysis comparing the HIV (p=0.657), TB (p=0.430) and HIV/TB (p=0.663) groups with the healthy control group revealed no significant differences in urinary 5-HIAA levels. The HIV and HIV/TB co-infected groups had only marginally lower means of 5-HIAA levels compared to the healthy controls. This is visually represented in a box and whiskers plot (Figure 4.7), which shows the distribution of 5-HIAA levels across the cohorts.

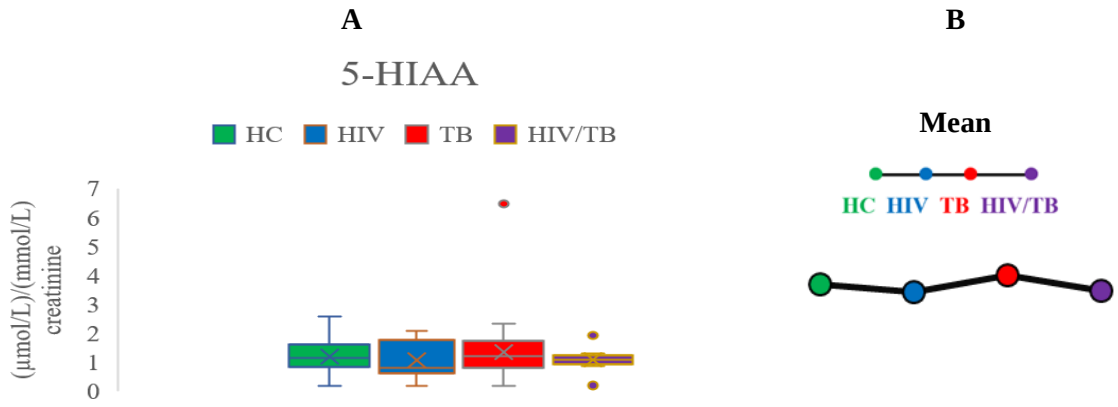

Figure 4.7: Urinary 5-hydroxyindoleacetic acid (5-HIAA) levels. *The box and whiskers diagram (A) compares urinary 5-HIAA levels among HIV, TB, HIV/TB co-infected groups, and healthy controls, with means indicated by a cross. The line graph (B) represents the mean urine 5-HIAA levels. Panels (A) and (B) demonstrates that there are no significant differences in 5-HIAA levels across the groups.*

4.6. Characterising the urine amino acid and acylcarnitine metabolome of the HIV/TB co-infected state

4.6.1. HIV-only infection and its impact on amino acids

In the HIV-only infected cohort, a noticeable trend of lower urine amino acid levels was observed. It is important to note that these findings represent comparisons between groups and not a decrease within the same individuals over time. All seven significantly altered amino acids and bioamines (i.e., isoleucine, tryptophan, α-aminoadipic acid, phosphoethanolamine, glutamic acid, argininosuccinic acid and ethanolamine) displayed lower levels compared to healthy controls. This overall lowering of amino acids might also relate to oxidative stress, potentially influenced by HIV's disruption of mitochondrial function, which impacts oxidative stress (Swanepoel *et al.*, 2021). Additionally, 32 out of 37 amino acids analysed showed lower mean values in the HIV-only infected group than in the healthy cohort (see Table 4.4). This trend is likely attributable to GI malabsorption due to HIV-associated enteropathy (as detailed in Section 2.1 and 2.6.1). This condition, coupled with a shift towards an anabolic protein turnover state, mirrors the metabolic alterations seen in inflammatory bowel disease, which, like HIV, often exhibit malabsorption due to chronic GI tract inflammation. For example, studies have noted decreased serum levels of several amino acids (such as glutamine, tyrosine, glycine, tryptophan, and asparagine) in a mouse colitis (an inflammatory bowel disease) model (Shiomi *et al.*, 2011). Stephens *et al.* (2013) also reported reduced levels of lysine, asparagine, and histidine in the urine of inflammatory bowel disease patients, linking these changes to malabsorption.

A study involving ^{15}N glycine stable isotope administration to individuals with HIV-only infection, TB-only and HIV/TB co-infection (Paton *et al.*, 2003) revealed a pronounced anabolic protein balance in the HIV-only infected individuals. Interestingly, this study did not observe significant alterations in protein flux, degradation, or synthesis in the TB-only and HIV/TB co-infected states. This indicates that the metabolic disruptions observed in HIV-only infection may not be as pronounced in HIV/TB co-infected individuals. Mercier *et al.* (2002) observed in a rat colitis model that colitis induced protein synthesis in the colon, spleen, and ileum, while reducing synthesis in skeletal muscle. This pattern suggests that conditions like HIV infection, which are characterised by GI tract malabsorption and chronic inflammation, may cause a shift towards increased reliance on skeletal muscle protein catabolism to supply amino acids to splanchnic organs (such as the spleen, intestines, and liver). However, the extent to which this pattern applies to HIV/TB co-infected individuals remains unclear and warrants further investigation. The colitis-induced rats exhibited lower levels of free plasma amino acids such as valine, methionine, phenylalanine, and leucine, indicating a redistribution of protein synthesis towards these splanchnic organs. Therefore, in conditions like colitis or potentially HIV infection, where malabsorption and chronic GI tract inflammation occur, there may be concurrent elevated protein catabolism in skeletal muscle, providing amino acid substrates for increased protein synthesis in splanchnic organs. The interaction between these metabolic processes in the context of HIV/TB co-infection, however, needs to be explicitly studied to understand its unique metabolic

implications fully. Amino acid metabolism, involved in various metabolic pathways, is influenced by factors beyond just absorption and protein turnover, including oxidative catabolism, ketogenesis, and gluconeogenesis processes utilising amino acids (Chandel, 2021). Specific amino acids, such as tryptophan, isoleucine, and glutamic acid, may diminish in HIV-only infection as they are converted into TCA cycle precursors (like pyruvate and acetyl-CoA) or intermediates to meet energy requirements. In the liver, these amino acid-derived intermediates can contribute to glucose synthesis via gluconeogenesis, maintaining glucose homeostasis. Tryptophan and isoleucine serve as precursors for acetyl-CoA, while glutamate and isoleucine can lead to TCA cycle intermediates like succinyl-CoA and α-ketoglutarate, respectively (Namikawa-Kanai *et al.*, 2020; Pasini *et al.*, 2018). The significant reduction of tryptophan levels in the HIV-only infected cohort seems unrelated to heightened kynurenine pathway activity, as there was no increase in kynurenine, hydroxykynurenine, or the kynurenine/tryptophan ratio. Glutamate plays a crucial role as a TCA cycle intermediate precursor, as it, along with oxidised nicotinamide adenine dinucleotide (phosphate) [NAD(P)+], converts to α-ketoglutarate and NAD(P)H in the mitochondria through the action of glutamate dehydrogenase, especially under conditions of low adenosine triphosphate (ATP) supply (Karaca *et al.*, 2018; Plaitakis *et al.*, 2017). The reduced glutamine/glutamic acid ratio in the HIV-only infected groups suggests increased metabolic flux via glutaminase-driven conversion of glutamine to glutamate in the mitochondria, aiding α-ketoglutarate synthesis (Mazat & Ransac, 2019).

In the HIV-only infected cohort, significant decreases were observed in ethanolamine and phosphoethanolamine. These compounds are crucial precursors in the biosynthesis of phosphatidyl-ethanolamine phospholipids, a major component of cellular membranes, via the cytidine diphosphate (CDP)-ethanolamine pathway (St Germain *et al.*, 2023). While the human body can synthesise these compounds, their levels can be significantly influenced by dietary intake and metabolic changes. Their decreased levels might thus be attributed to malabsorption (Patel & Witt, 2017). However, it is important to explore other potential mechanisms, such as direct impacts of HIV infection on metabolic pathways, which could also influence these levels. Reduced levels of phosphoethanolamine and phosphotidyl-ethanolamines, previously noted in untreated HIV-infected individuals, suggest that lower ethanolamine and phosphoethanolamine could impair the CDP-ethanolamine pathway in HIV infection (Peltenburg *et al.*, 2018). Phosphatidylethanolamines, constituting 15–25% of cellular phospholipids and about 30% of mitochondrial phospholipids, are crucial for mitochondrial functionality (Vance, 2015). Phosphatidylethanolamines facilitate mitochondrial respiration by creating a negative curvature in the inner mitochondrial membrane, thus augmenting the surface area and the binding capacity for electron transport proteins (St Germain *et al.*, 2023; Vance, 2015). This structural alteration enhances ATP production via oxidative phosphorylation (Joubert & Puff, 2021). Decreased levels of ethanolamine and/or phosphoethanolamine, leading to diminished levels of phosphatidylethanolamines, might contribute to the mitochondrial dysfunction observed in HIV-infected individuals (Schank *et al.*, 2021), although the extent to which these deficiencies impact mitochondrial respiration in humans remains unclear. The resulting mitochondrial dysfunction can have profound effects on cellular energy

metabolism, immune function, and overall health of HIV-infected individuals, underscoring the need to understand these metabolic alterations fully.

Furthermore, the notable decrease in argininosuccinic acid, an intermediate of the urea cycle, was observed in the HIV-only infected cohort, hinting at a decreased urea cycle activity (Madiraju *et al.*, 2016). The urea cycle activity, primarily functioning in the liver and to some extend in the kidneys, is crucial for detoxifying ammonia produced during amino acid catabolism (Lucarelli *et al.*, 2018; Olde Damink *et al.*, 2009). Ammonia, serving as a substrate for the initial and rate-limiting step of the urea cycle, is facilitated by carbamoyl phosphate synthetase I, where ammonia, along with bicarbonate, is converted to carbamoyl phosphate (Liu *et al.*, 2011). Decreased urea cycle activity in the HIV-only infected group may result from overall decreased amino acid levels, leading to reduced ammonia production via amino acid catabolism. This is supported by the findings of Brown *et al.* (1972), who observed that a protein-restricted diet alone led to reduced urea cycle activity in rats. In addition, significantly decreased levels of the urea cycle byproduct, urea, have also been noted in HIV-positive individuals, which was suggested to result from reduced urea cycle activity (Peltenburg *et al.*, 2018). Exploring the relationship between decreased urea cycle activity and HIV pathology could offer valuable insights into how this metabolic alteration affects the overall metabolic health of HIV-infected individuals.

4.6.2. TB and its impact on amino acids

In contrast to the lower urine amino acid levels of the HIV-only infection cohort, the significantly altered amino acids in our TB-only subjects were generally higher compared to controls, except for glycine and 3-methylhistidine. Moreover, 27 of the 37 amino acids analysed showed increased mean levels in the TB-only cohort compared to the healthy control group. This aligns with Zhou *et al.* (2013), who found increased plasma/serum amino acid levels and suggested this might result from impaired protein synthesis and net protein catabolism leading to amino acid oxidation. The significantly elevated amino acids, including kynurenine, hydroxykynurenine, leucine, isoleucine, α-aminoadipic acid, arginine, and asparagine, can be utilised for the synthesis of TCA cycle intermediates used for oxidative phosphorylation (Leandro & Houten, 2020; Namikawa-Kanai *et al.*, 2020; Pasini *et al.*, 2018). As not all elevated amino acids are proteinogenic, increased proteolysis alone does not fully explain this trend. Non-proteinogenic amino acids, such as kynurenine, carnosine, and α-aminoadipic acid, may be derived from the metabolism of the proteinogenic amino acids (Derave *et al.*, 2010; Sacksteder *et al.*, 2000; Savitz, 2020). Therefore, their elevated levels can be attributed to increased synthesis from their proteinogenic precursors and/or altered metabolism resulting from the infection. As such, an increase in urea cycle activity might be expected due to the deamination of generally increased amino acid levels. This is possibly reflected in the significantly elevated arginine levels within the TB-only cohort, as arginine is an essential urea cycle intermediate (Madiraju *et al.*, 2016).

Despite the decreased urinary levels of 3-methylhistidine in our TB-only cohort, increased excretion levels of 3-methylhistidine have been associated with skeletal muscle wasting (muscle atrophy) and cachexia, which is common in TB-positive individuals (Luies & Du Preez, 2020; Yang *et al.*, 2018). Muscle atrophy is the only endogenous source of plasma 3-methylhistidine, which is excreted without being metabolised. However, urinary and plasma 3-methylhistidine levels also dependent on dietary intake, particularly from red meat consumption (Cross *et al.*, 2011; Kochlik *et al.*, 2018). Therefore, the decreased 3-methylhistidine in our TB cohort might not necessarily indicate reduced muscle wasting but could be influenced by dietary factors and the heterogeneity among individuals in the group (Beukes *et al.*, 2023). This includes variations in diet and lifestyle associated with the geographical differences between the diseased samples and controls. It should be noted that our control group, drawn from surrounding areas in addition to the townships, was not perfectly matched to this context, possibly introducing additional complexity in comparing the TB cohort with the controls. Loss of appetite, a common occurrence in TB-positive individuals (Gupta *et al.*, 2009), could further explain the reduced 3-methylhistidine levels. Current recommendations advise adhering to a meat-free diet lasting for three days before testing plasma 3-methylhistidine levels (Tomas *et al.*, 1979).

The significantly decreased glycine levels in the TB-only cohort may indicate diabetes associated with hyperglycaemia, as glycine is typically reduced in people with hyperglycaemic conditions such as obesity and diabetes (Adeva-Andany *et al.*, 2018; Takashina *et al.*, 2016). Additionally, hyperglycaemia is frequently observed in untreated TB-positive patients; reports indicate that 17–87% (depending on the population) of TB-positive patients, who have no prior diabetes diagnosis, present with elevated glucose levels at the time of their TB diagnosis (Magee *et al.*, 2018; Ngo *et al.*, 2021). This may be due to undiagnosed diabetes, which is known to increase susceptibility to TB (Jeon & Murray, 2008). This observation is particularly concerning for South Africa, where high obesity rates and resource-limited settings complicate diabetes diagnosis and management (Pillay & Aldous, 2016). TB has also been shown to induce hyperglycaemic responses (Ngo *et al.*, 2021; Yorke *et al.*, 2017), known as stress hyperglycaemia, in patients without pre-existing diabetes (Vedantam *et al.*, 2022). The exact aetiology of TB-associated stress hyperglycaemia remains unclear, but it is thought to stem from prolonged inflammation. This inflammation may lead to secondary physiological stress, altered lipid and glucose metabolism, and insulin resistance in TB patients (Bisht *et al.*, 2023; Magee *et al.*, 2018; Menon *et al.*, 2020). The mechanism by which glycine levels decrease during hyperglycaemia is not fully understood. Increased glycine decarboxylase levels, observed in high-fat, insulin-resistant fed mice, suggest that elevated insulin might play a role in decreasing the expression of this enzyme (Jog *et al.*, 2021). Elevated glycine decarboxylase could be a primary contributor to reduced glycine levels, as it is the key rate-limiting enzyme of the glycine cleavage system responsible for most glycine degradation (Jog *et al.*, 2021; Lamers *et al.*, 2007). This system consists of three enzymes that oxidise glycine, tetrahydrofolate, and NAD+ to form carbon dioxide, ammonia, 5,10-methylene tetrahydrofolate, and NADH. The 5,10-methylene tetrahydrofolate formed is subsequently converted to formate, serving as a precursor for cytosolic-mediated one-carbon metabolism used in nucleotide and methionine biosynthesis (Kikuchi *et*

al., 2008; Tan *et al.*, 2020). Additionally, elevated levels of α-aminoadipic acid and arginine, also found in the TB-only cohort, have been proposed as strong indicators of type II diabetes, further supporting the link between TB and diabetes (Cao *et al.*, 2019; Luna *et al.*, 2021; Sell *et al.*, 2007). On the other hand, the significantly lower glycine levels in the TB-only cohort may be influenced by factors beyond potential hyperglycaemia. According to Amalia *et al.* (2022), TB alters amino acid metabolism in complex ways, potentially impacting glycine levels. This could be due to the metabolic demands of the host's immune response or the nutritional requirements of *Mtb*, offering a broader context to the observed changes in glycine and other amino acids in TB patients. These metabolic alterations in TB, as detailed in the review, emphasize the need to consider multiple factors influencing amino acid levels in TB patients, not solely focusing on diabetes-related mechanisms.

In contrast to the HIV-only cohort, tryptophan levels in the TB-only group were similar to the healthy control group. However, kynurenine pathway activity appears to be significantly increased in the TB-only cohort, as evidenced by significantly increased levels of kynurenine, hydroxykynurenine, and the kynurenine/tryptophan ratio. The reason for the unaffected tryptophan levels in the TB-only cohort may be attributed to increased proteolysis, since tryptophan is a proteogenic amino acid, and/or the ability of *Mtb* to synthesise tryptophan *de novo* (Gautam *et al.*, 2018).

The significantly elevated branched-chain amino acids (BCAAs), specifically leucine, isoleucine, and valine (although the latter was not significantly elevated and hence not reported in Table 4.5), in the TB-positive cohort, support the hypothesis that proteolysis is elevated in the skeletal muscle of these individuals. During metabolic stress, such as starvation or cachexia, most proteinogenic amino acids released from muscles are oxidised or used for gluconeogenesis in the liver, while the majority of BCAAs are catabolised in the muscles (Holeček, 2020). In these conditions, BCAA catabolism is inhibited in muscle tissue due to increased fatty acid oxidation and decreased glycolysis, leading to their accumulation in muscle tissue and plasma (De Blaauw *et al.*, 1996; Holeček, 2020; Pozefsky *et al.*, 1976). Additionally, increased BCAA levels are associated with type II diabetes, although it is unclear whether these elevated levels are a cause or biomarker of the disease (Cuomo *et al.*, 2022). The significant increase in carnosine, predominantly found in skeletal muscle, in our TB-only group further indicates skeletal muscle loss, as carnosine can be released during muscle atrophy (Derave *et al.*, 2010).

Lysine degradation via the saccharopine pathway seems to be enhanced in the TB-only population. This is evidenced by increased saccharopine and α-aminoadipic levels, and the saccharopine/lysine ratio, in the TB-positive group. The saccharopine pathway, which catabolises lysine in the mitochondrial matrix, is the primary regulator of lysine levels (Papes *et al.*, 1999). In this pathway, lysine reacts with α-ketoglutarate and NADPH to form saccharopine and NADP+ in a reaction facilitated by α-aminoadipic acid semialdehyde synthase. Saccharopine is then oxidised to α-aminoadipic acid semialdehyde and glutamate. Subsequently, α-aminoadipic semialdehyde and NAD(P)+ are converted to α-aminoadipic acid and NAD(P)H by α-aminoadipic semialdehyde dehydrogenase. The pathway

continues to produce α-ketoadipic acid and eventually glutaryl-CoA, which is used for the synthesis of glutaric acid or acetyl-CoA via the oxidation of glutaryl-CoA (Leandro & Houten, 2020; Sacksteder *et al.*, 2000). This elevated saccharopine pathway activity likely represents an adaptation where lysine is used to generate intermediates for the synthesis of NADH and reduced flavin adenine dinucleotide (FADH). In this process, the oxidation of glutaryl-CoA leads to the formation of acetyl-CoA, which then enter the TCA cycle. This contributes significantly to the formation of FADH and NADH via both the oxidation of glutaryl-CoA and the resulting acetyl-CoA entering the TCA cycle, thus supporting energy production through oxidative phosphorylation. This occurs despite the initial use of α-ketoglutarate, a TCA cycle intermediate, in the saccharopine pathway. The increased kynurenine pathway activity observed may also contribute to this process, as α-ketoadipic acid generated through kynurenine metabolism in the cytosol can be transported into the mitochondrial matrix and converted to glutaryl-CoA (Leandro & Houten, 2020).

4.6.3. Altered acylcarnitines and the link to a disrupted metabolic profile of the TB-only group

Although none of the acylcarnitines analysed were significantly altered in any of the infectious groups compared to the healthy control group a trend of elevated medium-chain acylcarnitines was observed in the TB-only group. Specifically, all mean values of medium-chain acylcarnitine levels were comparatively higher in the TB-positive group, with p-values lower than 0.05 for C6 and less than 0.1 for other medium-chain acylcarnitines. This trend may be linked to increased fatty oxidation associated with cachexia, as reported in previous studies on TB-positive cohorts (Che *et al.*, 2018; Fukawa *et al.*, 2016). Batchuluun *et al.* (2018) found that medium-chain acylcarnitines were particularly elevated in individuals with type II diabetes, complementing the deduction made earlier describing the amino acid phenotype in these individuals. Their research also demonstrated that elevated medium-chain acylcarnitines downregulated mitochondrial complex V of the electron transport chain in pancreatic islets of humans and mice, reducing mitochondrial oxidative capacity, a characteristic associated with type II diabetes. Although the short-chain acylcarnitines in the HIV-only group all had higher mean values compared to the healthy controls, the high p-values and FDR values obtained by the ANOVA for the short-chain acylcarnitines and considering that the HIV-only cohort was the smallest (n=7). This was likely due to a few outliers within the HIV-only group that had increased short-chain acylcarnitines rather than metabolic alterations associated with HIV-infection.

The suspected insulin resistance associated with this diabetic-like presentation could be responsible for the generally increased amino acid levels observed, which is postulated to originate from skeletal muscle wasting, as explained above. This is supported by previous studies indicating that insulin resistance induces skeletal muscle wasting through the activation of the ubiquitin-proteasome proteolytic pathway (Price *et al.*, 1996; Wang *et al.*, 2006).

4.6.4. The altered metabolism in HIV/TB co-infection

Unlike with the HIV-only infected and TB-only groups, the HIV/TB co-infected group did not exhibit a clear pattern in overall amino acid levels compared to the healthy control group. The decreased amino acid levels of the HIV-only infected cohort and the increased levels in the TB-only cohort suggested an increased anabolic and catabolic protein turnover state, respectively, in these single-infection states. A combined effect of HIV and *Mtb* infection might result in increased overall protein turnover in the HIV/TB co-infected group, with no net anabolic or catabolic effect. Paton *et al.* (2003) support this hypothesis, as the increased whole-body protein anabolism observed in their HIV-only cohort was not evident in their HIV/TB co-infected cohort. Although no significant changes in whole-body protein metabolism were observed in their TB-only group, their results indicated that *Mtb* infection could alter the net protein anabolic state in HIV-infected patients.

Since all significantly altered metabolites and metabolic trends within the HIV/TB co-infection group were also found in either the HIV-only or TB-only states, the driving agent of these metabolic alterations (HIV or *Mtb*) can be inferred based on the mono-infected state where similar alterations were observed. Therefore, it is probable that the metabolic alterations in the co-infected group have similar causes and/or metabolic effects as in the mono-infected groups. The lack of a clear net protein anabolic or catabolic shift in the HIV/TB co-infected group suggests that whole-body protein metabolism might not significantly contribute to the altered amino acids in this group. This could explain why the HIV/TB co-infected group had fewer significant amino acid features (n=4) compared to both the HIV-only infected (n=7) and TB-only (n=11) groups (Figure 4.6).

Compared to HIV, the altered urine metabolome in the HIV/TB co-infected cohort seems primarily driven by the *Mtb* infection. The HIV/TB co-infected cohort shared only a significant decrease in tryptophan with the HIV-only infected cohort. In contrast, this group mirrored the TB-only cohort with increased levels of hydroxykynurenine, and saccharopine, and a higher saccharopine/lysine ratio, and decreased glycine levels. A notable trend of increased medium-chain acylcarnitines, like the TB-only group, was also observed in the HIV/TB co-infected group. The significantly lowered tryptophan in the HIV/TB co-infected group may relate to malabsorption resulting from the HIV infection, as well as acetyl-CoA synthesis from elevated kynurenine pathway activity, likely due to *Mtb* infection. Although kynurenine pathway activity in the co-infected group was not as pronounced as in the TB-only group, hydroxykynurenine was the only kynurenine pathway metabolite significantly increased compared to healthy controls. The decreased glycine is likely due to hyperglycaemia, possibly related to diabetes or insulin resistance, while the increased saccharopine and saccharopine/lysine ratio levels strongly indicate enhanced lysine degradation via the saccharopine pathway to generate intermediates for oxidative phosphorylation. Although, lysine was not significantly altered in this study, enhanced saccharopine pathway activity may explain the significantly depleted lysine levels previously observed in the serum of our untreated co-infected HIV/TB patients (Herbert *et al.*, 2023). Furthermore, the generally increased medium-chain acylcarnitines hint at increased fatty acid oxidation and dysfunctional

mitochondrial respiration related to diabetes. In considering the metabolic alterations in the HIV/TB co-infected group, it is also important to consider the direct impact of HIV on mitochondrial function, which could be a contributing factor to the observed changes (Schank *et al.*, 2021).

As with the single-infection groups, 5-HIAA levels were not significantly affected compared to the controls. Yet, there appears to be a correlation between the mean tryptophan and 5-HIAA levels across the infection states, with both metabolites showing decreased mean values in the HIV-only and HIV/TB co-infected states and increased in the TB-only state compared to healthy controls.

4.6.5. The impact of amino acid and acylcarnitine alterations on health and metabolism

The observed disruptions in amino acid levels have significant implications for overall health and metabolic state. Amino acids are essential for numerous physiological processes, including protein synthesis, immune function, and energy metabolism (Wu, 2010, 2013). Thus, changes in proteinogenic amino acids could compromise protein synthesis, affecting skeletal muscle mass and strength, and potentially worsening skeletal muscle wasting often seen in HIV and TB patients (Luies & Du Preez, 2020). This condition, known as wasting syndrome or cachexia, is characterised by unintentional weight loss and can significantly impair physical functioning and quality of life (Evans *et al.*, 2008).

Amino acids, vital for immune function, show significant variations in our HIV-only infected group, where low levels typically activate an enzyme inhibiting HIV replication (see Section 2.6) (Afroz *et al.*, 2020; Del Pino *et al.*, 2012). The absence of these lowered amino acid levels in our HIV/TB co-infected cohort could lead to the inactivation of this enzyme, potentially explaining the enhanced HIV replication and contributing to increased disease severity in these individuals. In addition, the enhanced kynurenine pathway activity in our HIV/TB co-infected, absent in the HIV-only infected group, may exacerbate TB's immunosuppressive effects on HIV infection through the inactivation of CD8+ cells targeting HIV-infected cells (see Section 2.4) (Mbongue *et al.*, 2015).

Furthermore, amino acids are precursors to neurotransmitters, influencing mood, cognitive function, and overall neurological health — areas that are already of concern in especially HIV due to the virus' potential neurotoxic effects (Ling *et al.*, 2023). While our data did not show systemic alterations in the serotonin pathway, the significantly depleted tryptophan levels in both the HIV-only and HIV/TB co-infected cohorts could still the affect serotonin pathway in the CNS. Brain serotonin levels depend on tryptophan transport through the blood-brain barrier, facilitated by the large neutral amino acid transporter 1, for serotonin production (Ogawa *et al.*, 2023). HIV-infection may thus impact neurological health in HIV/TB co-infected individuals, as tryptophan levels, unaffected in the TB-only group, were significantly decreased in those with HIV/TB co-infection.

Therefore, understanding and addressing the alterations in amino acid metabolism in HIV, TB, and HIV/TB co-infection is critical, not only for understanding the disease's pathophysiology but also for

developing comprehensive treatment strategies aimed at improving the overall health and quality of life of affected individuals.

The observed changes in acylcarnitine levels, particularly in TB and HIV/TB co-infected patients, have profound implications for health and metabolic function. Acylcarnitines play a crucial role in fatty acid oxidation, an energy-generating process, especially under metabolic stress or increased energy demand (Dambrova *et al.*, 2022; Rinaldo *et al.*, 2008). Elevated medium-chain acylcarnitine levels, as observed in TB and HIV/TB co-infection, may indicate increased fatty acid oxidation (Che *et al.*, 2018; Li *et al.*, 2018), possibly a compensatory response to the chronic infection and inflammation. However, persistent alterations in acylcarnitine metabolism can lead to disrupted energy homeostasis and mitochondrial dysfunction, contributing to muscle wasting, fatigue, and reduced physiological resilience (Batchuluun *et al.*, 2018; Kuratsune *et al.*, 1994; Malaguarnera *et al.*, 2006). These changes also have implications for insulin resistance and diabetes, conditions frequently associated with chronic infections like TB (Batchuluun *et al.*, 2018). Therefore, the observed acylcarnitine profile alterations in these disease states highlight the complex interplay between infection, metabolism, and systemic health. Monitoring and addressing these changes are vital for comprehensive management of HIV, TB, and HIV/TB co-infection, aiming at controlling the infection and mitigating its metabolic and systemic consequences.

4.6.6. Conclusion

The amino acid metabolome was notably affected in the three disease states observed compared to the healthy controls, as depicted in Figure 4.8. The effects of infection with HIV-only and *Mtb*-only on the urine amino acid metabolome were substantially different. In the HIV-only infection cohort, the amino acid metabolome was characterised by generally decreased amino acid levels, likely due to a combination of net anabolic protein turnover, malabsorption, and increased gluconeogenesis. Conversely, the TB-only cohort showed a net protein catabolic state, possibly leading to the observed increase in amino acid levels. The amino acid profile in the TB-only group suggests the presence or risk of diabetes associated with hyperglycemia and indicates increased activity in the kynurenine and saccharopine pathways of tryptophan and lysine metabolism, respectively.

In the HIV/TB co-infected group, the metabolomic alterations were predominantly influenced by TB, since the amino acid and acylcarnitine profiles of this group compared to the healthy controls more closely resembled those of the TB-only group. A significant number of the amino acid features prominent in the HIV-only and TB-only cohorts were absent in co-infected cohort, suggesting possible attenuation of HIV's effects on the urine amino acid metabolome by TB, or vice versa. The urine metabolome of the HIV/TB co-infected metabolome suggests enhanced activity of the kynurenine and saccharopine pathways, as well as glycine cleavage system, and aberrant fatty acid oxidation, all of which appear to be predominantly influenced by TB. These findings, characterised using LC-MS metabolomics, provide crucial insights into the metabolic complexities associated with these conditions.

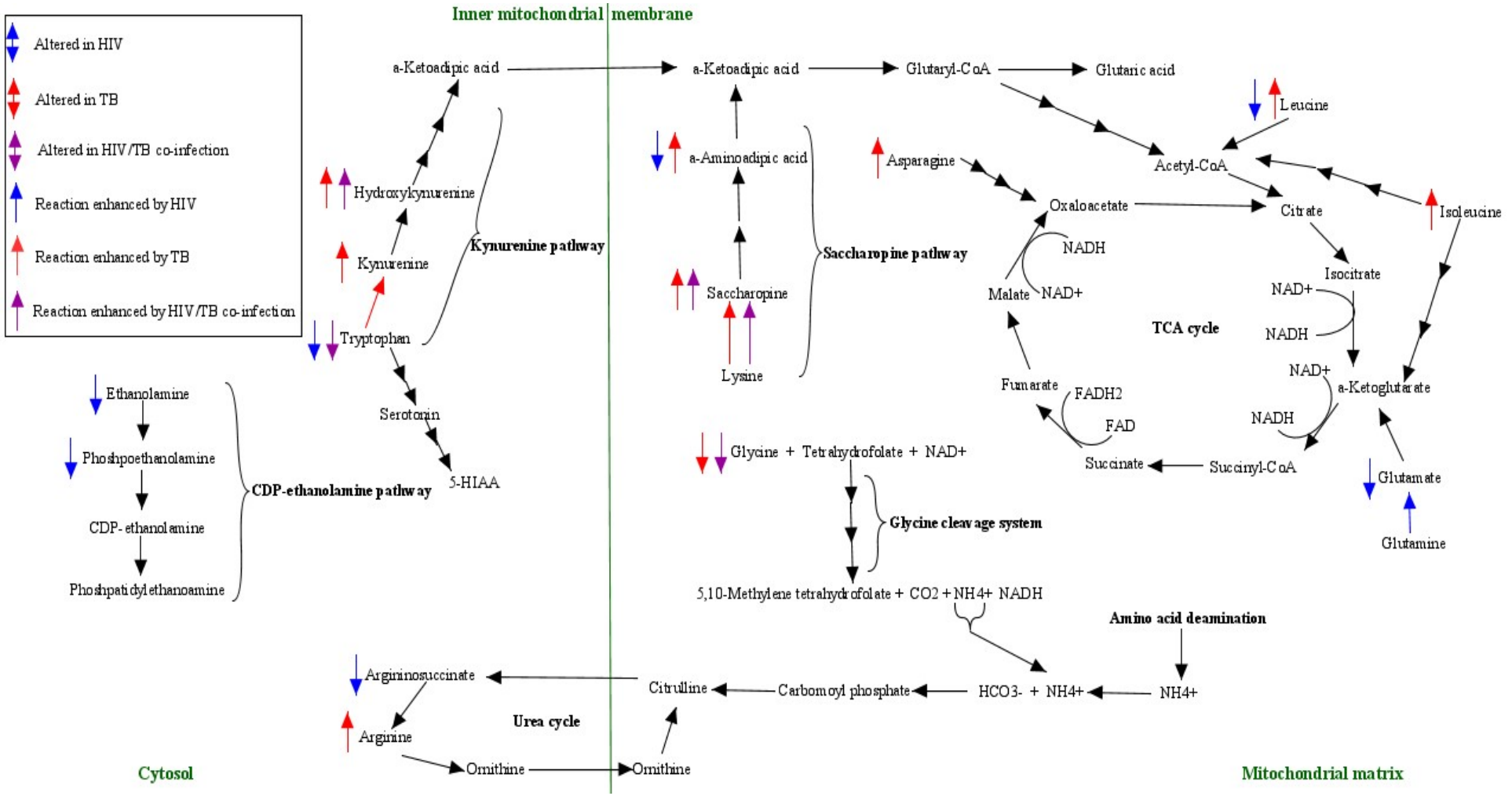

Figure 4.8: Amino acid metabolism pathways influenced by infection states. *This figure delineates the specific effects of HIV, TB, and HIV/TB co-infection on amino acid metabolic pathways, with alterations marked by colour-coded arrows. It highlights the reactions that are either upregulated or downregulated in the context of each infection, offering insight into the metabolic disturbances associated with these disease states. Abbreviations: 5-HIAA: 5-hydroxyindoleacetic acid; CDP-ethanolamine: cytidine diphosphate-ethanolamine; CO_2: carbon dioxide; HCO_3^-: bicarbonate; NH_4^+: ammonium; TCA cycle: tricarboxylic acid cycle; NAD+: nicotinamide adenine dinucleotide; FAD: flavin adenine dinucleotide.*

CHAPTER 5: CONCLUSIONS AND FUTURE PROSPECTS

5.1. Conclusions

The extensive analysis of the urinary metabolome in patients with HIV, TB, and HIV/TB co-infection has unveiled distinct metabolic alterations that provide deeper insights into the pathophysiological implications of these diseases. The HIV-only cohort exhibited a notable reduction in amino acid levels, which could be attributed to a combination of malnutrition and an anabolic protein turnover state. This finding underscores the complex metabolic challenges faced by HIV-infected individuals, highlighting the necessity for nutritional support and metabolic management in these patients.

Conversely, the TB-only group presented with a distinct increase in urinary amino acid levels, indicative of a catabolic protein turnover state. Several metabolic features in this group correlated with hyperglycaemia associated with diabetes, suggesting a significant interplay between TB and metabolic disorders like diabetes. This correlation is particularly important, given the rising prevalence of both TB and diabetes globally.

The HIV/TB co-infected state showcased a unique metabolic profile, characterised by significantly decreased tryptophan and glycine levels and increased hydroxykynurenine and saccharopine, with an elevated saccharopine/lysine ratio. These alterations suggest significant disruptions in the kynurenine and saccharopine pathways. Additionally, the presence of elevated medium-chain acylcarnitines, although not statistically significant, hints at enhanced fatty acid oxidation processes. This metabolic pattern is indicative of a state that potentially aligns with hyperglycaemia and metabolic conditions akin to diabetes. These metabolic insights underscore the intricate interplay between HIV infection and TB and their combined impact on the host's metabolic processes, emphasising the need for nuanced understanding and management strategies in co-infected individuals.

Interestingly, the metabolic changes observed in the co-infected state appear to be primarily driven by the *Mtb* infection, which could have significant implications for the management and treatment of HIV/TB co-infected patients. This study lays the groundwork for future research aiming to validate these findings and explore in greater depth the effect of HIV/TB co-infection on the host amino acid and lipid metabolism. The insights gained from this study can serve as a catalyst for developing targeted interventions that address the specific metabolic needs of individuals suffering from these complex infectious diseases.

In conclusion, this dissertation contributes significantly to our understanding of the metabolic alterations associated with HIV, TB, and their co-infection. It highlights the need for a comprehensive approach to the management of these diseases, considering not only the infectious agents but also the profound metabolic implications they bring. The findings from this study are pivotal for guiding future research directions and improving clinical strategies for managing the HIV/TB syndemic.

5.2. Future prospects

The results of this study illuminate the distinct urinary amino acid urine metabolome of individuals co-infected with HIV/TB, which not only differs from healthy individuals but also from those with either a single HIV or *Mtb* infection. This highlights the critical importance of including an HIV/TB co-infected group or establishing an exclusion criterion that prevents HIV/TB co-infected individuals from participating in studies aimed at observing the specific effects of HIV infection or TB disease on the metabolome. This is underscored by the significant portion of the metabolic perturbations typically associated with HIV-only or *Mtb*-only infection that was notably absent in the HIV/TB co-infected cohort. This finding is pivotal for guiding future research, particularly in the realm of metabolomics, to identify biomarkers for HIV/TB co-infection, develop robust diagnostic techniques, and monitor disease progression. The metabolic alterations commonly linked with HIV or *Mtb* infection are attenuated in co-infection, indicating that features significantly altered in the HIV/TB co-infected state, such as tryptophan and glycine, could serve as more reliable targets for future studies.

Repeating this study with larger sample cohorts, particularly those with HIV/TB co-infection (n=9) and HIV-only infection (n=7), would be beneficial to validate these findings. Additional clinical information about the subjects could also enhance the interpretation of the results. Complete viral load and CD4+ cell counts in the HIV and HIV/TB co-infected groups could provide valuable insights into the severity of HIV infection. Furthermore, blood glucose and insulin measurements would substantiate the link between diabetes and/or hyperglycaemia in TB and HIV/TB co-infected individuals. Investigating whole-body protein turnover using stable isotopic tracers, such as ^{15}N glycine, ^{13}C lysine, and ^{2}H phenylalanine administered intravenously, followed by analysis at isotopic steady state, would enable a more comprehensive understanding of whether a net protein anabolic or catabolic state could influence aberrant amino acid levels in a disease context.

Additionally, a broader metabolomic analysis encompassing lipids, specifically acyl-CoAs and phosphatidylethanolamines, would provide deeper insights into the lipid metabolism of the infected cohorts. The analysis of acyl-CoAs and phosphatidylethanolamines, in particular, could corroborate whether fatty acid oxidation and the CDP-ethanolamine pathway are altered in the infected cohorts, as suggested by the current findings. Targeted organic acid analysis indicative of mitochondrial function and oxidative stress markers could also contribute to our knowledge regarding HIV/TB co-infection. The integration of these additional analyses would not only validate the results obtained but also significantly enhance our understanding of the metabolic complexities associated with HIV, TB, and their co-infection.

REFERENCES

Abubakar, I., Pimpin, L., Ariti, C., Beynon, R., Mangtani, P., Sterne, J., Fine, P., Smith, P., Lipman, M. & Elliman, D. 2013. Systematic review and meta-analysis of the current evidence on the duration of protection by bacillus Calmette-Guérin vaccination against tuberculosis. *Health technology assessment (Winchester, England)*, 17(37):1.

Achouba, A., Dumas, P. & Ayotte, P. 2023. Simultaneous determination of ergothioneine, selenoneine, and their methylated metabolites in human blood using ID-LC–MS/MS. *Analytical and Bioanalytical Chemistry*:1-9.

Adeva-Andany, M., Souto-Adeva, G., Ameneiros-Rodríguez, E., Fernández-Fernández, C., Donapetry-García, C. & Domínguez-Montero, A. 2018. Insulin resistance and glycine metabolism in humans. *Amino Acids*, 50:11-27.

Adu-Gyamfi, C.G., Savulescu, D., George, J.A. & Suchard, M.S. 2019. Indoleamine 2, 3-dioxygenase-mediated tryptophan catabolism: a leading star or supporting act in the tuberculosis and HIV pas-de-deux? *Frontiers in cellular and infection microbiology*, 9:372.

Adu-Gyamfi, C.G., Snyman, T., Hoffmann, C.J., Martinson, N.A., Chaisson, R.E., George, J.A. & Suchard, M.S. 2017. Plasma indoleamine 2, 3-dioxygenase, a biomarker for tuberculosis in human immunodeficiency virus-infected patients. *Clinical Infectious Diseases*, 65(8):1356-1363.

Afroz, S., Battu, S., Giddaluru, J. & Khan, N. 2020. Dengue virus induced COX-2 signaling is regulated through nutrient sensor GCN2. *Frontiers in immunology*, 11:1831.

Alessio, L., Berlin, A., Dell'Orto, A., Toffoletto, F. & Ghezzi, I. 1985. Reliability of urinary creatinine as a parameter used to adjust values of urinary biological indicators. *International archives of occupational and environmental health*, 55(2):99-106.

Alexander, T.S. 2016. Human immunodeficiency virus diagnostic testing: 30 years of evolution. *Clinical and Vaccine Immunology*, 23(4):249-253.

Allers, K., Hütter, G., Hofmann, J., Loddenkemper, C., Rieger, K., Thiel, E. & Schneider, T. 2011. Evidence for the cure of HIV infection by CCR5Δ32/Δ32 stem cell transplantation. *Blood, The Journal of the American Society of Hematology*, 117(10):2791-2799.

Alonso, A., Marsal, S. & Julià, A. 2015. Analytical methods in untargeted metabolomics: state of the art in 2015. *Frontiers in bioengineering and biotechnology*, 3:23.

Amalia, F., Syamsunarno, M.R.A., Triatin, R.D., Fatimah, S.N., Chaidir, L. & Achmad, T.H. 2022. The role of amino acids in tuberculosis infection: A literature review. *Metabolites*, 12(10):933.

Angeles, L.F. & Aga, D.S. 2018. Establishing analytical performance criteria for the global reconnaissance of antibiotics and other pharmaceutical residues in the aquatic environment using liquid chromatography-tandem mass spectrometry. *Journal of analytical methods in chemistry*, 2018,

Anton, P.A., Elliott, J., Poles, M.A., McGowan, I.M., Matud, J., Hultin, L.E., Grovit-Ferbas, K., Mackay, C.R., Chen, I.S. & Giorgi, J.V. 2000. Enhanced levels of functional HIV-1 co-receptors on human mucosal T cells demonstrated using intestinal biopsy tissue. *Aids*, 14(12):1761-1765.

Arbeláez, M.P., Nelson, K.E. & Muñoz, A. 2000. BCG vaccine effectiveness in preventing tuberculosis and its interaction with human immunodeficiency virus infection. *International journal of epidemiology*, 29(6):1085-1091.

Armbruster, D.A. & Pry, T. 2008. Limit of blank, limit of detection and limit of quantitation. *The clinical biochemist reviews*, 29(Suppl 1):S49.

Armstrong, J. & Hart, P.D.A. 1971. Response of cultured macrophages to Mycobacterium tuberculosis, with observations on fusion of lysosomes with phagosomes. *The Journal of experimental medicine*, 134(3):713-740.

Arts, E.J. & Hazuda, D.J. 2012. HIV-1 antiretroviral drug therapy. *Cold Spring Harbor perspectives in medicine*, 2(4):a007161.

Bares, S.H. & Swindells, S. 2020. Latent Tuberculosis and HIV Infection. *Current Infectious Disease Reports*, 22(7):1-8.

Barker, L.P., George, K.M., Falkow, S. & Small, P. 1997. Differential trafficking of live and dead Mycobacterium marinum organisms in macrophages. *Infection and immunity*, 65(4):1497-1504.

Barré-Sinoussi, F., Chermann, J.-C., Rey, F., Nugeyre, M.T., Chamaret, S., Gruest, J., Dauguet, C., Axler-Blin, C., Vézinet-Brun, F. & Rouzioux, C. 1983. Isolation of a T-lymphotropic retrovirus from a patient at risk for acquired immune deficiency syndrome (AIDS). *Science*, 220(4599):868-871.

Batchuluun, B., Al Rijjal, D., Prentice, K.J., Eversley, J.A., Burdett, E., Mohan, H., Bhattacharjee, A., Gunderson, E.P., Liu, Y. & Wheeler, M.B. 2018. Elevated medium-chain acylcarnitines are associated with gestational diabetes mellitus and early progression to type 2 diabetes and induce pancreatic β-cell dysfunction. *Diabetes*, 67(5):885-897.

Bedimo, R., Maalouf, N.M., Zhang, S., Drechsler, H. & Tebas, P. 2012. Osteoporotic fracture risk associated with cumulative exposure to tenofovir and other antiretroviral agents. *Aids*, 26(7):825-831.

Bentsen, C., McLaughlin, L., Mitchell, E., Ferrera, C., Liska, S., Myers, R., Peel, S., Swenson, P., Gadelle, S. & Shriver, M.K. 2011. Performance evaluation of the Bio-Rad Laboratories GS HIV Combo Ag/Ab EIA, a 4th generation HIV assay for the simultaneous detection of HIV p24 antigen and antibodies to HIV-1 (groups M and O) and HIV-2 in human serum or plasma. *Journal of Clinical Virology*, 52:S57-S61.

Beukes, D., van Reenen, M., Loots, D.T. & du Preez, I. 2023. Tuberculosis is associated with sputum metabolome variations, irrespective of patient sex or HIV status: an untargeted GCxGC-TOFMS study. *Metabolomics*, 19(6):55.

Bisht, M.K., Dahiya, P., Ghosh, S. & Mukhopadhyay, S. 2023. The cause–effect relation of tuberculosis on incidence of diabetes mellitus. *Frontiers in Cellular and Infection Microbiology*, 13,

Black, G.F., Weir, R.E., Floyd, S., Bliss, L., Warndorff, D.K., Crampin, A.C., Ngwira, B., Sichali, L., Nazareth, B. & Blackwell, J.M. 2002. BCG-induced increase in interferon-gamma response to mycobacterial antigens and efficacy of BCG vaccination in Malawi and the UK: two randomised controlled studies. *The Lancet*, 359(9315):1393-1401.

Boasso, A., Shearer, G. & Chougnet, C. 2009. Immune dysregulation in human immunodeficiency virus infection: know it, fix it, prevent it? *Journal of internal medicine*, 265(1):78-96.

Boirivant, M., Viora, M., Giordani, L., Luzzati, A.L., Pronio, A.M., Montesani, C. & Pugliese, O. 1998. HIV-1 gp120 accelerates Fas-mediated activation-induced human lamina propria T cell apoptosis. *Journal of clinical immunology*, 18(1):39-47.

Borrow, P., Lewicki, H., Hahn, B.H., Shaw, G.M. & Oldstone, M. 1994. Virus-specific CD8+ cytotoxic T-lymphocyte activity associated with control of viremia in primary human immunodeficiency virus type 1 infection. *Journal of virology*, 68(9):6103-6110.

Bouatra, S., Aziat, F., Mandal, R., Guo, A.C., Wilson, M.R., Knox, C., Bjorndahl, T.C., Krishnamurthy, R., Saleem, F. & Liu, P. 2013. The human urine metabolome. *PloS one*, 8(9):e73076.

Branco, A.C.C.C., Yoshikawa, F.S.Y., Pietrobon, A.J. & Sato, M.N. 2018. Role of histamine in modulating the immune response and inflammation. *Mediators of inflammation*, 2018,

Brandt, L., Feino Cunha, J., Weinreich Olsen, A., Chilima, B., Hirsch, P., Appelberg, R. & Andersen, P. 2002. Failure of the Mycobacterium bovis BCG vaccine: some species of environmental mycobacteria block multiplication of BCG and induction of protective immunity to tuberculosis. *Infection and immunity*, 70(2):672-678.

Brenchley, J.M., Price, D.A., Schacker, T.W., Asher, T.E., Silvestri, G., Rao, S., Kazzaz, Z., Bornstein, E., Lambotte, O. & Altmann, D. 2006. Microbial translocation is a cause of systemic immune activation in chronic HIV infection. *Nature medicine*, 12(12):1365-1371.

Brennan, A., Evans, D., Maskew, M., Naicker, S., Ive, P., Sanne, I., Maotoe, T. & Fox, M. 2011. Relationship between renal dysfunction, nephrotoxicity and death among HIV adults on tenofovir. *AIDS (London, England)*, 25(13):1603.

Brown, C., Houghton, B.J., Souhami, R. & Richards, P. 1972. The effects of low-protein diet and uraemia upon urea-cycle enzymes and transaminases in rats. *Clinical science*, 43(3):371-376.

Butorov, E.V. 2017. Plasma L-carnitine and L-lysine concentrations in HIV-infected patients. *The open biochemistry journal*, 11:119.

Cambier, C., Falkow, S. & Ramakrishnan, L. 2014. Host evasion and exploitation schemes of Mycobacterium tuberculosis. *Cell*, 159(7):1497-1509.

Cao, Y.-F., Li, J., Zhang, Z., Liu, J., Sun, X.-Y., Feng, X.-F., Luo, H.-H., Yang, W., Li, S.-N. & Yang, X. 2019. Plasma levels of amino acids related to urea cycle and risk of type 2 diabetes mellitus in Chinese adults. *Frontiers in endocrinology*, 10:50.

Caradonna, L., Amati, L., Magrone, T., Pellegrino, N., Jirillo, E. & Caccavo, D. 2000. Invited review: Enteric bacteria, lipopolysaccharides and related cytokines in inflammatory bowel disease: biological and clinical significance. *Journal of endotoxin research*, 6(3):205-214.

Carranza, C., Pedraza-Sanchez, S., de Oyarzabal-Mendez, E. & Torres, M. 2020. Diagnosis for latent tuberculosis infection: New alternatives. *Frontiers in immunology*:2006.

Centers for Disease Control and Prevention. 1992. *1993 Revised Classification System for HIV Infection and Expanded Surveillance Case Definition for AIDS Among Adolescents and Adults* https://www.cdc.gov/mmwr/preview/mmwrhtml/00018871.htm Date of access: 15 June 2022.

Chandel, N.S. 2021. Amino acid metabolism. *Cold Spring Harbor Perspectives in Biology*, 13(4):a040584.

Chang, S.W., Pan, W.S., Lozano Beltran, D., Oleyda Baldelomar, L., Solano, M.A., Tuero, I., Friedland, J.S., Torrico, F. & Gilman, R.H. 2013. Gut hormones, appetite suppression and cachexia in patients with pulmonary TB. *PloS one*, 8(1):e54564.

Che, N., Ma, Y., Ruan, H., Xu, L., Wang, X., Yang, X. & Liu, X. 2018. Integrated semi-targeted metabolomics analysis reveals distinct metabolic dysregulation in pleural effusion caused by tuberculosis and malignancy. *Clinica Chimica Acta*, 477:81-88.

Che, N., Cheng, J., Li, H., Zhang, Z., Zhang, X., Ding, Z., Dong, F. & Li, C. 2013. Decreased serum 5-oxoproline in TB patients is associated with pathological damage of the lung. *Clinica Chimica Acta*, 423:5-9.

Chenneville, T., Gabbidon, K., Hanson, P. & Holyfield, C. 2020. The impact of COVID-19 on HIV treatment and research: a call to action. *International journal of environmental research and public health*, 17(12):4548.

Chiu, I.-M., Yaniv, A., Dahlberg, J.E., Gazit, A., Skuntz, S.F., Tronick, S.R. & Aaronson, S.A. 1985. Nucleotide sequence evidence for relationship of AIDS retrovirus to lentiviruses. *Nature*, 317(6035):366-368.

Cho, Y., Park, Y., Sim, B., Kim, J., Lee, H., Cho, S.-N., Kang, Y. & Lee, S.-G. 2020. Identification of serum biomarkers for active pulmonary tuberculosis using a targeted metabolomics approach. *Scientific reports*, 10(1):1-11.

Chojnacki, C., Medrek-Socha, M., Blonska, A., Zajdel, R., Chojnacki, J. & Poplawski, T. 2022. A reduced tryptophan diet in patients with diarrhoea-predominant irritable bowel syndrome improves their abdominal symptoms and their quality of life through reduction of serotonin Levels and its urinary metabolites. *International Journal of Molecular Sciences*, 23(23):15314.

Chun, T.-W., Finzi, D., Margolick, J., Chadwick, K., Schwartz, D. & Siliciano, R.F. 1995. In vivo fate of HIV-1-infected T cells: quantitative analysis of the transition to stable latency. *Nature medicine*, 1(12):1284-1290.

Chun, T.-W., Carruth, L., Finzi, D., Shen, X., DiGiuseppe, J.A., Taylor, H., Hermankova, M., Chadwick, K., Margolick, J. & Quinn, T.C. 1997. Quantification of latent tissue reservoirs and total body viral load in HIV-1 infection. *Nature*, 387(6629):183-188.

Chun, T.-W., Justement, J.S., Murray, D., Hallahan, C.W., Maenza, J., Collier, A.C., Sheth, P.M., Kaul, R., Ostrowski, M. & Moir, S. 2010. Rebound of plasma viremia following cessation of antiretroviral therapy despite profoundly low levels of HIV reservoir: implications for eradication. *AIDS (London, England)*, 24(18):2803.

Clark, Z.D., Cutler, J.M. & Frank, E.L. 2017. Practical LC-MS/MS method for 5-hydroxyindoleacetic acid in urine. *The Journal of Applied Laboratory Medicine*, 1(4):387-399.

Clemens, D.L. & Horwitz, M.A. 1995. Characterization of the Mycobacterium tuberculosis phagosome and evidence that phagosomal maturation is inhibited. *The Journal of experimental medicine*, 181(1):257-270.

Clish, C.B. 2015. Metabolomics: an emerging but powerful tool for precision medicine. *Molecular Case Studies*, 1(1):a000588.

Collins, J.M., Siddiqa, A., Jones, D.P., Liu, K., Kempker, R.R., Nizam, A., Shah, N.S., Ismail, N., Ouma, S.G. & Tukvadze, N. 2020. Tryptophan catabolism reflects disease activity in human tuberculosis. *JCI insight*, 5(10),

Craigie, R. 2012. The molecular biology of HIV integrase. *Future virology*, 7(7):679-686.

Cross, A.J., Major, J.M. & Sinha, R. 2011. Urinary biomarkers of meat consumption. *Cancer epidemiology, biomarkers & prevention*, 20(6):1107-1111.

Cuomo, P., Capparelli, R., Iannelli, A. & Iannelli, D. 2022. Role of branched-chain amino acid metabolism in type 2 diabetes, obesity, cardiovascular disease and non-alcoholic fatty liver disease. *International Journal of Molecular Sciences*, 23(8):4325.

Dambrova, M., Makrecka-Kuka, M., Kuka, J., Vilskersts, R., Nordberg, D., Attwood, M.M., Smesny, S., Sen, Z.D., Guo, A.C. & Oler, E. 2022. Acylcarnitines: nomenclature, biomarkers, therapeutic potential, drug targets, and clinical trials. *Pharmacological Reviews*, 74(3):506-551.

Das, B. 2011. Validation protocol: first step of a lean-total quality management principle in a new laboratory set-up in a tertiary care hospital in India. *Indian Journal of Clinical Biochemistry*, 26:235-243.

Davis, J.M. & Ramakrishnan, L. 2009. The role of the granuloma in expansion and dissemination of early tuberculous infection. *Cell*, 136(1):37-49.

De Blaauw, I., Deutz, N. & Von Meyenfeldt, M. 1996. In vivo amino acid metabolism of gut and liver during short and prolonged starvation. *American Journal of Physiology-Gastrointestinal and Liver Physiology*, 270(2):G298-G306.

De Deurwaerdère, P. & Di Giovanni, G. 2020. Serotonin in health and disease. *International journal of molecular sciences*, 21(10):3500.

De Martino, M., Lodi, L., Galli, L. & Chiappini, E. 2019. Immune response to Mycobacterium tuberculosis: a narrative review. *Frontiers in pediatrics*:350.

De Villiers, L. & Loots, D.T. 2013. Using metabolomics for elucidating the mechanisms related to tuberculosis treatment failure. *Current Metabolomics*, 1(4):306-317.

Deeks, S.G., Lewin, S.R. & Havlir, D.V. 2013. The end of AIDS: HIV infection as a chronic disease. *The lancet*, 382(9903):1525-1533.

Deeks, S.G., Overbaugh, J., Phillips, A. & Buchbinder, S. 2015. HIV infection. *Nature reviews Disease primers*, 1(1):1-22.

Del Pino, J., Jiménez, J.L., Ventoso, I., Castello, A., Muñoz-Fernández, M.Á., de Haro, C. & Berlanga, J.J. 2012. GCN2 has inhibitory effect on human immunodeficiency virus-1 protein synthesis and is cleaved upon viral infection. *PloS one*,

Derave, W., Everaert, I., Beeckman, S. & Baguet, A. 2010. Muscle carnosine metabolism and β-alanine supplementation in relation to exercise and training. *Sports medicine*, 40(3):247-263.

Ding, Y., Raterink, R.-J., Marín-Juez, R., Veneman, W.J., Egbers, K., van den Eeden, S., Haks, M.C., Joosten, S.A., Ottenhoff, T.H. & Harms, A.C. 2020. Tuberculosis causes highly conserved metabolic changes in human patients, mycobacteria-infected mice and zebrafish larvae. *Scientific reports*, 10(1):1-13.

Doitsh, G., Cavrois, M., Lassen, K.G., Zepeda, O., Yang, Z., Santiago, M.L., Hebbeler, A.M. & Greene, W.C. 2010. Abortive HIV infection mediates CD4 T cell depletion and inflammation in human lymphoid tissue. *Cell*, 143(5):789-801.

Drewes, J.L., Meulendyke, K.A., Liao, Z., Witwer, K.W., Gama, L., Ubaida-Mohien, C., Li, M., Notarangelo, F.M., Tarwater, P.M. & Schwarcz, R. 2015. Quinolinic acid/tryptophan ratios predict neurological disease in SIV-infected macaques and remain elevated in the brain under cART. *Journal of neurovirology*, 21:449-463.

Embretson, J., Zupancic, M., Ribas, J.L., Burke, A., Racz, P., Tenner-Racz, K. & Haase, A.T. 1993. Massive covert infection of helper T lymphocytes and macrophages by HIV during the incubation period of AIDS. *Nature*, 362(6418):359-362.

Emwas, A.-H.M. 2015. The strengths and weaknesses of NMR spectroscopy and mass spectrometry with particular focus on metabolomics research. In. *Metabonomics*: Springer. pp. 161-193.

Estaquier, J., Idziorek, T., Zou, W., Emilie, D., Farber, C.-M., Bourez, J.-M. & Ameisen, J.C. 1995. T helper type 1/T helper type 2 cytokines and T cell death: preventive effect of interleukin 12 on activation-induced and CD95 (FAS/APO-1)-mediated apoptosis of CD4+ T cells from human immunodeficiency virus-infected persons. *The Journal of experimental medicine*, 182(6):1759-1767.

Estaquier, J.M., Idziorek, T., De Bels, F., Barré-Sinoussi, F., Hurtrel, B., Aubertin, A.-M., Venet, A., Mehtali, M., Muchmore, E. & Michel, P. 1994. Programmed cell death and AIDS: significance of T-cell apoptosis in pathogenic and nonpathogenic primate lentiviral infections. *Proceedings of the National Academy of Sciences*, 91(20):9431-9435.

Evans, W.J., Morley, J.E., Argilés, J., Bales, C., Baracos, V., Guttridge, D., Jatoi, A., Kalantar-Zadeh, K., Lochs, H. & Mantovani, G. 2008. Cachexia: a new definition. *Clinical nutrition*, 27(6):793-799.

Exton, M.S. 1997. Infection-induced anorexia: active host defence strategy. *Appetite*, 29(3):369-383.

Falvo, J.V., Ranjbar, S., Jasenosky, L.D. & Goldfeld, A.E. 2011. Arc of a vicious circle: pathways activated by Mycobacterium tuberculosis that target the HIV-1 long terminal repeat. *American journal of respiratory cell and molecular biology*, 45(6):1116-1124.

Falzon, D., Zignol, M., Bastard, M., Floyd, K. & Kasaeva, T. 2023. The impact of the COVID-19 pandemic on the global tuberculosis epidemic. *Frontiers in Immunology*, 14,

Favre, D., Mold, J., Hunt, P.W., Kanwar, B., Loke, P.n., Seu, L., Barbour, J.D., Lowe, M.M., Jayawardene, A. & Aweeka, F. 2010. Tryptophan catabolism by indoleamine 2, 3-dioxygenase 1 alters the balance of TH17 to regulatory T cells in HIV disease. *Science translational medicine*, 2(32):32ra36-32ra36.

Fearon, M. 2005. The laboratory diagnosis of HIV infections. *Canadian Journal of Infectious Diseases and Medical Microbiology*, 16:26-30.

Finzi, D., Hermankova, M., Pierson, T., Carruth, L.M., Buck, C., Chaisson, R.E., Quinn, T.C., Chadwick, K., Margolick, J. & Brookmeyer, R. 1997. Identification of a reservoir for HIV-1 in patients on highly active antiretroviral therapy. *Science*, 278(5341):1295-1300.

Fløe, A., Hilberg, O., Wejse, C., Ibsen, R. & Løkke, A. 2018. Comorbidities, mortality and causes of death among patients with tuberculosis in Denmark 1998–2010: a nationwide, register-based case–control study. *Thorax*, 73(1):70-77.

Food and Drug Administration. 2018. Bioanalytical method validation. Guidance for industry. US Department of Health and Human Services. *Center for Drug Evaluation and Research (CDER), Center for Veterinary Medicine (CVM), Silver Spring, MD*,

Frumento, G., Rotondo, R., Tonetti, M., Damonte, G., Benatti, U. & Ferrara, G.B. 2002. Tryptophan-derived catabolites are responsible for inhibition of T and natural killer cell proliferation induced by indoleamine 2, 3-dioxygenase. *The Journal of experimental medicine*, 196(4):459-468.

Fukawa, T., Yan-Jiang, B.C., Min-Wen, J.C., Jun-Hao, E.T., Huang, D., Qian, C.-N., Ong, P., Li, Z., Chen, S. & Mak, S.Y. 2016. Excessive fatty acid oxidation induces muscle atrophy in cancer cachexia. *Nature medicine*, 22(6):666-671.

Gallo, R.C., Salahuddin, S.Z., Popovic, M., Shearer, G.M., Kaplan, M., Haynes, B.F., Palker, T.J., Redfield, R., Oleske, J. & Safai, B. 1984. Frequent detection and isolation of cytopathic retroviruses (HTLV-III) from patients with AIDS and at risk for AIDS. *science*, 224(4648):500-503.

Gandhi, R.T., Chen, B.K., Straus, S.E., Dale, J.K., Lenardo, M.J. & Baltimore, D. 1998. HIV-1 directly kills CD4+ T cells by a Fas-independent mechanism. *The Journal of experimental medicine*, 187(7):1113-1122.

Ganji, R., Dhali, S., Rizvi, A., Rapole, S. & Banerjee, S. 2016. Understanding HIV-Mycobacteria synergism through comparative proteomics of intra-phagosomal mycobacteria during mono-and HIV co-infection. *Scientific reports*, 6(1):1-14.

Gao, F., Bailes, E., Robertson, D.L., Chen, Y., Rodenburg, C.M., Michael, S.F., Cummins, L.B., Arthur, L.O., Peeters, M. & Shaw, G.M. 1999. Origin of HIV-1 in the chimpanzee Pan troglodytes troglodytes. *Nature*, 397(6718):436-441.

Gaschen, B., Taylor, J., Yusim, K., Foley, B., Gao, F., Lang, D., Novitsky, V., Haynes, B., Hahn, B.H. & Bhattacharya, T. 2002. Diversity considerations in HIV-1 vaccine selection. *Science*, 296(5577):2354-2360.

Gasper, M.A., Hesseling, A.C., Mohar, I., Myer, L., Azenkot, T., Passmore, J.-A.S., Hanekom, W., Cotton, M.F., Crispe, I.N. & Sodora, D.L. 2017. BCG vaccination induces HIV target cell activation in HIV-exposed infants in a randomized trial. *JCI insight*, 2(7),

Gautam, U.S., Foreman, T.W., Bucsan, A.N., Veatch, A.V., Alvarez, X., Adekambi, T., Golden, N.A., Gentry, K.M., Doyle-Meyers, L.A. & Russell-Lodrigue, K.E. 2018. In vivo inhibition of tryptophan catabolism reorganizes the tuberculoma and augments immune-mediated control of Mycobacterium tuberculosis. *Proceedings of the National Academy of Sciences*, 115(1):E62-E71.

Gelato, M., McNurlan, M. & Freedland, E. 2007. Role of recombinant human growth hormone in HIV-associated wasting and cachexia: pathophysiology and rationale for treatment. *Clinical Therapeutics*, 29(11):2269-2288.

Geldmacher, C., Ngwenyama, N., Schuetz, A., Petrovas, C., Reither, K., Heeregrave, E.J., Casazza, J.P., Ambrozak, D.R., Louder, M. & Ampofo, W. 2010. Preferential infection and depletion of Mycobacterium tuberculosis–specific CD4 T cells after HIV-1 infection. *Journal of Experimental Medicine*, 207(13):2869-2881.

Gerszten, R.E. & Wang, T.J. 2008. The search for new cardiovascular biomarkers. *Nature*, 451(7181):949-952.

Giesbertz, P., Ecker, J., Haag, A., Spanier, B. & Daniel, H. 2015. An LC-MS/MS method to quantify acylcarnitine species including isomeric and odd-numbered forms in plasma and tissues. *Journal of lipid research*, 56(10):2029-2039.

Gilboa, E., Mitra, S.W., Goff, S. & Baltimore, D. 1979. A detailed model of reverse transcription and tests of crucial aspects. *Cell*, 18(1):93-100.

Godzien, J., Alonso-Herranz, V., Barbas, C. & Armitage, E.G. 2015. Controlling the quality of metabolomics data: new strategies to get the best out of the QC sample. *Metabolomics*, 11:518-528.

González, O., Blanco, M.E., Iriarte, G., Bartolomé, L., Maguregui, M.I. & Alonso, R.M. 2014. Bioanalytical chromatographic method validation according to current regulations, with a special focus on the non-well defined parameters limit of quantification, robustness and matrix effect. *Journal of Chromatography A*, 1353:10-27.

Gottlieb, M.S., Schroff, R., Schanker, H.M., Weisman, J.D., Fan, P.T., Wolf, R.A. & Saxon, A. 1981. Pneumocystis carinii pneumonia and mucosal candidiasis in previously healthy homosexual men: evidence of a new acquired cellular immunodeficiency. *New England Journal of Medicine*, 305(24):1425-1431.

Gowda, G.N., Zhang, S., Gu, H., Asiago, V., Shanaiah, N. & Raftery, D. 2008. Metabolomics-based methods for early disease diagnostics. *Expert review of molecular diagnostics*, 8(5):617-633.

Grohmann, U. & Bronte, V. 2010. Control of immune response by amino acid metabolism. *Immunological reviews*, 236(1):243-264.

Guilhaudis, L., Jacobs, A. & Caffrey, M. 2002. Solution structure of the HIV gp120 C5 domain. *European journal of biochemistry*, 269(19):4860-4867.

Gupta, K.B., Gupta, R., Atreja, A., Verma, M. & Vishvkarma, S. 2009. Tuberculosis and nutrition. *Lung India*, 26(1):9-16.

Gupta, R.K., Lawn, S.D., Bekker, L.-G., Caldwell, J., Kaplan, R. & Wood, R. 2013. Impact of human immunodeficiency virus and CD4 count on tuberculosis diagnosis: analysis of city-wide data from Cape Town, South Africa. *The international journal of tuberculosis and lung disease*, 17(8):1014-1022.

Gupta, R.K., Peppa, D., Hill, A.L., Gálvez, C., Salgado, M., Pace, M., McCoy, L.E., Griffith, S.A., Thornhill, J. & Alrubayyi, A. 2020. Evidence for HIV-1 cure after CCR5Δ32/Δ32 allogeneic haemopoietic stem-cell transplantation 30 months post analytical treatment interruption: a case report. *The Lancet HIV*, 7(5):e340-e347.

Han, T.I., Kim, I.-O., Kim, W.S. & Yeon, K.M. 2000. Disseminated BCG infection in a patient with severe combined immunodeficiency. *Korean Journal of Radiology*, 1(2):114-117.

Hatamkhani, S., Khalili, H., Karimzadeh, I., Abdollahi, A., Jafari, S. & Khazaeipour, Z. 2013. Carnitine deficiency and its possible risk factors in TB patients: first report. *Immunotherapy*, 5(9):945-953.

Hellman, A.L. & Gram, M.C. 1993. The resurgence of tuberculosis: Risk in health care settings. *AAOHN Journal*, 41(2):66-72.

Herbert, C., Luies, L., Loots, D.T. & Williams, A.A. 2023. The metabolic consequences of HIV/TB co-infection. *BMC Infectious Diseases*, 23(1):536.

Herbst, S., Schaible, U.E. & Schneider, B.E. 2011. Interferon gamma activated macrophages kill mycobacteria by nitric oxide induced apoptosis. *PloS one*, 6(5):e19105.

Hermankova, M., Ray, S.C., Ruff, C., Powell-Davis, M., Ingersoll, R., Richard, T., Quinn, T.C., Siliciano, J.D., Siliciano, R.F. & Persaud, D. 2001. HIV-1 drug resistance profiles in children and adults with viral load of< 50 copies/ml receiving combination therapy. *Jama*, 286(2):196-207.

Hernandez-Vargas, E.A. & Middleton, R.H. 2013. Modeling the three stages in HIV infection. *Journal of theoretical biology*, 320:33-40.

Hewavitharana, A.K., Kassim, N.S.A. & Shaw, P.N. 2018. Standard addition with internal standardisation as an alternative to using stable isotope labelled internal standards to correct for matrix effects—Comparison and validation using liquid chromatography- tandem mass spectrometric assay of vitamin D. *Journal of Chromatography A*, 1553:101-107.

Heymsfield, S.B., Arteaga, C., McManus, C., Smith, J. & Moffitt, S. 1983. Measurement of muscle mass in humans: validity of the 24-hour urinary creatinine method. *The American journal of clinical nutrition*, 37(3):478-494.

Hirsch, V.M., Olmsted, R.A., Murphey-Corb, M., Purcell, R.H. & Johnson, P.R. 1989. An African primate lentivirus (SIVsmclosely related to HIV-2. *Nature*, 339(6223):389-392.

Höglund, E., Øverli, Ø. & Winberg, S. 2019. Tryptophan metabolic pathways and brain serotonergic activity: a comparative review. *Frontiers in endocrinology*:158.

Holeček, M. 2020. Why are branched-chain amino acids increased in starvation and diabetes? *Nutrients*, 12(10):3087.

Honig, A., Van Nieuwenhoven, M., Riedel, W. & Brummer, R.M. 2004. Acute tryptophan depletion affects brain-gut responses in irritable bowel syndrome patients and controls. *Gut*, 53(12):1794-1800.

Hou, Y. & Wu, G. 2018. Nutritionally essential amino acids. *Advances in Nutrition*, 9(6):849-851.

Hou, Y., Yin, Y. & Wu, G. 2015. Dietary essentiality of "nutritionally non-essential amino acids" for animals and humans. *Experimental Biology and Medicine*, 240(8):997-1007.

Hsu, D.C. & Sereti, I. 2016. Serious non-AIDS events: therapeutic targets of immune activation and chronic inflammation in HIV infection. *Drugs*, 76(5):533-549.

Huang, H., Li, Y., Liang, J. & Finkelman, F. 2018. Molecular regulation of histamine synthesis. Front Immunol 9: 1392. *Frontiers in Immunology*,

Hübner, W., McNerney, G.P., Chen, P., Dale, B.M., Gordon, R.E., Chuang, F.Y., Li, X.-D., Asmuth, D.M., Huser, T. & Chen, B.K. 2009. Quantitative 3D video microscopy of HIV transfer across T cell virological synapses. *Science*, 323(5922):1743-1747.

Jaffar, S., Wilkins, A., Ngom, P., Sabally, S., Corrah, T., Bangali, J., Rolfe, M. & Whittle, H. 1997. Rate of decline of percentage CD4+ cells is faster in HIV-1 than in HIV-2 infection. *JAIDS Journal of Acquired Immune Deficiency Syndromes*, 16(5):327-332.

Jankowska, M., Lemańska, M., Trocha, H., Gesing, M. & Smiatacz, T. 2001. Opportunistic infections in HIV-positive patients hospitalized in the Clinic of Infectious Diseases AMG. *Przeglad Epidemiologiczny*, 55:125-128.

Jeon, C.Y. & Murray, M.B. 2008. Diabetes mellitus increases the risk of active tuberculosis: a systematic review of 13 observational studies. *PLOS medicine*, 5(7):e152.

Jog, R., Chen, G., Wang, J. & Leff, T. 2021. Hormonal regulation of glycine decarboxylase and its relationship to oxidative stress. *Physiological Reports*, 9(15):e14991.

Johnson, L.F., Mossong, J., Dorrington, R.E., Schomaker, M., Hoffmann, C.J., Keiser, O., Fox, M.P., Wood, R., Prozesky, H. & Giddy, J. 2013. Life expectancies of South African adults starting antiretroviral treatment: collaborative analysis of cohort studies. *PLoS medicine*, 10(4):e1001418.

Joubert, F. & Puff, N. 2021. Mitochondrial cristae architecture and functions: lessons from minimal model systems. *Membranes*, 11(7):465.

Kandanearatchi, A. & Brew, B.J. 2012. The kynurenine pathway and quinolinic acid: pivotal roles in HIV associated neurocognitive disorders. *The FEBS journal*, 279(8):1366-1374.

Karaca, M., Martin-Levilain, J., Grimaldi, M., Li, L., Dizin, E., Emre, Y. & Maechler, P. 2018. Liver glutamate dehydrogenase controls whole-body energy partitioning through amino acid–derived gluconeogenesis and ammonia homeostasis. *Diabetes*, 67(10):1949-1961.

Kassa, D., de Jager, W., Gebremichael, G., Alemayehu, Y., Ran, L., Fransen, J., Wolday, D., Messele, T., Tegbaru, B. & Ottenhoff, T.H. 2016. The effect of HIV coinfection, HAART and TB treatment on cytokine/chemokine responses to Mycobacterium tuberculosis (Mtb) antigens in active TB patients and latently Mtb infected individuals. *Tuberculosis*, 96:131-140.

Keane, J. & Bresnihan, B. 2008. Tuberculosis reactivation during immunosuppressive therapy in rheumatic diseases: diagnostic and therapeutic strategies. *Current opinion in rheumatology*, 20(4):443-449.

Kema, I.P., de Vries, E.G. & Muskiet, F.A. 2000. Clinical chemistry of serotonin and metabolites. *Journal of Chromatography B: Biomedical Sciences and Applications*, 747(1-2):33-48.

Kerksick, C. & Willoughby, D. 2005. The antioxidant role of glutathione and N-acetyl-cysteine supplements and exercise-induced oxidative stress. *Journal of the international society of sports nutrition*, 2(2):38.

Khamis, M.M., Adamko, D.J. & El-Aneed, A. 2017. Mass spectrometric based approaches in urine metabolomics and biomarker discovery. *Mass spectrometry reviews*, 36(2):115-134.

Kikuchi, G., Motokawa, Y., Yoshida, T. & Hiraga, K. 2008. Glycine cleavage system: reaction mechanism, physiological significance, and hyperglycinemia. *Proceedings of the Japan Academy, Series B*, 84(7):246-263.

Klatzmann, D., Champagne, E., Chamaret, S., Gruest, J., Guetard, D., Hercend, T., Gluckman, J.-C. & Montagnier, L. 1984. T-lymphocyte T4 molecule behaves as the receptor for human retrovirus LAV. *Nature*, 312(5996):767-768.

Kochlik, B., Gerbracht, C., Grune, T. & Weber, D. 2018. The influence of dietary habits and meat consumption on plasma 3-methylhistidine—a potential marker for muscle protein turnover. *Molecular nutrition & food research*, 62(9):1701062.

Kogan, M.I., Naboka, Y.L., Ibishev, K.S., Gudima, I.A. & Naber, K.G. 2015. Human urine is not sterile-shift of paradigm. *Urologia internationalis*, 94(4):445-452.

Kulczyński, B., Sidor, A. & Gramza-Michałowska, A. 2019. Characteristics of selected antioxidative and bioactive compounds in meat and animal origin products. *Antioxidants*, 8(9):335.

Kumar, A., Kishore, L., Kaur, N. & Nair, A. 2012. Method development and validation: Skills and tricks. *Chronicles of young scientists*, 3(1):3-3.

Kumar, P. 2017. IFNγ-producing CD4+ T lymphocytes: the double-edged swords in tuberculosis. *Clinical and translational medicine*, 6(1):1-7.

Kuratsune, H., Yamaguti, K., Takahashi, M., Misaki, H., Tagawa, S. & Kitani, T. 1994. Acylcarnitine deficiency in chronic fatigue syndrome. *Clinical Infectious Diseases*, 18(Supplement_1):S62-S67.

Kuritzkes, D.R. 2016. Hematopoietic stem cell transplantation for HIV cure. *The Journal of clinical investigation*, 126(2):432-437.

Laforge, M., Petit, F., Estaquier, J. & Senik, A. 2007. Commitment to apoptosis in CD4+ T lymphocytes productively infected with human immunodeficiency virus type 1 is initiated by lysosomal membrane permeabilization, itself induced by the isolated expression of the viral protein Nef. *Journal of virology*, 81(20):11426-11440.

Lamers, Y., Williamson, J., Gilbert, L.R., Stacpoole, P.W. & Gregory III, J.F. 2007. Glycine turnover and decarboxylation rate quantified in healthy men and women using primed, constant infusions of [1, 2-13C2] glycine and [2H3] leucine. *The Journal of nutrition*, 137(12):2647-2652.

Lang, S., Mary-Krause, M., Cotte, L., Gilquin, J., Partisani, M., Simon, A., Boccara, F., Costagliola, D. & HIV, C.E.G.o.t.F.H.D.o. 2010. Impact of individual antiretroviral drugs on the risk of myocardial infarction in human immunodeficiency virus–infected patients: a case-control study nested within the French Hospital Database on HIV ANRS cohort CO4. *Archives of internal medicine*, 170(14):1228-1238.

Lawn, S.D., Myer, L., Bekker, L.-G. & Wood, R. 2006. Burden of tuberculosis in an antiretroviral treatment programme in sub-Saharan Africa: impact on treatment outcomes and implications for tuberculosis control. *Aids*, 20(12):1605-1612.

Le Hingrat, Q., Sereti, I., Landay, A.L., Pandrea, I. & Apetrei, C. 2021. The Hitchhiker Guide to CD4+ T-Cell Depletion in Lentiviral Infection. A Critical Review of the Dynamics of the CD4+ T Cells in SIV and HIV Infection. *Frontiers in Immunology*, 12,

Leandro, J. & Houten, S.M. 2020. The lysine degradation pathway: Subcellular compartmentalization and enzyme deficiencies. *Molecular Genetics and Metabolism*, 131(1-2):14-22.

Leonard, R., Zagury, D., Desportes, I., Bernard, J., Zagury, J.-F. & Gallo, R.C. 1988. Cytopathic effect of human immunodeficiency virus in T4 cells is linked to the last stage of virus infection. *Proceedings of the National Academy of Sciences*, 85(10):3570-3574.

Levy, J.A., Hoffman, A.D., Kramer, S.M., Landis, J.A., Shimabukuro, J.M. & Oshiro, L.S. 1984. Isolation of lymphocytopathic retroviruses from San Francisco patients with AIDS. *Science*, 225(4664):840-842.

Li, C., Chu, S., Tan, S., Yin, X., Jiang, Y., Dai, X., Gong, X., Fang, X. & Tian, D. 2021. Towards higher sensitivity of mass spectrometry: A perspective from the mass analyzers. *Frontiers in chemistry*, 9:813359.

Li, Q., Duan, L., Estes, J.D., Ma, Z.-M., Rourke, T., Wang, Y., Reilly, C., Carlis, J., Miller, C.J. & Haase, A.T. 2005. Peak SIV replication in resting memory CD4+ T cells depletes gut lamina propria CD4+ T cells. *Nature*, 434(7037):1148-1152.

Li, X., Wu, T., Jiang, Y., Zhang, Z., Han, X., Geng, W., Ding, H., Kang, J., Wang, Q. & Shang, H. 2018. Plasma metabolic changes in Chinese HIV-infected patients receiving lopinavir/ritonavir based treatment: Implications for HIV precision therapy. *Cytokine*, 110:204-212.

Liebenberg, C., Luies, L. & Williams, A.A. 2021. Metabolomics as a Tool to Investigate HIV/TB Co-Infection. *Frontiers in Molecular Biosciences*, 8,

Lin, C.-H., Lin, C.-J., Kuo, Y.-W., Wang, J.-Y., Hsu, C.-L., Chen, J.-M., Cheng, W.-C. & Lee, L.-N. 2014. Tuberculosis mortality: patient characteristics and causes. *BMC infectious diseases*, 14(1):1-8.

Ling, Z.-N., Jiang, Y.-F., Ru, J.-N., Lu, J.-H., Ding, B. & Wu, J. 2023. Amino acid metabolism in health and disease. *Signal Transduction and Targeted Therapy*, 8(1):345.

Liu, H., Dong, H., Robertson, K. & Liu, C. 2011. DNA methylation suppresses expression of the urea cycle enzyme carbamoyl phosphate synthetase 1 (CPS1) in human hepatocellular carcinoma. *The American journal of pathology*, 178(2):652-661.

Liu, Y.P. & Berkhout, B. 2014. HIV-1-based lentiviral vectors. In. *Human Retroviruses*: Springer. pp. 273-284.

Loddenkemper, R., Lipman, M. & Zumla, A. 2016. Clinical aspects of adult tuberculosis. *Cold Spring Harbor perspectives in medicine*, 6(1):a017848.

Lopez Angel, C.J. & Tomaras, G.D. 2020. Bringing the path toward an HIV-1 vaccine into focus. *PLoS Pathogens*, 16(9):e1008663.

Lu, Y.-J., Barreira-Silva, P., Boyce, S., Powers, J., Cavallo, K. & Behar, S.M. 2021. CD4 T cell help prevents CD8 T cell exhaustion and promotes control of Mycobacterium tuberculosis infection. *Cell reports*, 36(11):109696.

Lucarelli, G., Ferro, M., Ditonno, P. & Battaglia, M. 2018. The urea cycle enzymes act as metabolic suppressors in clear cell renal cell carcinoma. *Transl Cancer Res*, 7(Suppl 7):S766-S769.

Luies, L. & Loots, D.T. 2016. Tuberculosis metabolomics reveals adaptations of man and microbe in order to outcompete and survive. *Metabolomics*, 12(3):1-9.

Luies, L. & Du Preez, I. 2020. The echo of pulmonary tuberculosis: mechanisms of clinical symptoms and other disease-induced systemic complications. *Clinical Microbiology Reviews*, 33(4):e00036-00020.

Luies, L., Mienie, J., Motshwane, C., Ronacher, K., Walzl, G. & Loots, D.T. 2017. Urinary metabolite markers characterizing tuberculosis treatment failure. *Metabolomics*, 13:1-10.

Luna, C., Arjona, A., Dueñas, C. & Estevez, M. 2021. Allysine and α-aminoadipic acid as markers of the glyco-oxidative damage to human serum albumin under pathological glucose concentrations. *Antioxidants*, 10(3):474.

MacAllan, D.C., McNURLAN, M.A., Kurpad, A.V., De Souza, G., Shetty, P.S., Calder, A.G. & Griffin, G.E. 1998. Whole body protein metabolism in human pulmonary tuberculosis and undernutrition: evidence for anabolic block in tuberculosis. *Clinical science*, 94(3):321-331.

Madiraju, A.K., Alves, T., Zhao, X., Cline, G.W., Zhang, D., Bhanot, S., Samuel, V.T., Kibbey, R.G. & Shulman, G.I. 2016. Argininosuccinate synthetase regulates hepatic AMPK linking protein catabolism and ureagenesis to hepatic lipid metabolism. *Proceedings of the National Academy of Sciences*, 113(24):E3423-E3430.

Magee, M.J., Salindri, A.D., Kyaw, N.T.T., Auld, S.C., Haw, J.S. & Umpierrez, G.E. 2018. Stress hyperglycemia in patients with tuberculosis disease: epidemiology and clinical implications. *Current diabetes reports*, 18:1-10.

Makunde, W.H., Francis, F., Mmbando, B.P., Kamugisha, M.L., Rutta, A.M., Mandara, C.I. & Msangeni, H.A. 2012. Lost to follow up and clinical outcomes of HIV adult patients on antiretroviral therapy in care and treatment centres in Tanga City, north-eastern Tanzania. *Tanzania journal of health research*, 14(4),

Malaguarnera, M., Risino, C., Gargante, M.P., Oreste, G., Barone, G., Tomasello, A.V., Costanzo, M. & Cannizzaro, M.A. 2006. Decrease of serum carnitine levels in patients with or without gastrointestinal cancer cachexia. *World journal of gastroenterology: WJG*, 12(28):4541.

Malinowska, J.M. & Viant, M.R. 2019. Confidence in metabolite identification dictates the applicability of metabolomics to regulatory toxicology. *Current Opinion in Toxicology*, 16:32-38.

Masiá, M., Padilla, S., Alvarez, D., Lopez, J.C., Santos, I., Soriano, V., Hernández-Quero, J., Santos, J., Tural, C. & del Amo, J. 2013. Risk, predictors, and mortality associated with non-AIDS events in newly diagnosed HIV-infected patients: role of antiretroviral therapy. *Aids*, 27(2):181-189.

Mathiasen, V.D., Andersen, P.H., Johansen, I.S., Lillebaek, T. & Wejse, C. 2020. Clinical features of tuberculous lymphadenitis in a low-incidence country. *International Journal of Infectious Diseases*, 98:366-371.

Mattapallil, J.J., Douek, D.C., Hill, B., Nishimura, Y., Martin, M. & Roederer, M. 2005. Massive infection and loss of memory CD4+ T cells in multiple tissues during acute SIV infection. *Nature*, 434(7037):1093-1097.

Mazat, J.-P. & Ransac, S. 2019. The fate of glutamine in human metabolism. The interplay with glucose in proliferating cells. *Metabolites*, 9(5):81.

Mbongue, J.C., Nicholas, D.A., Torrez, T.W., Kim, N.-S., Firek, A.F. & Langridge, W.H. 2015. The role of indoleamine 2, 3-dioxygenase in immune suppression and autoimmunity. *Vaccines*, 3(3):703-729.

Mbuh, T.P., Ane-Anyangwe, I., Adeline, W., Thumamo Pokam, B.D., Meriki, H.D. & Mbacham, W. 2019. Bacteriologically confirmed extra pulmonary tuberculosis and treatment outcome of patients consulted and treated under program conditions in the littoral region of Cameroon. *BMC pulmonary medicine*, 19(1):1-7.

McKnight, T.R., Yoshihara, H.A., Sitole, L.J., Martin, J.N., Steffens, F. & Meyer, D. 2014. A combined chemometric and quantitative NMR analysis of HIV/AIDS serum discloses metabolic alterations associated with disease status. *Molecular BioSystems*, 10(11):2889-2897.

McQuaid, C.F., McCreesh, N., Read, J.M., Sumner, T., Houben, R.M., White, R.G., Harris, R.C. & Group, C.C.-W. 2020. The potential impact of COVID-19-related disruption on tuberculosis burden. *European Respiratory Journal*, 56(2),

Meghji, J., Simpson, H., Squire, S.B. & Mortimer, K. 2016. A systematic review of the prevalence and pattern of imaging defined post-TB lung disease. *PLoS One*, 11(8):e0161176.

Melone, M.A.B., Valentino, A., Margarucci, S., Galderisi, U., Giordano, A. & Peluso, G. 2018. The carnitine system and cancer metabolic plasticity. *Cell death & disease*, 9(2):1-12.

Mels, C., Jansen van Rensburg, P., van der Westhuizen, F.H., Pretorius, P.J. & Erasmus, E. 2011. Increased excretion of c4-carnitine species after a therapeutic acetylsalicylic Acid dose: evidence for an inhibitory effect on short-chain Fatty Acid metabolism. *International Scholarly Research Notices*, 2011,

Menon, S., Rossi, R., Dusabimana, A., Zdraveska, N., Bhattacharyya, S. & Francis, J. 2020. The epidemiology of tuberculosis-associated hyperglycemia in individuals newly screened for type 2 diabetes mellitus: systematic review and meta-analysis. *BMC infectious diseases*, 20(1):1-14.

Mercier, S., Breuille, D., Mosoni, L., Obled, C. & Patureau Mirand, P. 2002. Chronic inflammation alters protein metabolism in several organs of adult rats. *The Journal of nutrition*, 132(7):1921-1928.

Moosavi, S.M. & Ghassabian, S. 2018. Linearity of calibration curves for analytical methods: A review of criteria for assessment of method reliability. *Calibration and validation of analytical methods: a sampling of current approaches*, 109,

Mugusi, F., Villamor, E., Urassa, W., Saathoff, E., Bosch, R. & Fawzi, W. 2006. HIV co-infection, CD4 cell counts and clinical correlates of bacillary density in pulmonary tuberculosis. *The International Journal of Tuberculosis and Lung Disease*, 10(6):663-669.

Muller, W.A. & Randolph, G.J. 1999. Migration of leukocytes across endothelium and beyond: molecules involved in the transmigration and fate of monocytes. *Journal of leukocyte biology*, 66(5):698-704.

Mulu, W., Mekkonnen, D., Yimer, M., Admassu, A. & Abera, B. 2015. Risk factors for multidrug resistant tuberculosis patients in Amhara National Regional State. *African health sciences*, 15(2):368-377.

Munshi, S.U., Rewari, B.B., Bhavesh, N.S. & Jameel, S. 2013. Nuclear magnetic resonance based profiling of biofluids reveals metabolic dysregulation in HIV-infected persons and those on anti-retroviral therapy. *PloS one*, 8(5):e64298.

Namikawa-Kanai, H., Miyazaki, T., Matsubara, T., Shigefuku, S., Ono, S., Nakajima, E., Morishita, Y., Honda, A., Furukawa, K. & Ikeda, N. 2020. Comparison of the amino acid profile between the nontumor and tumor regions in patients with lung cancer. *American Journal of Cancer Research*, 10(7):2145.

Nazli, A., Chan, O., Dobson-Belaire, W.N., Ouellet, M., Tremblay, M.J., Gray-Owen, S.D., Arsenault, A.L. & Kaushic, C. 2010. Exposure to HIV-1 directly impairs mucosal epithelial barrier integrity allowing microbial translocation. *PLoS pathogens*, 6(4):e1000852.

Ndlovu, H. & Marakalala, M.J. 2016. Granulomas and inflammation: host-directed therapies for tuberculosis. *Frontiers in immunology*, 7:434.

Newsholme, P. & Newsholme, E.A. 1989. Rates of utilization of glucose, glutamine and oleate and formation of end-products by mouse peritoneal macrophages in culture. *Biochemical Journal*, 261(1):211-218.

Newsholme, P., Procopio, J., Lima, M.M.R., Pithon-Curi, T.C. & Curi, R. 2003. Glutamine and glutamate—their central role in cell metabolism and function. *Cell biochemistry and function*, 21(1):1-9.

Ngabonziza, J.C.S., Ssengooba, W., Mutua, F., Torrea, G., Dushime, A., Gasana, M., Andre, E., Uwamungu, S., Nyaruhirira, A.U. & Mwaengo, D. 2016. Diagnostic performance of smear microscopy and incremental yield of Xpert in detection of pulmonary tuberculosis in Rwanda. *BMC infectious diseases*, 16(1):1-7.

Ngo, M.D., Bartlett, S. & Ronacher, K. 2021. Diabetes-associated susceptibility to tuberculosis: contribution of hyperglycemia vs. Dyslipidemia. *Microorganisms*, 9(11):2282.

Nyamweya, S., Hegedus, A., Jaye, A., Rowland-Jones, S., Flanagan, K.L. & Macallan, D.C. 2013. Comparing HIV-1 and HIV-2 infection: Lessons for viral immunopathogenesis. *Reviews in medical virology*, 23(4):221-240.

Ogawa, M., Shimizu, F., Ishii, Y., Takao, T. & Takada, A. 2023. Uniqueness of Tryptophan in the Transport System in the Brain and Peripheral Tissues. *Food and Nutrition Sciences*, 14(5):401-414.

Olde Damink, S.W., Jalan, R. & Dejong, C.H. 2009. Interorgan ammonia trafficking in liver disease. *Metabolic brain disease*, 24:169-181.

Oliveira, S.M.d.V.L.d., Trajman, A., Paniago, A.M.M., Motta-Castro, A.R.C., Ruffino-Netto, A., Maciel, E.L.N., Croda, J. & Bonecini-Almeida, M.d.G. 2017. Frequency of indeterminate results from an interferon-gamma release assay among HIV-infected individuals. *Jornal Brasileiro de Pneumologia*, 43:215-218.

Ong, R.Y.L., Chan, S.-W.B., Chew, S.J., Liew, W.K., Thoon, K.C., Chong, C.-Y., Yung, C.F., Sng, L.-H., Tan, A.M. & Bhattacharyya, R. 2020. Disseminated Bacillus-Calmette-Guérin infections and primary immunodeficiency disorders in Singapore: a single center 15-year retrospective review. *International Journal of Infectious Diseases*, 97:117-125.

Pagán, A.J. & Ramakrishnan, L. 2015. Immunity and immunopathology in the tuberculous granuloma. *Cold Spring Harbor perspectives in medicine*, 5(9):a018499.

Papes, F., Kemper, E.L., Cord-neto, G., Langone, F. & Arruda, P. 1999. Lysine degradation through the saccharopine pathway in mammals: involvement of both bifunctional and monofunctional lysine-degrading enzymes in mouse. *Biochemical Journal*, 344(2):555-563.

Pasini, E., Corsetti, G., Aquilani, R., Romano, C., Picca, A., Calvani, R. & Dioguardi, F.S. 2018. Protein-amino acid metabolism disarrangements: The hidden enemy of chronic age-related conditions. *Nutrients*, 10(4):391.

Patel, D. & Witt, S.N. 2017. Ethanolamine and phosphatidylethanolamine: partners in health and disease. *Oxidative medicine and cellular longevity*, 2017,

Paton, N.I., Ng, Y.-M., Chee, C.B., Persaud, C. & Jackson, A.A. 2003. Effects of tuberculosis and HIV infection on whole-body protein metabolism during feeding, measured by the [15N] glycine method. *The American journal of clinical nutrition*, 78(2):319-325.

Peltenburg, N.C., Schoeman, J.C., Hou, J., Mora, F., Harms, A.C., Lowe, S.H., Bierau, J., Bakker, J.A., Verbon, A. & Hankemeier, T. 2018. Persistent metabolic changes in HIV-infected patients during the first year of combination antiretroviral therapy. *Scientific Reports*, 8(1):1-11.

Perez, E.R., Knapp, J.A., Horn, C.K., Stillman, S.L., Evans, J.E. & Arfsten, D.P. 2016. Comparison of LC–MS-MS and GC–MS analysis of benzodiazepine compounds included in the drug demand reduction urinalysis program. *Journal of analytical toxicology*, 40(3):201-207.

Petit, F., Arnoult, D., Lelievre, J.-D., Moutouh-de Parseval, L., Hance, A.J., Schneider, P., Corbeil, J., Ameisen, J.C. & Estaquier, J. 2002. Productive HIV-1 infection of primary CD4+ T cells induces mitochondrial membrane permeabilization leading to a caspase-independent cell death. *Journal of Biological Chemistry*, 277(2):1477-1487.

Phipps, W.S., Crossley, E., Boriack, R., Jones, P.M. & Patel, K. 2020. Quantitative amino acid analysis by liquid chromatography-tandem mass spectrometry using low cost derivatization and an automated liquid handler. *JIMD reports*, 51(1):62-69.

Phuoc Long, N., Heo, D.Y., Park, S., Thi Hai Yen, N., Cho, Y.-S., Shin, J.-G., Oh, J.Y. & Kim, D.-H. 2022. Molecular perturbations in pulmonary tuberculosis patients identified by pathway-level analysis of plasma metabolic features. *Plos one*, 17(1):e0262545.

Pillay, S. & Aldous, C. 2016. Introducing a multifaceted approach to the management of diabetes mellitus in resource-limited settings. *SAMJ: South African Medical Journal*, 106(5):456-458.

Piot, P. & Colebunders, R. 1987. Clinical manifestations and the natural history of HIV infection in adults. *Western Journal of Medicine*, 147(6):709.

Pitt, J.J. 2009. Principles and applications of liquid chromatography-mass spectrometry in clinical biochemistry. *The Clinical Biochemist Reviews*, 30(1):19.

Plaitakis, A., Kalef-Ezra, E., Kotzamani, D., Zaganas, I. & Spanaki, C. 2017. The glutamate dehydrogenase pathway and its roles in cell and tissue biology in health and disease. *Biology*, 6(1):11.

Poles, M.A., Elliott, J., Taing, P., Anton, P.A. & Chen, I.S. 2001. A preponderance of CCR5+ CXCR4+ mononuclear cells enhances gastrointestinal mucosal susceptibility to human immunodeficiency virus type 1 infection. *Journal of virology*, 75(18):8390-8399.

Pozefsky, T., TANcREDI, R.G., MoxLEY, R.T., DuPRE, J. & Tobin, J.D. 1976. Effects of brief starvation on muscle amino acid metabolism in nonobese man. *The Journal of clinical investigation*, 57(2):444-449.

Pradipta, I.S., Idrus, L.R., Probandari, A., Lestari, B.W., Diantini, A., Alffenaar, J.-W.C. & Hak, E. 2021. Barriers and strategies to successful tuberculosis treatment in a high-burden tuberculosis setting: a qualitative study from the patient's perspective. *BMC Public Health*, 21:1-12.

Price, S.R., Bailey, J.L., Wang, X., Jurkovitz, C., England, B.K., Ding, X., Phillips, L.S. & Mitch, W.E. 1996. Muscle wasting in insulinopenic rats results from activation of the ATP-dependent, ubiquitin-proteasome proteolytic pathway by a mechanism including gene transcription. *The Journal of clinical investigation*, 98(8):1703-1708.

Qian, S., Chen, X., Wu, T., Sun, Y., Li, X., Fu, Y., Zhang, Z., Xu, J., Han, X. & Ding, H. 2021. The accumulation of plasma acylcarnitines are associated with poor immune recovery in HIV-infected individuals. *BMC Infectious Diseases*, 21(1):1-12.

Qu, Q., Zeng, F., Liu, X., Wang, Q. & Deng, F. 2016. Fatty acid oxidation and carnitine palmitoyltransferase I: emerging therapeutic targets in cancer. *Cell death & disease*, 7(5):e2226-e2226.

Rachlis, B., Ochieng, D., Geng, E., Rotich, E., Ochieng, V., Maritim, B., Ndege, S., Naanyu, V., Martin, J.N. & Keter, A. 2015. Implementation and operational research: evaluating outcomes of patients lost to follow-up in a

large comprehensive care treatment program in western Kenya. *JAIDS Journal of Acquired Immune Deficiency Syndromes*, 68(4):e46-e55.

Ranjbar, S., Jasenosky, L.D., Chow, N. & Goldfeld, A.E. 2012. Regulation of Mycobacterium tuberculosis-dependent HIV-1 transcription reveals a new role for NFAT5 in the toll-like receptor pathway. *PLoS pathogens*, 8(4):e1002620.

Rao, S., Schieber, A.M.P., O'Connor, C.P., Leblanc, M., Michel, D. & Ayres, J.S. 2017. Pathogen-mediated inhibition of anorexia promotes host survival and transmission. *Cell*, 168(3):503-516. e512.

Reilly, S.M., Cheng, T. & DuMond, J. 2020. Method validation approaches for analysis of constituents in ENDS. *Tobacco regulatory science*, 6(4):242.

Rinaldo, P., Cowan, T.M. & Matern, D. 2008. Acylcarnitine profile analysis. *Genetics in Medicine*, 10(2):151-156.

Roberts, L.D., Souza, A.L., Gerszten, R.E. & Clish, C.B. 2012. Targeted metabolomics. *Current protocols in molecular biology*, 98(1):30.32. 31-30.32. 24.

Roth, W., Zadeh, K., Vekariya, R., Ge, Y. & Mohamadzadeh, M. 2021. Tryptophan metabolism and gut-brain homeostasis. *International journal of molecular sciences*, 22(6):2973.

Rusli, H., Putri, R.M. & Alni, A. 2022. Recent Developments of Liquid Chromatography Stationary Phases for Compound Separation: From Proteins to Small Organic Compounds. *Molecules*, 27(3):907.

Sacksteder, K.A., Biery, B.J., Morrell, J.C., Goodman, B.K., Geisbrecht, B.V., Cox, R.P., Gould, S.J. & Geraghty, M.T. 2000. Identification of the α-aminoadipic semialdehyde synthase gene, which is defective in familial hyperlysinemia. *The American Journal of Human Genetics*, 66(6):1736-1743.

Saharia, K.K. & Koup, R.A. 2013. T cell susceptibility to HIV influences outcome of opportunistic infections. *Cell*, 155(3):505-514.

Sankaranantham, M. 2019. HIV–Is a cure possible? *Indian journal of sexually transmitted diseases and AIDS*, 40(1):1.

Sashindran, V.K. & Thakur, R. 2020. Malnutrition in HIV/AIDS: aetiopathogenesis. *Nutrition and HIV/AIDS-Implication for Treatment, Prevention and Cure [series online]*,

Savitz, J. 2020. The kynurenine pathway: a finger in every pie. *Molecular psychiatry*, 25(1):131-147.

Sawhney, M. & Sharma, Y. 2006. Significance of tuberculin testing in HIV infection: An Indian perspective. *Medical Journal Armed Forces India*, 62(2):104-107.

Scarpelini, B., Zanoni, M., Sucupira, M.C.A., Truong, H.-H.M., Janini, L.M.R., Segurado, I.D.C. & Diaz, R.S. 2016. Plasma metabolomics biosignature according to HIV stage of infection, pace of disease progression, viremia level and immunological response to treatment. *PLoS One*, 11(12):e0161920.

Schank, M., Zhao, J., Moorman, J.P. & Yao, Z.Q. 2021. The impact of HIV-and ART-induced mitochondrial dysfunction in cellular senescence and aging. *Cells*, 10(1):174.

Schober, P., Boer, C. & Schwarte, L.A. 2018. Correlation coefficients: appropriate use and interpretation. *Anesthesia & analgesia*, 126(5):1763-1768.

Schooneman, M.G., Vaz, F.M., Houten, S.M. & Soeters, M.R. 2013. Acylcarnitines: reflecting or inflicting insulin resistance? *Diabetes*, 62(1):1-8.

Schutz, C., Meintjes, G., Almajid, F., Wilkinson, R.J. & Pozniak, A. 2010. Clinical management of tuberculosis and HIV-1 co-infection. *European Respiratory Journal*,

Schwenk, A. & Macallan, D.C. 2000. Tuberculosis, malnutrition and wasting. *Current Opinion in Clinical Nutrition & Metabolic Care*, 3(4):285-291.

Selik, R.M. & Linley, L. 2018. Viral loads within 6 weeks after diagnosis of HIV infection in early and later stages: Observational study using national surveillance data. *JMIR Public Health and Surveillance*, 4(4):e10770.

Sell, D.R., Strauch, C.M., Shen, W. & Monnier, V.M. 2007. 2-aminoadipic acid is a marker of protein carbonyl oxidation in the aging human skin: effects of diabetes, renal failure and sepsis. *Biochemical Journal*, 404(2):269-277.

Selwyn, P.A., Hartel, D., Lewis, V.A., Schoenbaum, E.E., Vermund, S.H., Klein, R.S., Walker, A.T. & Friedland, G.H. 1989. A prospective study of the risk of tuberculosis among intravenous drug users with human immunodeficiency virus infection. *New England journal of medicine*, 320(9):545-550.

Seung, K.J., Keshavjee, S. & Rich, M.L. 2015. Multidrug-resistant tuberculosis and extensively drug-resistant tuberculosis. *Cold Spring Harbor perspectives in medicine*, 5(9):a017863.

Seyed Mohammad, A. & Nejad, S. 2008. The causes of death among patients with tuberculosis in Khuzestan, Iran. *Pakistan journal of medical sciences*

Shankar, E.M., Vignesh, R., Ellegård, R., Barathan, M., Chong, Y.K., Bador, M.K., Rukumani, D.V., Sabet, N.S., Kamarulzaman, A. & Velu, V. 2014. HIV–Mycobacterium tuberculosis co-infection: a 'danger-couple model'of disease pathogenesis. *Pathogens and disease*, 70(2):110-118.

Shiomi, Y., Nishiumi, S., Ooi, M., Hatano, N., Shinohara, M., Yoshie, T., Kondo, Y., Furumatsu, K., Shiomi, H. & Kutsumi, H. 2011. GCMS-based metabolomic study in mice with colitis induced by dextran sulfate sodium. *Inflammatory bowel diseases*, 17(11):2261-2274.

Shrivastava, A. & Gupta, V.B. 2011. Methods for the determination of limit of detection and limit of quantitation of the analytical methods. *Chron. Young Sci*, 2(1):21-25.

Siddiqui, J., Phillips, A.L., Freedland, E.S., Sklar, A.R., Darkow, T. & Harley, C.R. 2009. Prevalence and cost of HIV-associated weight loss in a managed care population. *Current medical research and opinion*, 25(5):1307-1317.

Siddiqui, J., Samuel, S.K., Hayward, B., Wirka, K.A., Deering, K.L., Harshaw, Q., Phillips, A. & Harbour, M. 2022. HIV-associated wasting prevalence in the era of modern antiretroviral therapy. *AIDS (London, England)*, 36(1):127.

Sidhu, A., Verma, G., Humar, A. & Kumar, D. 2014. Outcome of latent tuberculosis infection in solid organ transplant recipients over a 10-year period. *Transplantation*, 98(6):671-675.

Silva, C.A., Graham, B., Webb, K., Ashton, L.V., Harton, M., Luetkemeyer, A.F., Bokatzian, S., Almubarak, R., Mahapatra, S. & Hovind, L. 2019. A pilot metabolomics study of tuberculosis immune reconstitution inflammatory syndrome. *International Journal of Infectious Diseases*, 84:30-38.

Silva Miranda, M., Breiman, A., Allain, S., Deknuydt, F. & Altare, F. 2012. The tuberculous granuloma: an unsuccessful host defence mechanism providing a safety shelter for the bacteria? *Clinical and Developmental Immunology*, 2012,

Silva, N.M., Rodrigues, C.V., Santoro, M.M., Reis, L.F., Alvarez-Leite, J.I. & Gazzinelli, R.T. 2002. Expression of indoleamine 2, 3-dioxygenase, tryptophan degradation, and kynurenine formation during in vivo infection with Toxoplasma gondii: induction by endogenous gamma interferon and requirement of interferon regulatory factor 1. *Infection and immunity*, 70(2):859-868.

Sitole, L.J., Tugizimana, F. & Meyer, D. 2019. Multi-platform metabonomics unravel amino acids as markers of HIV/combination antiretroviral therapy-induced oxidative stress. *Journal of Pharmaceutical and Biomedical Analysis*, 176:112796.

Sivanandham, R., Brocca-Cofano, E., Krampe, N., Falwell, E., Venkatraman, S.M.K., Ribeiro, R.M., Apetrei, C. & Pandrea, I. 2018. Neutrophil extracellular trap production contributes to pathogenesis in SIV-infected nonhuman primates. *The Journal of clinical investigation*, 128(11):5178-5183.

Sloand, E.M., Young, N.S., Kumar, P., Weichold, F.F., Sato, T. & Maciejewski, J.P. 1997. Role of Fas ligand and receptor in the mechanism of T-cell depletion in acquired immunodeficiency syndrome: effect on CD4+

lymphocyte depletion and human immunodeficiency virus replication. *Blood, The Journal of the American Society of Hematology*, 89(4):1357-1363.

Sofi, M.H., Li, W., Kaplan, M.H. & Chang, C.-H. 2009. Elevated IL-6 expression in CD4 T cells via PKCθ and NF-κB induces Th2 cytokine production. *Molecular immunology*, 46(7):1443-1450.

Sourisseau, M., Sol-Foulon, N., Porrot, F., Blanchet, F. & Schwartz, O. 2007. Inefficient human immunodeficiency virus replication in mobile lymphocytes. *Journal of virology*, 81(2):1000-1012.

St Germain, M., Iraji, R. & Bakovic, M. 2023. Phosphatidylethanolamine homeostasis under conditions of impaired CDP-ethanolamine pathway or phosphatidylserine decarboxylation. *Frontiers in Nutrition*, 9:1094273.

Stephens, N.S., Siffledeen, J., Su, X., Murdoch, T.B., Fedorak, R.N. & Slupsky, C.M. 2013. Urinary NMR metabolomic profiles discriminate inflammatory bowel disease from healthy. *Journal of Crohn's and Colitis*, 7(2):e42-e48.

Stone, P., Glauner, T., Kuhlmann, F., Schlabach, T. & Miller, K. 2009. New dynamic MRM mode improves data quality and triple quad quantification in complex analyses. *Agilent publication*,

Sultana, Z.Z., Hoque, F.U., Beyene, J., Akhlak-Ul-Islam, M., Khan, M.H.R., Ahmed, S., Hawlader, D.H. & Hossain, A. 2021. HIV infection and multidrug resistant tuberculosis: a systematic review and meta-analysis. *BMC infectious diseases*, 21(1):1-13.

Swanepoel, A., Bester, J., Kruger, Y., Davoren, E. & Du Preez, I. 2021. The effect of combined oral contraceptives containing drospirenone and ethinylestradiol on serum levels of amino acids and acylcarnitines. *Metabolomics*, 17:1-11.

Takashina, C., Tsujino, I., Watanabe, T., Sakaue, S., Ikeda, D., Yamada, A., Sato, T., Ohira, H., Otsuka, Y. & Oyama-Manabe, N. 2016. Associations among the plasma amino acid profile, obesity, and glucose metabolism in Japanese adults with normal glucose tolerance. *Nutrition & metabolism*, 13(1):1-10.

Tan, Y.-L., Sou, N.-L., Tang, F.-Y., Ko, H.-A., Yeh, W.-T., Peng, J.-H. & Chiang, E.-P.I. 2020. Tracing metabolic fate of mitochondrial glycine cleavage system derived formate in vitro and in vivo. *International journal of molecular sciences*, 21(22):8808.

Terness, P., Bauer, T.M., Röse, L., Dufter, C., Watzlik, A., Simon, H. & Opelz, G. 2002. Inhibition of allogeneic T cell proliferation by indoleamine 2, 3-dioxygenase–expressing dendritic cells: mediation of suppression by tryptophan metabolites. *The Journal of experimental medicine*, 196(4):447-457.

Terracciano, E., Amadori, F., Zaratti, L. & Franco, E. 2020. Tuberculosis: an ever present disease but difficult to prevent. *Igiene e sanita pubblica*, 76(1):59-66.

Tomas, F., Ballard, F. & Pope, L. 1979. Age-dependent changes in the rate of myofibrillar protein degradation in humans as assessed by 3-methylhistidine and creatinine excretion. *Clinical Science (London, England: 1979)*, 56(4):341-346.

Tomé, D. 2021. Amino acid metabolism and signalling pathways: potential targets in the control of infection and immunity. *European Journal of Clinical Nutrition*, 75(9):1319-1327.

Triebl, A. & Wenk, M.R. 2018. Analytical considerations of stable isotope labelling in lipidomics. *Biomolecules*, 8(4):151.

UNAIDS. 2023. *FACTSHEET - WORLD AIDS DAY 2023*. https://www.unaids.org/en/resources/fact-sheet Date of access: 15 November 2023.

Van Donkelaar, E., Blokland, A., Ferrington, L., Kelly, P., Steinbusch, H. & Prickaerts, J. 2011. Mechanism of acute tryptophan depletion: is it only serotonin? *Molecular psychiatry*, 16(7):695-713.

Vance, J.E. 2015. Phospholipid synthesis and transport in mammalian cells. *Traffic*, 16(1):1-18.

Vedantam, D., Poman, D.S., Motwani, L., Asif, N., Patel, A. & Anne, K.K. 2022. Stress-induced hyperglycemia: Consequences and management. *Cureus*, 14(7),

Volkman, H.E., Clay, H., Beery, D., Chang, J.C.W., Sherman, D.R., Ramakrishnan, L. & Akira, S. 2004. Tuberculous granuloma formation is enhanced by a mycobacterium virulence determinant. *PLoS biology*, 2(11):e367.

Vrieling, F., Ronacher, K., Kleynhans, L., Van Den Akker, E., Walzl, G., Ottenhoff, T.H. & Joosten, S.A. 2018. Patients with concurrent tuberculosis and diabetes have a pro-atherogenic plasma lipid profile. *EBioMedicine*, 32:192-200.

Vrieling, F., Alisjahbana, B., Sahiratmadja, E., van Crevel, R., Harms, A.C., Hankemeier, T., Ottenhoff, T.H. & Joosten, S.A. 2019. Plasma metabolomics in tuberculosis patients with and without concurrent type 2 diabetes at diagnosis and during antibiotic treatment. *Scientific reports*, 9(1):1-12.

Wagner, B.D., Accurso, F.J. & Laguna, T.A. 2010. The applicability of urinary creatinine as a method of specimen normalization in the cystic fibrosis population. *Journal of Cystic Fibrosis*, 9(3):212-216.

Walsh, M.C., Brennan, L., Malthouse, J.P.G., Roche, H.M. & Gibney, M.J. 2006. Effect of acute dietary standardization on the urinary, plasma, and salivary metabolomic profiles of healthy humans. *The American journal of clinical nutrition*, 84(3):531-539.

Wang, M., Dong, X., Huang, Y., Su, J., Dai, X., Guo, Y., Hu, C., Zhou, Q. & Zhu, B. 2019. Activation of the kynurenine pathway is associated with poor outcome in Pneumocystis pneumonia patients infected with HIV: results of 2 months cohort study. *BMC Infectious Diseases*, 19(1):1-6.

Wang, X., Hu, Z., Hu, J., Du, J. & Mitch, W.E. 2006. Insulin resistance accelerates muscle protein degradation: activation of the ubiquitin-proteasome pathway by defects in muscle cell signaling. *Endocrinology*, 147(9):4160-4168.

Wanke, C. 2004. Pathogenesis and consequences of HIV-associated wasting. *JAIDS Journal of Acquired Immune Deficiency Syndromes*, 37:S277-S279.

Weiner, J., Parida, S.K., Maertzdorf, J., Black, G.F., Repsilber, D., Telaar, A., Mohney, R.P., Arndt-Sullivan, C., Ganoza, C.A. & Fae, K.C. 2012. Biomarkers of inflammation, immunosuppression and stress are revealed by metabolomic profiling of tuberculosis patients. *PloS one*, 7(7):e40221.

Weiner, J., Maertzdorf, J., Sutherland, J.S., Duffy, F.J., Thompson, E., Suliman, S., McEwen, G., Thiel, B., Parida, S.K. & Zyla, J. 2018. Metabolite changes in blood predict the onset of tuberculosis. *Nature communications*, 9(1):1-12.

Weiss, G. & Schaible, U.E. 2015. Macrophage defense mechanisms against intracellular bacteria. *Immunological reviews*, 264(1):182-203.

Whitmire, M., Ammerman, J., De Lisio, P., Killmer, J., Kyle, D., Mainstone, E., Porter, L. & Zhang, T. 2011. LC-MS/MS bioanalysis method development, validation, and sample analysis: points to consider when conducting nonclinical and clinical studies in accordance with current regulatory guidances. *J Anal Bioanal Techniques S*, 4(2),

Willcox, P. & Ferguson, A. 1989. Chronic obstructive airways disease following treated pulmonary tuberculosis. *Respiratory medicine*, 83(3):195-198.

Williams, A., Koekemoer, G., Lindeque, Z., Reinecke, C. & Meyer, D. 2012. Qualitative serum organic acid profiles of HIV-infected individuals not on antiretroviral treatment. *Metabolomics*, 8(5):804-818.

Wolfe, A.J. & Brubaker, L. 2015. "Sterile urine" and the presence of bacteria. *European urology*, 68(2):173.

World Health Organization. 2007. Revised BCG vaccination guidelines for infants at risk for HIV infection. *Weekly Epidemiological Record= Relevé épidémiologique hebdomadaire*, 82(21):193-196.

World Health Organization. 2013. *Global tuberculosis report 2013*. https://apps.who.int/iris/bitstream/handle/10665/91355/9789241564656_eng.pdf?sequence=1&isAllowed=y Date of access: 7 June.

World Health Organization. 2015. *The use of lateral flow urine lipoarabinomannan assay (LF-LAM) for the diagnosis and screening of active tuberculosis in people living with HIV: policy guidance*. https://apps.who.int/iris/bitstream/handle/10665/193633/9789241509633_eng.pdf?sequence=1&isAllowed=y Date of access: 22 June 2022.

World Health Organization. 2021. *Global tuberculosis report 2021*. https://apps.who.int/iris/rest/bitstreams/1379788/retrieve Date of access: 7 June.

Wu, G. 2010. Functional amino acids in growth, reproduction, and health. *Advances in nutrition*, 1(1):31-37.

Wu, G. 2013. Functional amino acids in nutrition and health. *Amino Acids*, 45(3):407-411.

Wu, G., Field, C.J. & Marliss, E.B. 1991. Glutamine and glucose metabolism in rat splenocytes and mesenteric lymph node lymphocytes. *American Journal of Physiology-Endocrinology and Metabolism*, 260(1):E141-E147.

Xiao, J.F., Zhou, B. & Ressom, H.W. 2012. Metabolite identification and quantitation in LC-MS/MS-based metabolomics. *TrAC Trends in Analytical Chemistry*, 32:1-14.

Xu, S., Cooper, A., Sturgill-Koszycki, S., Van Heyningen, T., Chatterjee, D., Orme, I., Allen, P. & Russell, D.G. 1994. Intracellular trafficking in Mycobacterium tuberculosis and Mycobacterium avium-infected macrophages. *The Journal of Immunology*, 153(6):2568-2578.

Yang, F., Yang, Y., Zeng, L., Chen, Y. & Zeng, G. 2021. Nutrition metabolism and infections. *Infectious Microbes & Diseases*, 3(3):134-141.

Yang, Q.J., Zhao, J.R., Hao, J., Li, B., Huo, Y., Han, Y.L., Wan, L.L., Li, J., Huang, J. & Lu, J. 2018. Serum and urine metabolomics study reveals a distinct diagnostic model for cancer cachexia. *Journal of cachexia, sarcopenia and muscle*, 9(1):71-85.

Yang, R., Masters, A.R., Fortner, K.A., Champagne, D.P., Yanguas-Casás, N., Silberger, D.J., Weaver, C.T., Haynes, L. & Rincon, M. 2016. IL-6 promotes the differentiation of a subset of naive CD8+ T cells into IL-21–producing B helper CD8+ T cells. *Journal of Experimental Medicine*, 213(11):2281-2291.

Yang, W.-C., Hwang, Y.-S., Chen, Y.-Y., Liu, C.-L., Shen, C.-N., Hong, W.-H., Lo, S.-M. & Shen, C.-R. 2017. Interleukin-4 supports the suppressive immune responses elicited by regulatory T cells. *Frontiers in immunology*, 8:1508.

Yorke, E., Atiase, Y., Akpalu, J., Sarfo-Kantanka, O., Boima, V. & Dey, I.D. 2017. The bidirectional relationship between tuberculosis and diabetes. *Tuberculosis research and treatment*, 2017,

Yoshida, M., Hatano, N., Nishiumi, S., Irino, Y., Izumi, Y., Takenawa, T. & Azuma, T. 2012. Diagnosis of gastroenterological diseases by metabolome analysis using gas chromatography–mass spectrometry. *Journal of gastroenterology*, 47(1):9-20.

Zhai, L., Ladomersky, E., Bell, A., Dussold, C., Cardoza, K., Qian, J., Lauing, K.L. & Wainwright, D.A. 2019. Quantification of IDO1 enzyme activity in normal and malignant tissues. In. *Methods in enzymology*. 629: Elsevier. pp. 235-256.

Zhang, Y.J. & Rubin, E.J. 2013. Feast or famine: the host–pathogen battle over amino acids. *Cellular microbiology*, 15(7):1079-1087.

Zhang, Y.J., Reddy, M.C., Ioerger, T.R., Rothchild, A.C., Dartois, V., Schuster, B.M., Trauner, A., Wallis, D., Galaviz, S. & Huttenhower, C. 2013. Tryptophan biosynthesis protects mycobacteria from CD4 T-cell-mediated killing. *Cell*, 155(6):1296-1308.

Zhou, A., Ni, J., Xu, Z., Wang, Y., Lu, S., Sha, W., Karakousis, P.C. & Yao, Y.-F. 2013. Application of 1H NMR spectroscopy-based metabolomics to sera of tuberculosis patients. *Journal of proteome research*, 12(10):4642-4649.

Zimmer, A.J., Klinton, J.S., Oga-Omenka, C., Heitkamp, P., Nyirenda, C.N., Furin, J. & Pai, M. 2022. Tuberculosis in times of COVID-19. *J Epidemiol Community Health*, 76(3):310-316.

Zolopa, A.R., Andersen, J., Komarow, L., Sanne, I., Sanchez, A., Hogg, E., Suckow, C., Powderly, W. & Team, A.A.S. 2009. Early antiretroviral therapy reduces AIDS progression/death in individuals with acute opportunistic infections: a multicenter randomized strategy trial. *PloS one,* 4(5):e5575.

Zou, S., Glynn, S., Kuritzkes, D., Shah, M., Cook, N. & Berliner, N. 2013. Hematopoietic cell transplantation and HIV cure: where we are and what next? *Blood, The Journal of the American Society of Hematology*, 122(18):3111-3115.

APPENDIX A

Table A1: Summary of acylcarnitine stock and working solutions.

Compound	C2	C3	C4	C5	C6	C8	C10	C12
Stock solution (µmol/L)	98.4	115.1	108.1	107	104.1	86.1	82.4	72.8
Work solutions for method standardisation (µmol/L)	AC standardisation solution							
	12.3	14.4	13.5	13.4	13	10.8	10.3	9.1
Work solutions for calibration curves (µmol/L)	Solution 1	Solution 2			Solution 3			
	24	8	n/a	8	016	0.16	0.16	0.16
Work solutions for the preparation of LQC, MQC and HQC samples (µmol/L)	Solution 1	Solution 2			Solution 3			
	18	2.6	n/a	1.2	0.14	0.14	0.14	0.14
Work solutions for LLOQ preparations (µmol/L)	Solution 1			Solution 2				
	0.64	0.32	n/a	0.026	0.0052	0.006	0.0172	0.022

Table A2: Expected values of prepared calibrators for acylcarnitines and 5-HIAA.

Calibrator (µmol/L)	1	2	3	4	5	6	7	8	9	10
C2	0.05	0.1	0.2	0.3	0.75	1.5	3	4	12	25
C3, C5	0.005	0.015	0.05	0.1	0.2	0.3	0.750	1.5	3	4
C6, C8, C10, C12	0.0002	0.0004	0.0008	0.0024	0.005	0.0075	0.01	0.02	0.03	0.08
5-HIAA	0.1	0.25	0.5	3	8	12.5	25	50	75	100

Table A3: Expected values of analytes in prepared quality control samples used during the precision and accuracy experiments.

	C2	C3	C5	C6	C8	C10	C12	5-HIAA
Low QC(µmol/L)	3.3750	0.5000	0.2300	0.0300	0.0300	0.0300	0.0300	20.0000
Medium QC(µmol/L)	6.0000	0.8000	0.3700	0.0500	0.0500	0.0500	0.0500	40.0000
High QC(µmol/L)	9.0000	1.3000	0.6000	0.0700	0.0700	0.0700	0.0700	80.0000
LLOQ (µmol/L)	0.3200	0.1624	0.0130	0.0026	0.0030	0.0086	0.0100	5.6810

APPENDIX B

Table B1: Calibration curves for all acylcarnitines and 5-HIAA analysed with the acylcarnitine and 5-HIAA analysis method respectively.

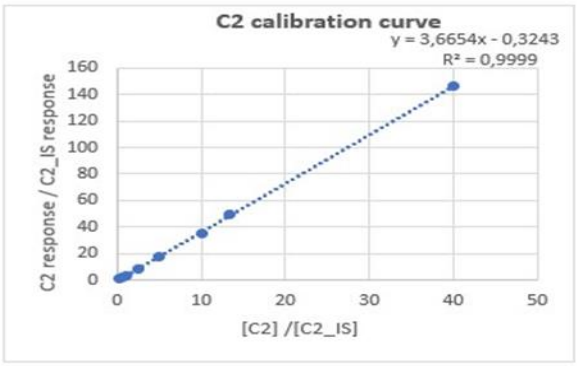

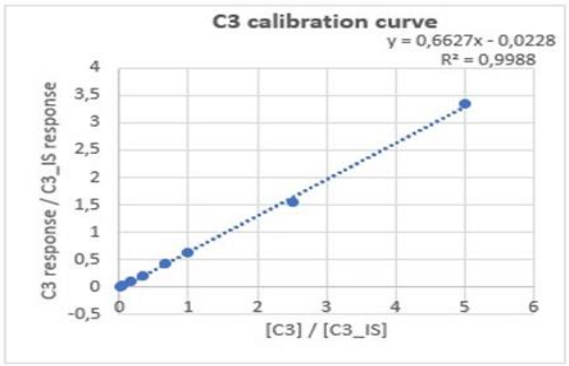

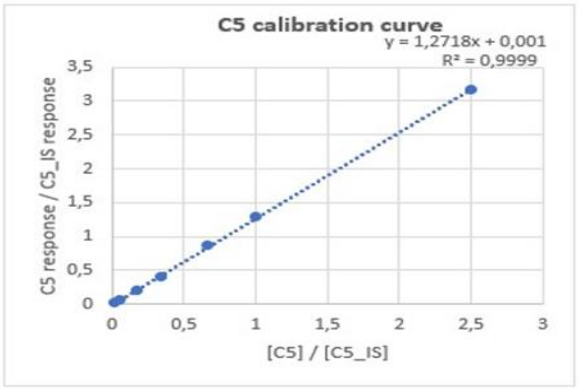

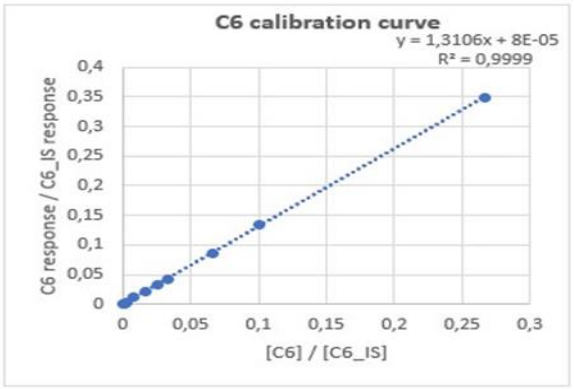

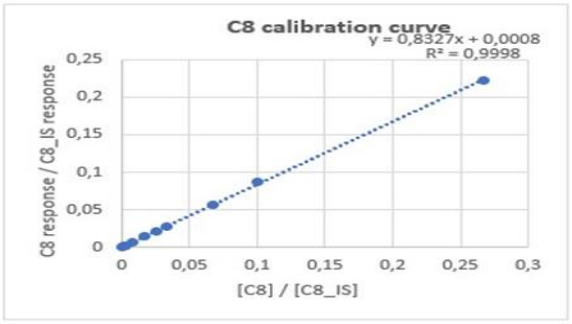

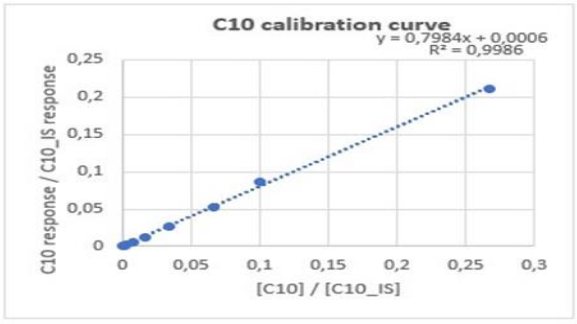

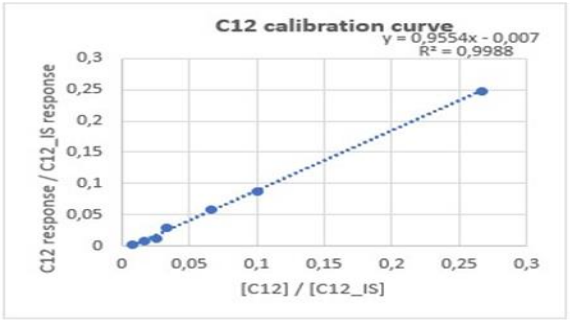

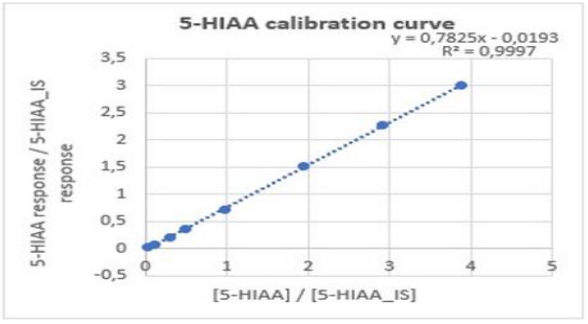

Table B2: Concentration of acylcarnitines and 5-HIAA with reference ranges given in (µmol/L)/(mmol/L) creatinine.

ID	Group	C2 (0.4-7.5)	C3 (0.01-0.2)	C5 (0.04-0.44)	C6 (0.03-0.07)	C8 (0.03-0.09)	C10 (0.02-0.06)	C12 (0.01-0.04)	5-HIAA (0.4-5.8)
34	HIV-/TB-	0.7729	0.1237	0.0071	0.0038	0.0103	0.0059	0.0030	0.845
36	HIV-/TB-	1.5111	0.5770	0.0568	0.0039	0.0155	0.0053	0	0
43	HIV-/TB-	1.9667	0	0	0	0	0	0	0
44	HIV-/TB-	0.6221	0.1659	0.0060	0.0011	0.0035	0.0035	0	1.073
45	HIV-/TB-	0	0	0	0	0	0	0	0
47	HIV-/TB-	0	0	0.0033	0.0041	0.0063	0.0072	0.0026	1.351
49	HIV-/TB-	1.3247	0.2982	0.0164	0.0033	0.0130	0.0081	0.0033	0.833
59	HIV-/TB-	0.9326	0.3386	0.0338	0.0029	0.0106	0.0081	0.0040	1.237
61	HIV-/TB-	0.8717	0.3182	0.0267	0.0021	0.0084	0.0026	0.0019	0.498
64	HIV-/TB-	1.5487	0.3717	0.0573	0.0050	0.0240	0.0112	0.0031	1.184
65	HIV-/TB-	0.8246	0.3838	0.0412	0.0025	0.0186	0.0048	0.0029	1.293
67	HIV-/TB-	0	0	0.0032	0.0011	0.0015	0	0.0029	1.009
69	HIV-/TB-	0.1264	0	0.0056	0.0013	0.0037	0.0033	0	1.018
116	HIV-/TB-	2.1963	0.2092	0.0697	0	0	0.0034	0	0.38
127	HIV-/TB-	0.2167	0.0734	0.0042	0.0010	0.0018	0.0023	0	1.661
147	HIV-/TB-	0.2333	0.1050	0.0219	0.0012	0.0038	0.0035	0.0014	1.092
148	HIV-/TB-	0.1876	0.0672	0.0140	0.0012	0.0027	0.0028	0	1.844
155	HIV-/TB-	0	0	0.0086	0.0046	0.0073	0.0102	0	1.573
158	HIV-/TB-	0.0666	0	0.0033	0.0029	0.0055	0.0060	0.0026	1.641
159	HIV-/TB-	1.0723	0.2896	0.0219	0.0056	0.0189	0.0127	0.0016	1.143
161	HIV-/TB-	0	0	0	0	0	0	0	0
162	HIV-/TB-	0.5809	0.0837	0.0097	0.0064	0.0131	0.0160	0.0047	1.239
163	HIV-/TB-	0.7501	0.2970	0.0601	0	0.0088	0	0	1.617
165	HIV-/TB-	0.5900	0.1593	0.0162	0.0026	0.0084	0.0059	0.0018	1.330
166	HIV-/TB-	0	0	0	0	0.0053	0	0.0159	1.922
167	HIV-/TB-	0.3970	0.0970	0.0185	0.0014	0.0064	0.0052	0.0035	2.579
170	HIV-/TB-	0.9278	0.2998	0.0609	0.0025	0.0176	0.0058	0.0011	0.771
171	HIV-/TB-	0.6039	0.1298	0.0055	0.0014	0.0038	0.0032	0.0022	1.085
172	HIV-/TB-	0.8186	0.2597	0.0203	0.0073	0.0158	0.0226	0.0119	2.330
173	HIV-/TB-	0.8666	0.1490	0.0110	0.0032	0.0119	0.0066	0.0030	2.230
184	HIV-/TB-	3.7493	0.3025	0.0380	0.0021	0.0108	0.0067	0.0023	1.151
185	HIV-/TB-	1.3966	0.1975	0.0294	0.0033	0.0145	0.0127	0.0040	0.946
1	HIV-/TB+	0.4842	0.2290	0.0319	0.0022	0.0078	0.0042	0.0014	1.093
3	HIV-/TB+	1.0650	0.3583	0.0271	0.0067	0.0224	0.0114	0.0023	1.695
7	HIV-/TB+	0.0542	0.0149	0.0048	0.0141	0.0190	0.0193	0.0082	1.655
12	HIV-/TB+	0.1754	0.0511	0.0062	0.0012	0.0023	0.0023	0.0015	0.751
14	HIV-/TB+	0.1204	0.0371	0.0061	0.0098	0.0159	0.0197	0.0047	0.769
19	HIV-/TB+	0.2112	0	0.0043	0.0122	0.0182	0.0314	0.0124	1.527

22	HIV-/TB+	0.0895	0.0556	0.0131	0.0032	0.0051	0.0051	0.0030	6.467
23	HIV-/TB+	0.5562	0.2206	0.0206	0.0053	0.0157	0.0135	0.0043	0.540
27	HIV-/TB+	0.0793	0.0275	0.0075	0.0020	0.0037	0.0046	0.0015	0.768
90	HIV-/TB+	0.6923	0.1848	0.0063	0.0018	0.0061	0.0043	0.0013	0.871
91	HIV-/TB+	1.9794	0.1255	0.0067	0.0031	0.0068	0.0043	0.0015	0.943
123	HIV-/TB+	0.3527	0.0635	0.0033	0.0025	0.0067	0.0071	0.0026	0
124	HIV-/TB+	0	0	0.0163	0.0076	0.0139	0.0169	0.0104	0
128	HIV-/TB+	0.0222	0	0.0023	0.0034	0.0050	0.0061	0.0022	0.51
130	HIV-/TB+	0.3325	0.2024	0.0188	0.0043	0.0067	0.0082	0.0028	1.362
132	HIV-/TB+	0.4018	0.0572	0.0058	0.0028	0.0066	0.0059	0.0036	1.960
135	HIV-/TB+	0	0	0.0027	0.0008	0.0017	0.0025	0.0014	1.874
140	HIV-/TB+	0.1908	0	0.0279	0.0015	0.0025	0	0	1.139
141	HIV-/TB+	0.4518	0.2039	0.0199	0.0030	0.0068	0	0.0075	0.874
144	HIV-/TB+	1.9352	0.6454	0.0402	0.0032	0.0097	0.0050	0.0013	1.843
146	HIV-/TB+	5.6139	2.3635	0.3677	0.0465	1.3254	0.0863	0.0051	0.991
152	HIV-/TB+	0.2970	0.0690	0.0057	0.0026	0.0049	0.0043	0.0015	0.916
154	HIV-/TB+	0.5154	0	0	0	0.0063	0	0	1.807
157	HIV-/TB+	0	0	0.0049	0.0012	0.0017	0	0.0034	2.106
168	HIV-/TB+	1.9535	0.6477	0.0873	0.0055	0.0219	0.0081	0.0062	1.063
169	HIV-/TB+	0.6924	0.2716	0.0285	0.0024	0.0088	0.0043	0.0020	1.377
175	HIV-/TB+	0.0837	0	0.0088	0.0064	0.0104	0.0149	0.0053	1.204
176	HIV-/TB+	1.9441	0.8310	0.0634	0.0035	0.0121	0.0039	0.0011	0.801
178	HIV-/TB+	0.7928	0.1811	0.0128	0.0031	0.0068	0.0051	0.0038	2.335
180	HIV-/TB+	4.3313	1.9602	0.1058	0.0148	0.0885	0.0204	0.0031	1.781
181	HIV-/TB+	0	0	0	0.0023	0.0034	0.0047	0.0028	1.270
182	HIV-/TB+	0.0470	0	0.0037	0.0048	0.0085	0.0096	0.0036	1.535
183	HIV-/TB+	0.2266	0.1247	0.0111	0.0056	0.0096	0.0091	0.0023	0.656
188	HIV-/TB+	0	0	0	0	0	0	0	0
189	HIV-/TB+	0.0741	0	0.0043	0.0018	0.0038	0.0058	0.0024	1.187
190	HIV-/TB+	1.9781	0.8620	0.0377	0.0089	0.0239	0.0104	0.0029	1.293
191	HIV-/TB+	0	0	0.0051	0.0023	0.0039	0.0045	0.0033	1.898
192	HIV-/TB+	1.6443	0.4633	0.0248	0	0.0052	0	0	0
193	HIV-/TB+	1.3789	0.6275	0.0491	0	0.0320	0	0	2.233
194	HIV/TB+	5.7494	1.6737	0.0484	0.0090	0.0473	0.0195	0.0031	1.646
198	HIV-/TB+	1.4538	0.2342	0.0296	0.0108	0.0282	0.0223	0.0042	1.288
46	HIV+/TB-	0.9325	0.2111	0.0091	0.0014	0.0058	0	0	0.789
48	HIV+/TB-	0.0916	0.0322	0.0055	0.0030	0.0049	0.0057	0.0027	0.713
57	HIV+/TB-	0.7125	0.1897	0.0109	0.0013	0.0035	0	0	2.071
62	HIV+/TB-	0.2142	0.0675	0.0151	0.0011	0.0017	0	0	1.770
63	HIV+/TB-	0.6366	0.3253	0.0504	0.0029	0.0106	0.0073	0.0023	1.260
77	HIV+/TB-	3.8444	1.1001	0.1861	0.0068	0.0309	0.0126	0.0057	0.622
80	HIV+/TB-	0.2762	0.1502	0.0123	0	0.0029	0	0	0

13	HIV+/TB+	0	0	0	0.0072	0.0115	0.0153	0.0043	1.053
21	HIV+/TB+	0.0958	0.0339	0.0084	0.0026	0.0045	0.0056	0.0018	0.862
92	HIV+/TB+	0.9907	0.3460	0	0.0147	0.0314	0.0093	0	0
100	HIV+/TB+	1.4438	0.8893	0.0811	0.0115	0.0977	0.0257	0.0066	1.912
103	HIV+/TB+	2.8819	0.0759	0.0069	0.0146	0.0227	0.0284	0.0115	1.078
129	HIV+/TB+	2.5412	0.8695	0.0459	0.0129	0.0631	0.0152	0.0031	1.299
145	HIV+/TB+	0.6020	0.1236	0.0167	0.0051	0.0104	0.0130	0.0053	1.199
151	HIV+/TB+	0	0	0.0098	0.0013	0.0018	0	0	1.140
186	HIV+/TB+	0.8146	0.3737	0.0198	0.0032	0.0106	0.0047	0.0025	0.978

Values outside of reference ranges (besides the zero values that were below the detection level) are indicated in red font.

Table B3: All amino acid concentrations values given in (µmol/L)/(mmol/L) creatinine

ID	Group	Acetyl-tyrosine	Ethanol-amine	B-amino-isobutyric acid	Pyro-glutamic acid	B-Alanine	Tryptophan	Leucine	Kynurenine
34	HIV-/TB-	0	30.162	0	15.839	0	1.929	0.689	0
36	HIV-/TB-	0.12	23.363	0	20.07	0	3.47	0	0
43	HIV-/TB-	3.941	35.956	27.085	17.957	3.917	6.551	0	7.372
44	HIV-/TB-	0	89.242	0	21.903	0	18.814	2.755	0.41
45	HIV-/TB-	35.074	103.264	74.146	13.773	7.874	14.12	0	20.811
47	HIV-/TB-	0	20.93	0	18.783	0	5.223	1.378	0
49	HIV-/TB-	0	25.757	0	16.113	0	4.919	0.728	0
59	HIV-/TB-	0.015	24.981	0	14.41	0.074	5.683	2.722	0
61	HIV-/TB-	0	13.099	8.124	24.812	2.331	5.217	1.732	0
64	HIV-/TB-	0	7.201	0	25.589	0	2.822	0.173	0
65	HIV-/TB-	0	25.018	16.736	18.939	0.758	1.359	1.042	0.08
67	HIV-/TB-	0	23.482	0	14.095	0	2.086	0.291	0
69	HIV-/TB-	0	30.295	0	14.258	0	1.997	0	0
116	HIV-/TB-	0	61.556	0	29.434	0.61	7.62	0	0
127	HIV-/TB-	0.013	36.416	5.299	21.352	0	3.768	1.909	0
147	HIV-/TB-	0.019	29.093	4.216	18.41	0.277	5.115	2.678	0.307
148	HIV-/TB-	0	28.042	5.452	15.741	3.937	1.909	1.939	0.051
155	HIV-/TB-	0	12.488	0	24.906	0	0	0	0
158	HIV-/TB-	0	6.154	0	20.326	0	1.502	0.872	0
159	HIV-/TB-	0	56.656	13.587	28.926	0.044	6.41	2.858	0.38
161	HIV-/TB-	6.592	100.203	66.348	61.278	6.259	8.666	0	12.831
162	HIV-/TB-	0	25.007	2.443	8.968	0	2.336	0.787	0
163	HIV-/TB-	0	18.983	121.169	32.554	0	0	0	0
165	HIV-/TB-	0.045	31.235	0	16.195	0	5.74	1.162	0.049
166	HIV-/TB-	3.951	53.662	29.698	52.95	3.309	3.703	0.589	5.985
167	HIV-/TB-	0	22.464	5.278	15.915	8.107	11.299	3.265	0.236
170	HIV-/TB-	0	18.955	0.743	20.381	0.096	3.939	1.336	0.371
171	HIV-/TB-	0	31.94	13.098	19.122	0.709	11.02	2.602	0

172	HIV-/TB-	2.065	63.713	133.604	24.058	3.222	2.848	1.035	4.356
173	HIV-/TB-	0	24.645	42.345	15.409	0	0	0.744	0
184	HIV-/TB-	0	34.047	133.05	18.413	12.618	1.109	1.345	0
185	HIV-/TB-	0	30.997	7.583	62.478	0	2.124	1.42	0.053
1	HIV-/TB+	0.08	11.084	14.577	18.433	0.21	1.873	1.186	0.132
3	HIV-/TB+	0	21.99	0	35.226	0.116	1.552	2.053	1.031
7	HIV-/TB+	0.404	5.358	0.995	29.378	0.236	1.297	2.59	0.939
12	HIV-/TB+	0	45.627	2.139	23.034	0	3.415	3.851	2.895
14	HIV-/TB+	0	35.247	0	33.237	0	6.251	7.35	1.154
19	HIV-/TB+	0.588	49.309	3.436	28.933	3.112	0.725	3.852	1.632
22	HIV-/TB+	0	23.596	0	34.664	0.225	7.839	6.218	0.198
23	HIV-/TB+	0.731	27.098	6.049	20.86	2.119	1.09	1.898	1.908
27	HIV-/TB+	0	19.102	2.912	19.305	0	3.607	1.547	0.559
90	HIV-/TB+	0.115	49.219	1.016	20.491	0	5.591	2.812	0.325
91	HIV-/TB+	0.017	4.229	21.833	25.687	0	1.981	9.278	0
123	HIV-/TB+	0	43.821	55.094	22.33	0	0.797	0.604	0
124	HIV-/TB+	1.873	48.983	161.046	29.176	2.413	2.412	0	3.973
128	HIV-/TB+	0.085	20.873	73.451	24.948	0.754	3.878	2.007	1.681
130	HIV-/TB+	0	34.597	0	26.189	2.419	5.818	5.311	0.619
132	HIV-/TB+	0.373	42.291	15.951	23.35	2.114	0.61	3.366	1.262
135	HIV-/TB+	0	20.877	1.635	21.309	0.001	2.208	1.554	0.134
140	HIV-/TB+	0	35.166	9.271	26.467	0	5.191	0.996	0.261
141	HIV-/TB+	1.53	37.203	36.854	24.202	2.364	2.569	1.681	3.111
144	HIV-/TB+	0.021	147.11	1.085	33.387	0.084	5.023	2.422	1.774
146	HIV-/TB+	0	43.113	0.655	21.989	0.286	5.658	2.428	1.755
152	HIV-/TB+	0.036	25.026	0	22.637	0	1.59	1.321	0.146
154	HIV-/TB+	2.589	53.69	45.386	36.383	4.175	3.614	2.235	5.599
157	HIV-/TB+	0	17.016	0	26.249	0	1.455	0	0
168	HIV-/TB+	0	12.123	0	35.678	0	0.899	0.611	0.314
169	HIV-/TB+	0	30.035	13.471	31.314	0	3.379	3.436	0.455
175	HIV-/TB+	0	47.026	105.791	31.555	0	2.321	1.518	0.11
176	HIV-/TB+	0.005	18.755	6.134	40.097	0.188	2.751	2.616	2.112
178	HIV-/TB+	0.906	66.131	5.934	33.669	3.024	1.299	3.763	2.492
180	HIV-/TB+	0.286	34.638	1.918	46.041	2.171	0.519	1.281	0.901
181	HIV-/TB+	0.565	28.13	4.521	24.654	1.537	0.821	1.218	1.279
182	HIV-/TB+	0	58.376	20.038	25.164	0	5.885	2.159	11.477
183	HIV-/TB+	0	19.449	0	34.73	2.772	5.166	2.71	0.989
188	HIV-/TB+	3.187	51.678	24.368	71.682	5.701	4.091	0.7	5.595
189	HIV-/TB+	0	25.591	0.071	16.098	0.063	3.659	1.257	0.319
190	HIV-/TB+	0	23.424	46.136	26.194	0.288	0.67	1.297	0.336
191	HIV-/TB+	0.66	42.254	76.264	23.631	3.164	3.685	3.345	2.019
192	HIV-/TB+	2.521	44.509	42.162	28.75	3.849	4.157	1.297	4.827

193	HIV-/TB+	4.158	67.999	25.498	14.355	3.836	4.977	0.693	7.506
194	HIV/TB+	0	50.429	2.176	53.591	0	4.968	4.311	1.72
198	HIV-/TB+	0.128	21.001	0.552	31.742	0.246	6.422	1.743	0.817
46	HIV+/TB-	0	12.148	0	13.205	0	0	0	0
48	HIV+/TB-	0	23.744	0	17.794	0	0	0	0
57	HIV+/TB-	0	11.259	0	18.707	0	5.091	0.98	0
62	HIV+/TB-	0	26.484	0	19.049	0	3.871	0.696	0
63	HIV+/TB-	1.326	14.569	0.121	22.702	0.047	6.466	2.743	0.219
77	HIV+/TB-	0	0	0	14.505	0	0	2.91	0
80	HIV+/TB-	0	3.739	13.032	13.621	2.424	0	0	0
13	HIV+/TB+	0	134.461	58.676	24.434	0	0	1.261	0
21	HIV+/TB+	0	20.38	1.089	20.972	1.693	4.29	2.099	0.859
92	HIV+/TB+	0	252.886	0	19.817	0	0	18.685	0
100	HIV+/TB+	0	2.5	239.479	21.431	0	3.607	3.843	6.386
103	HIV+/TB+	0.759	39.889	128.028	26.641	2.441	1.281	0.869	2.057
129	HIV+/TB+	0	27.884	0	25.619	0	1.55	3.113	0
145	HIV+/TB+	0	21.781	2.898	16.999	1.724	1.551	1.374	0.044
151	HIV+/TB+	0	49.355	124.83	25.379	0.732	1.173	0.6	0.659
186	HIV+/TB+	0	17.76	2.147	27.118	1.963	1.927	1.882	1.767

ID	Group	Isoleucine	Phenyl-alanine	Allo-isoleucine	Hydroxy-kynurenine	Methionine	Valine	Tyrosine	a-amino-butyric acid
34	HIV-/TB-	0.062	2.192	0	0	0	0.887	4.163	0
36	HIV-/TB-	0.178	2.644	0	0	0	1.374	7.242	0
43	HIV-/TB-	4.72	3.933	4.678	3.361	13.76	1.786	3.887	1.765
44	HIV-/TB-	0.108	7.681	0	0	0	3.804	16.259	0.01
45	HIV-/TB-	13.864	10.638	5.952	10.446	22.291	4.695	9.739	4.461
47	HIV-/TB-	0	3.812	0	0	0	0.257	4.942	0.362
49	HIV-/TB-	0	3.408	0	0	0	0.925	5.024	0
59	HIV-/TB-	0.618	4.662	0	0	0	2.682	9.303	0.345
61	HIV-/TB-	0.4	2.429	0	0	0	1.586	2.663	0.493
64	HIV-/TB-	0	2.136	0	0	0	0	2.946	0
65	HIV-/TB-	0.611	1.589	0	0	0	1.09	1.651	0.304
67	HIV-/TB-	0	2.554	0	0	0	0	3.379	0
69	HIV-/TB-	0	0.28	0	0	0	0	1.867	0
116	HIV-/TB-	0	2.549	0	0	0	2.492	7.653	0.62
127	HIV-/TB-	0.7	2.759	0	0	0	2.116	2.899	0.247
147	HIV-/TB-	0.9	5.135	0.026	0.1	0.558	2.905	5.454	0.425
148	HIV-/TB-	0.928	2.068	0	0	0	1.505	4.257	0.069
155	HIV-/TB-	0	1.162	0	0	0	0	0	0
158	HIV-/TB-	0	2.297	0	0	0	1.306	1.961	0
159	HIV-/TB-	0.74	5.989	0	0.267	0.414	2.462	5.848	1.234
161	HIV-/TB-	8.289	5.413	7.171	6.063	18.172	3.571	7.668	3.406
162	HIV-/TB-	0.179	1.947	0	0	0	0.862	3.373	0.371

163	HIV-/TB-	0	0.543	0	0	0	0	4.044	0
165	HIV-/TB-	0	6.807	0	0	0	0.384	8.073	0.429
166	HIV-/TB-	3.783	2.632	4.428	2.688	11.962	1.323	4.193	1.527
167	HIV-/TB-	1.325	4.753	0	0	0	2.154	12.414	0.546
170	HIV-/TB-	0.384	3.25	0	0.338	0.289	1.349	3.908	0.279
171	HIV-/TB-	0.373	7.625	0	0	0	3.379	13.802	0.368
172	HIV-/TB-	2.505	1.727	5.163	1.818	8.824	1.111	3.255	1.406
173	HIV-/TB-	0.221	0.945	0	0	0	1.109	0.917	0.003
184	HIV-/TB-	0	1.57	0	0	0	2.501	1.512	0.195
185	HIV-/TB-	0.715	2.207	0	0.015	5.321	1.537	1.579	0.149
1	HIV-/TB+	0.54	2.711	0	0.03	0.068	1.085	1.004	0.135
3	HIV-/TB+	0.635	4.848	0	5.619	0.208	1.954	1.799	0.481
7	HIV-/TB+	0.687	3.347	0	0.228	0.204	2.221	2.186	0.176
12	HIV-/TB+	0.466	8.565	0	5.512	0	2.809	6.564	0.586
14	HIV-/TB+	2.305	9.78	0	13.409	0	7.794	10.867	1.141
19	HIV-/TB+	3.374	0.456	4.266	13.061	4.126	0.292	2.905	0.772
22	HIV-/TB+	1.841	11.326	0	0.141	0.236	8.231	12.026	1.553
23	HIV-/TB+	1.023	0.613	3.498	0.718	5.006	0.313	2.493	0.874
27	HIV-/TB+	0.314	5.735	0	0.158	0	1.742	2.684	0.275
90	HIV-/TB+	0.736	4.467	0	0	0.043	2.604	5.696	0.851
91	HIV-/TB+	0.342	2.582	0	0	0	0.946	1.745	0
123	HIV-/TB+	0	0.354	0	0	0	0	0.847	0
124	HIV-/TB+	2.704	1.46	3.523	1.598	7.117	0.92	3.136	0.813
128	HIV-/TB+	0.744	4.509	1.049	0.614	0.15	2.375	4.863	0.427
130	HIV-/TB+	0.313	7.498	0	0	0	7.096	8.212	0.65
132	HIV-/TB+	0.712	0.351	2.498	0.413	3.01	0.582	1.91	0.7
135	HIV-/TB+	0.605	2.675	0	0.051	0.071	1.46	3.468	0.081
140	HIV-/TB+	0.993	3.56	0	0	0	0.478	8.641	0
141	HIV-/TB+	1.877	1.168	3.164	1.256	6.391	0.59	2.772	0.814
144	HIV-/TB+	0.655	6.681	0	13.133	0.441	2.277	7.239	0.288
146	HIV-/TB+	1.078	5.056	0	0.916	0.179	2.065	5.992	1.017
152	HIV-/TB+	0.409	2.707	0	0	0.082	1.56	2.282	0.22
154	HIV-/TB+	3.275	2.468	4.937	2.403	9.882	1.998	5.291	1.388
157	HIV-/TB+	0	1.728	0	0	0	0	1.794	0
168	HIV-/TB+	0.787	1.319	0	0	0	0	1.266	0
169	HIV-/TB+	1.372	4.898	0	0.201	0.557	3.208	4.349	0.889
175	HIV-/TB+	0.574	4.744	0	9.163	0	1.423	3.901	0.53
176	HIV-/TB+	0.5	5.538	0	3.635	0.089	1.978	2.761	0.548
178	HIV-/TB+	1.546	0.895	3.561	1.268	8.836	1.063	3.694	0.688
180	HIV-/TB+	1.127	0.282	3.235	2.124	2.826	0.644	2.077	0.431
181	HIV-/TB+	0.659	0.526	2.495	0.498	2.883	0.618	1.45	0.453
182	HIV-/TB+	0.232	4.375	0	2.14	0	0.782	7.463	0

183	HIV-/TB+	0	5.872	0	1.295	0	0.482	4.93	0
188	HIV-/TB+	3.647	3.918	4.694	2.725	9.501	2.705	3.57	1.501
189	HIV-/TB+	0.698	9.397	0	0.118	0.301	1.409	5.882	0.338
190	HIV-/TB+	0.536	2.006	0	0.262	0.375	1.38	1.445	0.353
191	HIV-/TB+	1.238	0.739	5.434	1.284	6.501	1.036	2.98	0.614
192	HIV-/TB+	3.11	2.67	5.262	2.395	7.125	2.684	3.951	1.64
193	HIV-/TB+	4.867	3.037	5.63	3.34	14.119	2.118	4.623	1.421
194	HIV/TB+	0.781	8.557	0	0.651	0	3.475	8.589	0.07
198	HIV-/TB+	0.642	4.165	0	1.431	0.41	1.534	4.921	0.539
46	HIV+/TB-	0	0	0	0	0	0	0	0
48	HIV+/TB-	0	1.962	0	0	0	0.549	1.526	0
57	HIV+/TB-	0	5.075	0	0	0	0.393	9.013	0
62	HIV+/TB-	0	4.662	0	0	0	0.624	7.182	0
63	HIV+/TB-	0.536	3.012	0	0	0	2.332	4.663	0.57
77	HIV+/TB-	0	1.481	0	0	0	0.158	3.51	0.746
80	HIV+/TB-	0	1.651	0	0	0	0	5.562	0
13	HIV+/TB+	0.597	3.24	1.141	1.243	0	1.266	4.173	0.292
21	HIV+/TB+	0.859	5.979	0.613	0.721	0.052	2.165	5.573	0.397
92	HIV+/TB+	0	13.792	0	0	0	3.392	2.642	0
100	HIV+/TB+	0	6.141	0	29.055	0	1.851	6.935	0
103	HIV+/TB+	1.683	0.638	3.985	10.43	5.427	0.38	2.624	1.083
129	HIV+/TB+	0.262	4.497	0	0	0	2.13	3.147	0.058
145	HIV+/TB+	0.862	2.769	0.145	0	0	1.277	1.451	0.632
151	HIV+/TB+	0.697	5.067	0	1.355	0	0.651	2.623	0
186	HIV+/TB+	0.617	4.044	0	4.275	0	1.948	2.647	0.635

ID	Group	Taurine	Pipecolic acid	Alanine	a-amino-adipic acid	Threonine	Proline	Glycine	Sarcosine
34	HIV-/TB-	46.179	0	17.528	0.222	8.387	0	245.505	0
36	HIV-/TB-	76.59	0	9.903	1.547	3.755	0	213.376	0
43	HIV-/TB-	183.178	4.327	71.411	16.126	3.436	1.845	641.971	2.075
44	HIV-/TB-	147.072	0	123.343	3.036	80.608	0	632.171	0
45	HIV-/TB-	249.576	10.792	90.651	33.58	6.699	1.092	180.805	3.771
47	HIV-/TB-	48.275	0	13.455	0	6.587	0	458.867	0
49	HIV-/TB-	88.89	0	9.815	0	4.009	0	247.683	0
59	HIV-/TB-	135.694	0	29.417	2.957	6.843	0	130.47	0
61	HIV-/TB-	92.319	0	40.426	2.525	15.086	0	471.712	0
64	HIV-/TB-	116.485	0	4.05	0	12.384	0	204.432	0
65	HIV-/TB-	57.799	0	17.378	0.556	10.085	0	360.901	0
67	HIV-/TB-	60.709	0	8.3	0	1.972	0	48.359	0
69	HIV-/TB-	48.306	0	3.361	0	1.973	0	115.289	0
116	HIV-/TB-	139.677	0	17.103	1.267	11.207	0	344.346	0
127	HIV-/TB-	112.279	0	19.986	1.238	9.59	0	130.461	0
147	HIV-/TB-	65.191	0.036	14.696	1.106	8.08	0.016	70.084	0.053

148	HIV-/TB-	124.311	0	15.079	0.85	10.043	0	104.37	0
155	HIV-/TB-	229.239	0	6.521	0	0	0	109.225	0
158	HIV-/TB-	161.278	0	18.22	0	1.079	0	34.326	0
159	HIV-/TB-	93.091	0.017	24.891	2.019	9.655	0.348	262.233	0.014
161	HIV-/TB-	103.237	6.599	54.42	23.651	6.896	2.103	138.197	2.641
162	HIV-/TB-	61.03	0	6.099	0.016	6.971	0	70.904	0
163	HIV-/TB-	746.182	0	0	0.01	0	0	47.904	0
165	HIV-/TB-	60.239	0.029	22.612	2.762	8.061	0.265	108.856	0
166	HIV-/TB-	54.236	2.894	26.17	17.54	3.864	0.786	103.523	1.177
167	HIV-/TB-	72.488	0	28.971	1.723	18.453	0	206.136	0
170	HIV-/TB-	98.423	0.121	17.4	1.21	8.132	0.062	78.522	0
171	HIV-/TB-	120.572	0	45.147	2.357	22.379	0	740.212	0
172	HIV-/TB-	163.968	1.913	28.328	13.886	2.371	0.658	406.709	0.888
173	HIV-/TB-	42.97	0	6.956	0.909	4.236	0	49.318	0
184	HIV-/TB-	134.528	0	4.652	1.751	0	0	177.756	0
185	HIV-/TB-	16.965	0	9.358	0.795	3.187	0	77.625	0
1	HIV-/TB+	98.976	0	2.644	0.877	1.644	0	16.919	0
3	HIV-/TB+	181.991	0	9.036	0.878	3.328	0.071	18.54	0.079
7	HIV-/TB+	8.17	0.089	19.351	0.433	4.043	0.156	35.419	0.179
12	HIV-/TB+	107.607	0	24.365	1.838	5.925	0	101.536	0
14	HIV-/TB+	168.74	0	72.952	2.416	15.173	0	89.007	0.635
19	HIV-/TB+	184.477	0.475	8.537	7.979	5.701	0.768	50.478	1.203
22	HIV-/TB+	181.126	0	61.368	5.368	11.294	0.395	57.641	0
23	HIV-/TB+	124.305	0.695	10.765	9.585	1.997	0.571	100.506	0.317
27	HIV-/TB+	164.066	0	7.1	3.705	4.582	0	76.935	0
90	HIV-/TB+	102.964	0.038	18.449	2.403	8.132	0.325	158.225	0
91	HIV-/TB+	34.281	0	7.197	0.451	2.526	0.083	22.849	0.151
123	HIV-/TB+	91.893	0	10.611	0.722	5.671	0	303.382	0
124	HIV-/TB+	41.092	1.721	12.063	3.15	1.881	1.553	93.4	0.65
128	HIV-/TB+	233.458	0	14.125	2.404	6.471	0.144	35.913	0
130	HIV-/TB+	357.058	0	47.568	2.889	9.196	0	70.483	0
132	HIV-/TB+	39.683	0.353	8.228	5.173	1.478	0.213	74.497	0.175
135	HIV-/TB+	55.065	0	8.515	0.196	3.554	0.196	70.314	0
140	HIV-/TB+	208.941	0	23.146	0	8.292	0	338.579	0
141	HIV-/TB+	112.358	1.377	17.38	8.917	1.989	0.73	85.154	0.545
144	HIV-/TB+	133.709	0	29.334	0.506	6.974	0.083	35.987	0
146	HIV-/TB+	143.858	0	18.526	2.589	7.29	0	146.145	0
152	HIV-/TB+	88.602	0	7.42	0.438	4.094	0.127	43.077	0
154	HIV-/TB+	149.406	2.651	39.379	16.795	2.325	1.412	204.489	1.187
157	HIV-/TB+	35.506	0	8.857	0	0.853	0	98.967	0
168	HIV-/TB+	71.457	0	7.384	0	1.549	0	30.562	0
169	HIV-/TB+	16.685	0	14.475	1.292	9.503	0	116.93	0

175	HIV-/TB+	56.252	0	15.716	0.864	10.565	0.87	58.298	0
176	HIV-/TB+	268.549	0	18.126	7.212	7.348	0.062	87.462	0
178	HIV-/TB+	17.621	0.868	19.444	10.881	1.808	1.244	112.626	0.386
180	HIV-/TB+	155.708	0.301	14.492	8.842	1.951	0.387	38.743	0.112
181	HIV-/TB+	64.753	0.5	11.557	4.555	1.025	0.471	48.273	0.26
182	HIV-/TB+	12.266	0	30.154	0.674	6.408	0	68.482	0
183	HIV-/TB+	197.516	0	13.208	2.907	4.334	0	41.199	0
188	HIV-/TB+	69.545	2.817	41.305	13.108	3.031	1.677	40.762	1.503
189	HIV-/TB+	170.588	0	13.275	0.306	6.258	0	62.904	0
190	HIV-/TB+	141.412	0	13.304	0.35	4.286	0	52.991	0
191	HIV-/TB+	108.735	0.641	15.541	11.608	2.712	0.7	96.466	0.428
192	HIV-/TB+	239.992	2.473	28.511	11.551	2.687	1.817	41.676	1.384
193	HIV-/TB+	117.853	3.601	25.969	10.572	2.474	1.032	101.325	1.261
194	HIV/TB+	126.71	0	39.746	0.804	17.223	0	141.349	0
198	HIV-/TB+	144.62	0	6.556	0.692	4.101	0	30.926	0
46	HIV+/TB-	102.628	0	34.294	0	1.865	0	185.931	0
48	HIV+/TB-	60.774	0	0.68	0	2.26	0	124.509	0
57	HIV+/TB-	22.36	0	76.098	0.367	20.34	0	660.126	0
62	HIV+/TB-	125.133	0	16.869	0	5.096	0	106.194	0
63	HIV+/TB-	260.078	0	32.984	3.76	10.008	0	81.431	0
77	HIV+/TB-	167.808	0	32.005	0	0	0	70.737	0
80	HIV+/TB-	82.051	0	50.386	1.16	21.531	0	199.128	0
13	HIV+/TB+	59.236	0	3.887	0.025	7.316	0	82.533	0
21	HIV+/TB+	110.914	0	12.016	2.004	5.29	0	33.953	0
92	HIV+/TB+	96.915	0	5.589	0	0	0.692	139.6	0
100	HIV+/TB+	55.115	0	12.161	0	9.968	1.153	12.454	0
103	HIV+/TB+	82.724	0.717	12.723	7.57	2.541	0.472	50.169	0.419
129	HIV+/TB+	52.985	0	10.855	0.537	8.682	0	60.275	0
145	HIV+/TB+	150.958	0	5.908	3.445	3.676	0	64.863	0
151	HIV+/TB+	235.083	0	8.055	6.302	2.569	0	40.361	0
186	HIV+/TB+	215.422	0.004	11.562	1.612	4.959	0.116	24.617	0
ID	**Group**	**Glutamic acid**	**Glutamine**	**Serine**	**4-Hydroxy-proline**	**Arginine**	**Histidine**	**Asparagine**	**1-methyl-histidine**
34	HIV-/TB-	1.033	4.037	39.333	0	0.057	42.455	1.76	11.326
36	HIV-/TB-	5.785	8.88	39.893	0	0	60.408	0	17.327
43	HIV-/TB-	3.272	63.876	9.057	1.917	7.351	90.413	89.531	20.843
44	HIV-/TB-	1.589	0	90.666	0	0	352.105	28.845	25.895
45	HIV-/TB-	0	44.843	5.914	5.021	22.79	105.005	163.589	25.05
47	HIV-/TB-	0	0	38.231	0	0	57.015	1.87	13.55
49	HIV-/TB-	0	0	30.316	0	0	39.5	0	14.763
59	HIV-/TB-	1.424	5.516	30.412	0	1.76	91.716	7.016	24.143
61	HIV-/TB-	4.785	4.425	85.401	0.206	1.259	73.847	13.775	24.641
64	HIV-/TB-	0.206	0	44.94	0	0.124	91.946	5.927	17.925

65	HIV-/TB-	0	7.057	43.064	0	0.748	40.5	4.656	18.929
67	HIV-/TB-	0	0	24.223	0	0	55.675	0	16.018
69	HIV-/TB-	0.378	0	33.783	0	0	53.065	0.399	18.835
116	HIV-/TB-	18.906	3.635	9.056	0.585	0.875	76.076	0	21.233
127	HIV-/TB-	1.99	5.389	29	0	1.588	24.599	5.413	22.747
147	HIV-/TB-	1.203	2.812	16.024	0.024	1.321	34.374	4.239	18.069
148	HIV-/TB-	5.929	7.685	21.347	0.174	0.682	53.824	4.704	23.133
155	HIV-/TB-	2.438	9.576	29.235	0	0.212	23.329	2.927	21.395
158	HIV-/TB-	0.327	0	15.752	0	0.983	14.649	0.462	17.397
159	HIV-/TB-	36.983	3.813	32.635	0	1.11	102.462	5.568	19.212
161	HIV-/TB-	0.335	50.352	3.791	6.482	22.495	86.048	95.998	18.535
162	HIV-/TB-	0.937	5.04	42.582	0	0.794	45.33	4.083	16.419
163	HIV-/TB-	1.907	15.917	20.784	0	0.73	40.501	3.271	19.902
165	HIV-/TB-	4.448	2.132	19.773	0.514	0.015	99.481	1.188	16.958
166	HIV-/TB-	0	27.73	1.552	1.903	9.913	67.635	66.015	8.451
167	HIV-/TB-	2.444	7.965	45.701	0	0.359	145.371	14.546	22.126
170	HIV-/TB-	0.362	1.574	19.226	0	0.594	49.758	4.459	16.892
171	HIV-/TB-	0.23	0	65.718	0	0.291	129.155	8.079	20.019
172	HIV-/TB-	0.446	45.631	1.064	1.794	11.821	63.96	76.807	13.024
173	HIV-/TB-	0.399	3.297	11.736	0	0.805	12.07	2.395	22.673
184	HIV-/TB-	1.999	0	31.254	0	0	32.884	0.487	34.691
185	HIV-/TB-	1.288	8.148	21.674	0	0.815	26.398	4.564	20.724
1	HIV-/TB+	0	2.578	10.989	0	0.53	7.229	2.883	15.053
3	HIV-/TB+	2.393	2.35	15.45	0	0.821	8.149	4.825	13.39
7	HIV-/TB+	1.294	2.569	17.78	0	0.335	10.909	3.719	15.836
12	HIV-/TB+	0.082	2.456	26.086	0	0.689	58.29	10.534	23.992
14	HIV-/TB+	3.058	6.497	43.511	0	2.225	56.964	15.213	18.058
19	HIV-/TB+	1.563	23.813	0.349	1.541	7.869	47.541	26.116	6.105
22	HIV-/TB+	1.053	7.47	37.409	0	3.312	41.57	10.004	18.178
23	HIV-/TB+	2.938	32.522	0.504	1.302	6.548	40.518	45.915	9.023
27	HIV-/TB+	1.054	2.486	30.165	0	0.546	27.254	6.313	13.708
90	HIV-/TB+	0.667	2.461	27.144	0.147	1.046	55.386	7.493	20.912
91	HIV-/TB+	0.245	2.886	9.577	0	0.75	16.463	6.433	16.617
123	HIV-/TB+	8.436	9.281	23.965	0	0.133	54.384	1.138	19.111
124	HIV-/TB+	1.039	37.905	3.183	2.115	5.098	33.351	17.103	6.725
128	HIV-/TB+	1.596	1.837	20.099	0	0.798	9.334	5.686	11.343
130	HIV-/TB+	4.2	0	35.908	0	1.004	29.131	5.967	19.751
132	HIV-/TB+	20.478	15.708	0.262	1.617	4.173	29.735	35.034	4.284
135	HIV-/TB+	1.833	2.704	13.406	0	0.537	10.11	3.227	16.321
140	HIV-/TB+	5.03	18.933	39.338	0	0.753	62.314	7.889	18.295
141	HIV-/TB+	0	24.649	0.794	1.266	7.239	52.6	38.418	5.82
144	HIV-/TB+	1.444	2.701	31.105	0	0.836	35.586	7.629	18.514

146	HIV-/TB+	0.223	7.39	33.549	0	1.242	52.988	7.767	17.428
152	HIV-/TB+	0.798	1.112	16.589	0.059	0.663	8.239	3.734	12.992
154	HIV-/TB+	0.255	29.323	1.667	2.727	11.366	67.14	68.035	7.701
157	HIV-/TB+	0	0	27.88	0	0	31.031	0	15.469
168	HIV-/TB+	0	12.327	22.239	0	0.122	12.817	3.543	22.046
169	HIV-/TB+	0.411	4.473	23.197	0	0.969	33.134	6.444	19.757
175	HIV-/TB+	5.568	10.601	37.349	0.021	1.007	9.112	7.155	13.468
176	HIV-/TB+	2.433	3.49	31.381	0	0.907	18.425	10.424	17.945
178	HIV-/TB+	1.187	15.205	0.659	2.239	6.775	21.423	36.243	6.442
180	HIV-/TB+	1.453	27.761	0.192	1.146	4.454	8.385	21.993	2.914
181	HIV-/TB+	0.258	14.24	0.514	0.911	3.79	9.504	22.22	2.395
182	HIV-/TB+	1.489	0	40.301	0	1.751	56.807	10.706	14.711
183	HIV-/TB+	6.629	0	28.716	0	0	27.603	6.719	11.359
188	HIV-/TB+	4.79	12.527	2.282	3.256	10.838	49.44	41.187	8.844
189	HIV-/TB+	0	4.91	30.943	0	1.022	31.742	5.233	14.523
190	HIV-/TB+	1.784	2.899	18.932	0	0.717	17.228	4.279	15.28
191	HIV-/TB+	1.263	36.469	0.764	1.289	7.33	28.179	45.539	7.241
192	HIV-/TB+	1.613	21.76	1.108	3.333	9.413	30.569	45.326	8.755
193	HIV-/TB+	6.123	27.297	1.893	2.248	10.693	64.492	73.932	11.155
194	HIV/TB+	0	0	50.262	0	1.945	20.305	12.412	27.86
198	HIV-/TB+	0.827	11.696	19.209	0	0.633	19.733	4.777	15.094
46	HIV+/TB-	2.639	0	38.331	0	0	53.826	0	18.75
48	HIV+/TB-	0	0	21.836	0	0.725	11.38	0	9.075
57	HIV+/TB-	0	0	78.044	0	0	148.573	17.282	25.167
62	HIV+/TB-	0	6.39	32.651	0	0.076	49.673	3.883	18.185
63	HIV+/TB-	1.352	3.359	20.664	0	3.569	62.89	7.425	44.989
77	HIV+/TB-	0	0	27.174	0	0	35.575	0	18.446
80	HIV+/TB-	0	13.404	59.035	0	0.472	120.903	15.915	24.855
13	HIV+/TB+	1.854	4.879	33.491	0	1.068	24.893	5.971	17.262
21	HIV+/TB+	1.118	4.16	20.377	0	1.292	44.388	6.064	18.706
92	HIV+/TB+	5.657	0	26.645	0	2.506	0	0	11.875
100	HIV+/TB+	3.346	0	36.963	0	0.812	60.945	10.596	32.938
103	HIV+/TB+	0.467	24.911	0.418	1.122	6.411	17.357	37.37	4.324
129	HIV+/TB+	5.516	2.305	28.158	0	1.031	24.294	4.958	23.148
145	HIV+/TB+	0.138	6.369	19.68	0	0.984	16.195	4.471	20.922
151	HIV+/TB+	2.361	8.478	22.745	0	0.88	14.118	4.623	13.018
186	HIV+/TB+	0.902	2.294	19.062	0	0.644	27.403	4.149	15.98
ID	**Group**	**Lysine**	**Carnosine**	**Homo-citrulline**	**Ornithine**	**3-Methyl-histidine**	**Adenosyl-homo-cysteine**	**Hydroxy-lysine**	**Citrulline**
34	HIV-/TB-	0	0	0	0	4.392	0	0	0
36	HIV-/TB-	4.648	0	0	0	27.154	0	0	0
43	HIV-/TB-	8.427	10.74	3.083	8.642	0	0	19.78	2.632

44	HIV-/TB-	41.612	0	0	1.624	185.617	0	3.477	0.483
45	HIV-/TB-	0	28.143	4.287	22.397	0	0	29.819	6.553
47	HIV-/TB-	0	0	0	0	7.171	0	0	0
49	HIV-/TB-	4.105	0	0	0	87.565	0	0	0
59	HIV-/TB-	19.8	0	0	0	237.527	0	0.13	0
61	HIV-/TB-	13.443	6.637	0.07	0	134.589	0	1.643	0
64	HIV-/TB-	27.981	0	0	0	53.94	0	2.573	0
65	HIV-/TB-	1.942	1.716	0.328	0.696	17.646	0	0	0
67	HIV-/TB-	0	1.26	0	0	8.981	0	0	0
69	HIV-/TB-	2.284	0	0	0	66.016	0	0	0
116	HIV-/TB-	6.383	0	0	0	2.019	0	5.134	0
127	HIV-/TB-	6.734	1.103	0.731	3.05	145.413	0	0	0
147	HIV-/TB-	6.663	0.848	1.132	0.84	118.3	0	0.219	0.216
148	HIV-/TB-	2.136	0.93	0.029	0.625	89.736	0	0.024	0
155	HIV-/TB-	10.786	1.581	0	0	106.073	0	0.612	0
158	HIV-/TB-	3.116	0	0	0	35.918	0	0	0
159	HIV-/TB-	6.403	0.117	2.675	0.596	3.589	0	0.247	0.171
161	HIV-/TB-	0	17.748	3.065	16.078	0	0	15.162	4.947
162	HIV-/TB-	6.924	0.519	0	0	41.987	0	0	0
163	HIV-/TB-	3.209	0	0	0	42.012	0	0	0
165	HIV-/TB-	10.707	0.193	1.539	0	3.147	0	0.307	0.876
166	HIV-/TB-	17.405	7.964	2.244	7.601	0	0	6.74	2.008
167	HIV-/TB-	22.348	14.887	0	0.78	137.949	0	0.093	0
170	HIV-/TB-	1.586	1.207	0.454	0.367	14.948	0	0.022	0.028
171	HIV-/TB-	28.919	0	0	0	128.805	0	0	0
172	HIV-/TB-	13.621	4.959	0.823	4.496	0	0	6.303	1.796
173	HIV-/TB-	8.19	0	1.631	0	14.749	0	0.517	0
184	HIV-/TB-	2.041	10.182	0.538	0	211.626	0	0.181	0
185	HIV-/TB-	1.393	0	2.681	0.787	30.341	0	0	0
1	HIV-/TB+	1.553	7.296	0.43	0.603	7.508	0	0.028	0
3	HIV-/TB+	1.383	0.285	0	0.513	0.315	0	0.05	0
7	HIV-/TB+	1.615	0.516	0	0.719	9.37	0.076	0.091	0
12	HIV-/TB+	4.01	0.812	0.232	0	18.95	0	0.273	0
14	HIV-/TB+	13.171	0	0	0	17.541	0	0.557	0
19	HIV-/TB+	19.63	1.616	0.375	1.941	0	0	2.462	1.334
22	HIV-/TB+	30.839	0	0	1.657	30.27	0	0.557	0
23	HIV-/TB+	15.495	2.295	0.521	2.063	0	0	2.227	0.833
27	HIV-/TB+	4.506	0.661	0.685	0	12.189	0	0.184	0
90	HIV-/TB+	3.143	0.673	0.996	5.179	46.679	0.007	0.313	0
91	HIV-/TB+	0.473	0.265	0.2	0	7.493	0	0	0
123	HIV-/TB+	3.226	0.058	0	0	16.236	0	0	0
124	HIV-/TB+	12.476	6.713	2.363	3.986	0	0	5.935	2.391

128	HIV-/TB+	2.771	1.562	0.062	0	1.829	0.009	0	0
130	HIV-/TB+	10.96	0.475	0	0	9.797	0	2.56	0
132	HIV-/TB+	23.102	2.552	0.533	1.357	0	0	1.464	1.05
135	HIV-/TB+	0.864	1.607	0	0.493	35.436	0	0.02	0
140	HIV-/TB+	10.282	2.068	0	1.012	40.239	0	0	0
141	HIV-/TB+	12.244	4.169	1.586	3.199	0	0	4.207	1.22
144	HIV-/TB+	2.313	1.078	0.23	0.728	5.149	0	0.223	0.051
146	HIV-/TB+	7.385	1.014	0.194	0.859	44.832	0	0.159	0
152	HIV-/TB+	2.703	0.388	0.088	4.672	18.232	0.045	0.107	0
154	HIV-/TB+	10.914	7.359	1.011	5.856	0	0	6.575	2.223
157	HIV-/TB+	0	0	0	0	26.286	0	0	0
168	HIV-/TB+	0	0.795	0	1.416	74.335	0	0	0
169	HIV-/TB+	1.715	0.035	0	0.74	6.268	0	0.002	0
175	HIV-/TB+	5.172	0.464	0	0	0.107	0	0	0
176	HIV-/TB+	2.483	0.139	0.109	0	9.028	0	0	0
178	HIV-/TB+	18.89	3.436	1.353	2.646	0	0	2.633	1.154
180	HIV-/TB+	28.675	1.022	1.639	0.856	0	0	1.042	0.592
181	HIV-/TB+	16.49	1.518	1.019	1.348	0	0	1.435	0.674
182	HIV-/TB+	25.693	0	0	0.59	12.017	0	0.969	0
183	HIV-/TB+	0	0.009	0	0	4.852	0	0	0
188	HIV-/TB+	11.329	8.055	2.361	7.886	0	0	6.069	2.779
189	HIV-/TB+	2.173	1.18	0	0.957	3.412	0	0	0
190	HIV-/TB+	2.752	1.38	0.032	0.506	1.45	0	0.053	0
191	HIV-/TB+	26.239	1.817	2.44	2.118	0	0	2.271	1.001
192	HIV-/TB+	14.649	6.267	2.18	6.666	0	0	6.632	2.733
193	HIV-/TB+	2.921	9.792	2.549	7.709	0	0	9.873	2.812
194	HIV/TB+	10.102	1.227	0	0	32.708	0	1.203	0
198	HIV-/TB+	1.382	0	0	0.567	3.884	0	0	0
46	HIV+/TB-	0	0	0	0	86.222	0	6.012	0
48	HIV+/TB-	0	0	0	0	14.85	0	0	0
57	HIV+/TB-	28.946	0	0	0	19.571	0	93.054	0
62	HIV+/TB-	0	0	0	0	37.58	0	0	0
63	HIV+/TB-	20.149	1.03	0.252	8.864	384.335	0	2.631	0.397
77	HIV+/TB-	0.499	0	0	0	10.582	0	0	0
80	HIV+/TB-	24.685	1.249	0	0	327.305	0	0	0
13	HIV+/TB+	9.109	0	0	0	1.817	0	0.02	0
21	HIV+/TB+	19.783	0.319	2.868	0.974	99.911	0	0.39	0.05
92	HIV+/TB+	0	0	0	0	0	0	0	0
100	HIV+/TB+	13.838	0	0	0	47.12	0	0.333	0
103	HIV+/TB+	16.031	2.72	0.682	2.182	0	0	2.325	0.994
129	HIV+/TB+	2.44	0	0	0.188	95.488	0	1.278	0
145	HIV+/TB+	5.933	2.08	0.135	2.102	97.059	0	0.427	0

151	HIV+/TB+	0.149	0	0.034	0.858	5.439	0	0	0
186	HIV+/TB+	3.17	9.254	1.173	0.695	70.151	0	0.08	0
ID	**Group**	**Anserine**	**Aspartic acid**	**Homo-cystine**	**Arginino-succinic acid**	**Cystat-hionine**	**Phospho-ethanol-amine**	**Cystine**	**Saccharo-pine**
34	HIV-/TB-	0	6.143	0	0.332	0	0	3.077	0
36	HIV-/TB-	0	3.789	0	0	0	0.258	3.769	0
43	HIV-/TB-	23.978	1.26	1.166	5.622	4.796	5.116	10.095	0.617
44	HIV-/TB-	3.18	27.769	0	0.023	1.512	2.954	10.145	0
45	HIV-/TB-	33.848	4.849	3.094	14.336	11.254	17.147	17.437	1.532
47	HIV-/TB-	0	0	0	0	0	0	4.232	0
49	HIV-/TB-	0	0	0	0	0	0	4.669	0
59	HIV-/TB-	4.715	0	0	0	0	0.507	6.89	0
61	HIV-/TB-	31.322	0	0	0.473	0.196	0	3.85	0
64	HIV-/TB-	0	0	0	0	0	0	5.685	0
65	HIV-/TB-	0.205	0	0	0.888	0	0	3.813	0.03
67	HIV-/TB-	0	0	0	0	0	1.362	1.616	0
69	HIV-/TB-	0	0	0	0	0	0	2.014	0
116	HIV-/TB-	0	1.371	0	0	0	0	6.193	0
127	HIV-/TB-	2.88	0	0	0.055	0.274	1.803	3.677	0
147	HIV-/TB-	1.065	0	0.679	0.794	0.404	0.758	2.507	0.206
148	HIV-/TB-	2.912	0	0	0.563	0.064	2.252	3.553	0.099
155	HIV-/TB-	16.759	0	0	0	0	0	6.806	0
158	HIV-/TB-	0	0	0	0	0	0	5.847	0
159	HIV-/TB-	0	0	0	0.829	0.297	0.615	4.267	0.135
161	HIV-/TB-	106.868	2.794	2.734	10.616	11.847	11.62	14.344	1.553
162	HIV-/TB-	0	0	0	0	0	0	3.656	0
163	HIV-/TB-	0	0	0	0	0	0	4.373	0
165	HIV-/TB-	0	1.303	0	0.713	0.164	0.838	4.079	0.004
166	HIV-/TB-	71.224	1.337	1.003	4.843	3.993	7.994	7.407	0.588
167	HIV-/TB-	57.399	0	0	0.161	0.256	4.614	5.739	0.044
170	HIV-/TB-	0.036	0	0	0.548	0.2	1.025	3.278	0.093
171	HIV-/TB-	0.055	0	0	0	0	0	12.886	0
172	HIV-/TB-	12.456	0.743	0.685	3.167	2.889	3.885	8.357	0.404
173	HIV-/TB-	0	0	0	0.38	0.067	1.974	4.472	0
184	HIV-/TB-	50.315	0	0	0	0	1.737	2.35	0
185	HIV-/TB-	0	0	0	0.315	0.288	0	4.089	0.111
1	HIV-/TB+	2.141	0	0	0.392	0.042	0.528	3.116	0.119
3	HIV-/TB+	0	0	0	0.179	0.054	0.179	5.115	0.476
7	HIV-/TB+	0.13	0	0	0.65	0.06	0.409	7.423	0.272
12	HIV-/TB+	0	0	0	0.41	0.227	0.34	5.281	0.033
14	HIV-/TB+	0	0	0	0.258	2.635	1.503	12.918	0.195
19	HIV-/TB+	5.794	0.206	0.188	1.165	1.326	4.07	7.832	0.685

22	HIV-/TB+	0.158	0	0	0.584	0.347	2.854	13.226	0.363
23	HIV-/TB+	24.226	0.288	0.301	1.481	1.069	1.69	4.592	0.32
27	HIV-/TB+	0	0	0	0	0	1.916	5.328	0
90	HIV-/TB+	0.171	0	0	0.344	0.177	8.212	4.625	0
91	HIV-/TB+	0	0.113	0	0.788	0	0.615	3.62	0.235
123	HIV-/TB+	0	0.503	0	0	0	0.919	5.665	0
124	HIV-/TB+	19.979	2.322	0.646	2.939	3.503	3.908	8.183	0.605
128	HIV-/TB+	0	0.144	0	0.444	0.154	0	4.715	0.091
130	HIV-/TB+	0	0	0	0	0	0.335	9.526	0
132	HIV-/TB+	46.548	0.278	0.101	1.081	0.595	1.313	3.168	0.171
135	HIV-/TB+	0.05	0	0	0.716	0	0.351	3.36	0.082
140	HIV-/TB+	0.366	0	0	0.093	0.176	0	8.348	0
141	HIV-/TB+	0	0.519	0.407	2.199	1.805	2.125	4.855	0.317
144	HIV-/TB+	0	0	0	0.761	0.617	0.891	4.576	0.247
146	HIV-/TB+	0.297	0	0	0.399	0.917	1.094	5.677	0.337
152	HIV-/TB+	0.008	0	0	0.533	0.052	0.103	3.12	0.088
154	HIV-/TB+	10.846	1.124	1.381	4.749	3.732	4.494	7.662	0.903
157	HIV-/TB+	0	0	0	0	0	0	3.474	0
168	HIV-/TB+	4.512	0	0	0	1.039	0	3.978	0
169	HIV-/TB+	0	0	0	0.723	0.107	1.609	3.591	0.115
175	HIV-/TB+	0	0	0	0.113	0	0.01	3.441	0.022
176	HIV-/TB+	0	0	0	0.396	0	0.008	5.161	0.091
178	HIV-/TB+	4.148	0.423	0.369	2.257	1.069	2.842	4.075	0.376
180	HIV-/TB+	25.345	0.566	0.058	0.956	0.409	0.603	4.195	0.387
181	HIV-/TB+	30.935	0.336	0.26	1.604	0.833	2.95	2.883	0.312
182	HIV-/TB+	5.325	0	0	0	0.871	0.115	12.965	0
183	HIV-/TB+	0	0	0	0	0	0	4.598	0
188	HIV-/TB+	12.543	1.365	1.538	5.059	3.832	5.088	6.25	1.201
189	HIV-/TB+	0	0	0	0.55	0.035	2.358	3.936	0.084
190	HIV-/TB+	0	0	0	0.689	0.18	0.229	3.983	0.392
191	HIV-/TB+	81.815	1.348	0.351	1.387	2.754	1.148	4.877	0.46
192	HIV-/TB+	16.675	1.267	1.482	4.241	3.564	4.019	5.744	1.16
193	HIV-/TB+	35.69	1.466	1.116	5.052	3.906	5.566	7.709	0.511
194	HIV/TB+	1.338	0	0	0	0	2.398	4.935	0
198	HIV-/TB+	0	0	0	0.47	0	0	3.299	0.224
46	HIV+/TB-	9.598	0	0	0	0	0	2.44	0
48	HIV+/TB-	0	0	0	0	0	0	2.11	0
57	HIV+/TB-	0	0	0	0	0	0	10.081	0
62	HIV+/TB-	0	0	0	0	0	0	4.528	0
63	HIV+/TB-	4.518	0	0	0.335	0.985	0.742	3.844	0
77	HIV+/TB-	0	0	0	0	0	0	2.139	0
80	HIV+/TB-	2.6	0	0	0	0	0	8.38	0

13	HIV+/TB+	0	0	0	0.179	0	4.175	5.167	0
21	HIV+/TB+	0.449	0	0	0.125	0.81	1.578	6.952	0.123
92	HIV+/TB+	0	0	0	0	0	0	0	0
100	HIV+/TB+	0.445	0	0	0	0	0	9.156	0.223
103	HIV+/TB+	6.273	0.244	0.231	1.476	2.026	2.53	6.425	0.484
129	HIV+/TB+	0	0.038	0	0	0	0	4.764	0.157
145	HIV+/TB+	19.159	0	0	1.143	0.345	0	3.645	0.083
151	HIV+/TB+	0	0	0	0.301	0	0	2.867	0.354
186	HIV+/TB+	47.836	0	0	0.292	0.418	2.16	2.822	0.326
ID	**Group**	**Cysteine-sulfate**	**Phospho-serine**						
34	HIV-/TB-	0	0						
36	HIV-/TB-	0.572	0						
43	HIV-/TB-	1.98	1.271						
44	HIV-/TB-	0	0						
45	HIV-/TB-	5.113	3.43						
47	HIV-/TB-	0	0						
49	HIV-/TB-	0	0						
59	HIV-/TB-	0	0						
61	HIV-/TB-	0.25	0						
64	HIV-/TB-	0	0						
65	HIV-/TB-	0	0						
67	HIV-/TB-	0	0						
69	HIV-/TB-	0	0						
116	HIV-/TB-	0	0						
127	HIV-/TB-	0	0						
147	HIV-/TB-	0	0						
148	HIV-/TB-	0	0						
155	HIV-/TB-	0	0						
158	HIV-/TB-	0	0						
159	HIV-/TB-	0	0						
161	HIV-/TB-	6.656	3.7						
162	HIV-/TB-	0	0						
163	HIV-/TB-	0	0						
165	HIV-/TB-	0	0						
166	HIV-/TB-	1.899	1.106						
167	HIV-/TB-	0	0						
170	HIV-/TB-	0	0						
171	HIV-/TB-	0	0						
172	HIV-/TB-	3.128	0.791						
173	HIV-/TB-	0	0						
184	HIV-/TB-	0	0						
185	HIV-/TB-	0	0						

1	HIV-/TB+	0	0						
3	HIV-/TB+	0	0						
7	HIV-/TB+	0	0						
12	HIV-/TB+	0	0						
14	HIV-/TB+	0	0						
19	HIV-/TB+	0.896	0.199						
22	HIV-/TB+	0	0						
23	HIV-/TB+	1.704	0.45						
27	HIV-/TB+	0	0						
90	HIV-/TB+	0.192	0						
91	HIV-/TB+	2.081	0						
123	HIV-/TB+	0	0						
124	HIV-/TB+	7.634	0.931						
128	HIV-/TB+	0.074	0						
130	HIV-/TB+	0	0						
132	HIV-/TB+	0.325	0.112						
135	HIV-/TB+	0	0						
140	HIV-/TB+	0	0						
141	HIV-/TB+	4.711	0.447						
144	HIV-/TB+	0	0						
146	HIV-/TB+	0	0						
152	HIV-/TB+	0	0						
154	HIV-/TB+	2.263	2.595						
157	HIV-/TB+	0	0						
168	HIV-/TB+	0	0						
169	HIV-/TB+	0	0						
175	HIV-/TB+	0	0						
176	HIV-/TB+	1.406	0						
178	HIV-/TB+	1.362	0.455						
180	HIV-/TB+	0.441	0.062						
181	HIV-/TB+	0.828	0.365						
182	HIV-/TB+	0	0						
183	HIV-/TB+	0	0						
188	HIV-/TB+	3.479	1.82						
189	HIV-/TB+	0	0						
190	HIV-/TB+	0	0						
191	HIV-/TB+	1.507	0.429						
192	HIV-/TB+	4.225	1.847						
193	HIV-/TB+	1.826	1.164						
194	HIV/TB+	0	0						
198	HIV-/TB+	0	0						
46	HIV+/TB-	0	0						

48	HIV+/TB-	0	0						
57	HIV+/TB-	0	0						
62	HIV+/TB-	0	0						
63	HIV+/TB-	0	0						
77	HIV+/TB-	0	0						
80	HIV+/TB-	0	0						
13	HIV+/TB+	0	0						
21	HIV+/TB+	0	0						
92	HIV+/TB+	0	0						
100	HIV+/TB+	0	0						
103	HIV+/TB+	0.847	0.241						
129	HIV+/TB+	0	0						
145	HIV+/TB+	0	0						
151	HIV+/TB+	0	0						
186	HIV+/TB+	0	0						